Nazarbayev University School of Engineering and Digital Sciences Chemical and Materials Engineering Department
ENG 400 Capstone Project II

Report 4

Design of an Industrial Plant for Production of MTBE in Kazakhstan

Group members:

Asset Aliyev 202064719

Assiya Baigarina 201932931

Assem Sauirbayeva 202056246

Bek Madiyar 202053571

Yernur Shyntassov 201921466

Amina Baktybayeva 202043382

Instructor: Prof. Dhawal Shah

Supervisor: Prof. Cevat Erisken

Spring 2025

Astana, Kazakhstan

20.04.2025

Work Distribution Table

Chapter	Chapter Name	Assem	Assiya	Yernur	Asset	Amina	Bek
1	**Process Introduction**						
1.1	General Physical and Chemical Properties of MTBE					**2nd**	**1st**
1.2	MTBE Application and Production Rate					**1st**	
1.3	Review on the Selected Production Route					**1st**	
2	**Process Summary**						
2.1	Process Flow Diagram				**2nd**		**1st**
2.2	Material Balance of MTBE Production		**1st**		**2nd**		
2.3	Energy Balance of MTBE Production	**1st**			**2nd**		
3	**Major Equipment Design**						
3.1	H-101 Heat Exchanger	**1st**					
3.2	Heat Exchanger H-102			**1st**			
3.3	PFR Reactor R-101						
3.3	Reactor overall design	**2nd**				**1st**	
3.3	Cooling system of reactor	**1st**					
3.3	R-101 Unit Residence Time and Cost					**1st**	
3.4	MTBE Distillation Column T-101				**1st**		
3.5	T-102 Absorption Column		**1st**		**2nd**		
3.6	Methanol Distillation Column T-103				**1st**		**2nd**

4	**Minor Equipment Design**						
4.1	Temperature Changers	**2nd**	**1st**				
4.2	Pressure Changers		**1st**		**2nd**		
4.3	Storage Tanks					**1st**	
5	**Plant Location and Layout**						
5.1	Plant Site Location				**2nd**		**1st**
5.2	Plant Layout				**2nd**		**1st**
6	**Environment and Waste Streams**			**1st**			
7	**Total Investment and Profitability**						
7.1	Price of Raw Materials and Final Products		**1st**				
7.2	Cost of Equipment and Storage Tanks	**1st**	**2nd**				
7.3	Capital Investment Estimation	**2nd**	**1st**				
7.4	Fixed and Operating Labor Costs	**1st**	**2nd**				
7.5	Variable Cost of Production	**2nd**		**1st**			
7.6	Economic Analysis	**1st**					
8	**Conclusions and Future Work**						
8.1	Conclusion				**1st**	**2nd**	
8.2	Future Work				**1st**	**2nd**	

Table of Contents

List of Figures

List of Tables

Chapter 1: Process Introduction

Kazakhstan's substantial hydrocarbon reserves and strategic location position it as a key player in the global energy market. The Kashagan oil field, one of the world's largest offshore oil fields, boasts recoverable reserves estimated between 9 and 13 billion barrels of crude oil [1]. In

2024, Kashagan produced approximately 378 500 barrels per day, contributing significantly to the nation's oil output [2]. Additionally, Kazakhstan ranks among the top ten coal producers globally, with coal production reaching around 117.7 million tons in recent years [3].

However, the country's energy sector is also the primary source of greenhouse gas emissions, accounting for approximately 87.4% of total emissions in 2021 . Recognizing the environmental challenges, Kazakhstan has committed to achieving carbon neutrality by 2060, as outlined in its Strategy for Achieving Carbon Neutrality [4].

In alignment with these goals, the development of an industrial plant for the production of methyl tertiary-butyl ether (MTBE) in Kazakhstan represents a strategic initiative. MTBE, a high-octane additive used to improve gasoline combustion efficiency, can be synthesized from methanol and isobutylene - both of which can be derived from Kazakhstan's abundant natural gas and oil resources. The establishment of such a facility not only leverages domestic feedstocks but also contributes to cleaner fuel production, aligning with the nation's environmental objectives.

This capstone project aims to design and simulate an efficient, cost-optimized MTBE production plant in Kazakhstan. The project scope encompasses the selection of an appropriate manufacturing pathway, determination of final product specifications, identification of suitable reaction kinetics and catalysts, design of major and minor equipment, selection of an optimal plant location, and comprehensive economic and market analyses. By integrating these elements, the project seeks to support Kazakhstan's transition towards sustainable energy practices while capitalizing on its existing resource base.

1.1. General Physical and Chemical Properties of MTBE

Methyl tertiary-butyl ether (MTBE) is a volatile, colorless, and combustible organic compound formed by the reaction of isobutylene, derived from the C4 fraction of catalytic cracking or other low-cost sources, and methanol, which is typically produced from synthesis gas. Originally introduced in the late 1970s as a gasoline additive to replace lead and enhance octane ratings, MTBE gained widespread use following the 1990 U.S. Clean Air Act, which promoted its use to reduce motor vehicle emissions, including carbon monoxide, hydrocarbons, and ground-level ozone precursors. Compared to other gasoline components, MTBE is more soluble in water, has a smaller molecular size, and is less biodegradable, making it more mobile in groundwater and often detectable even when other gasoline constituents are absent [5].

While MTBE has proven effective in the fuel industry, especially as an octane enhancer and for reducing emissions, it poses significant environmental risks. Due to its high mobility in groundwater, MTBE can travel over long distances, contaminating drinking water sources and threatening both human and animal health [6]. Studies have indicated that long-term exposure to MTBE may cause damage to the nervous system, liver, and respiratory organs [7]. The primary environmental concern arises from leaks at gas stations and fuel transport accidents, where large quantities of MTBE-blended gasoline can enter and persist in the environment. Traditional approach to prevent the damage by MTBE to the environment suggests stricter control for the transportation and storage tanks, particularly in European countries [5]. The agricultural regions of Persian Gulf countries, particularly, in Iran are investigated for the potentially prospective use

of bioethanol as replacement for MTBE, however, it brings other issues such as soil erosion by source agricultures [8]. Alternatively, the ways to mitigate already present pollution by biological activated carbon treatment and catalytic degradation are investigated to avoid discarding MTBE as fuel dopant [9, 10].

MTBE is produced through the reaction of methanol with isobutene, facilitated by a solid acid catalyst. Industrial-scale production typically utilizes macroporous acidic ion-exchange resins, though other catalysts such as bentonites and zeolites can also be employed. A commonly used catalyst is sulfonated poly(styrene-divinylbenzene) resin. The reaction of MTBE formation proceeds according to a well-established chemical equation:

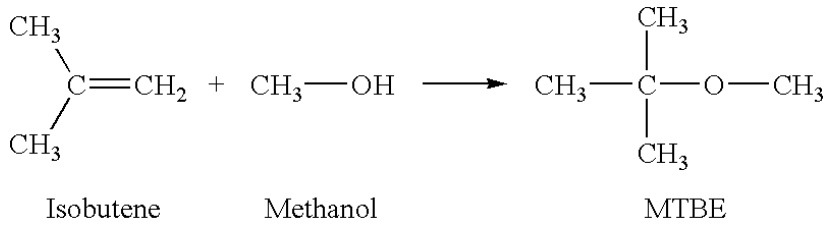

Figure 1.1.1. Synthesis of MTBE [5]

The chemical and physical properties of methyl tertiary-butyl ether (MTBE) were collected from multiple reputable sources, including the Aspen Plus database, NIST Chemistry WebBook, the article by Viswanathan et al. (2000), and the GESTIS Substance Database [11-13]. A detailed comparison of these properties is provided in Appendix A, Table A.1.

MTBE has a molar mass of approximately 88.15 g/mol, consistently reported across all sources. It exhibits a relatively low boiling point of around 55 °C, indicating that it is a volatile liquid under standard ambient conditions. The melting point is approximately –109 °C, which reflects the compound's broad liquid range and stability at low temperatures.

The critical temperature of MTBE lies in the range of 223.25 to 223.95 °C, while the critical pressure is reported between 3.286 and 3.397 MPa. These values are essential for understanding MTBE's behavior under high-temperature and high-pressure conditions, particularly in industrial processes.

At 20 °C and 1 atm, the density of MTBE is around 740–742.5 kg/m³, slightly less than that of water. Its dynamic viscosity under the same conditions is relatively low, approximately 0.35–0.39 cP, indicating that the fluid is easily flowable. The flash point of MTBE, measured in a closed cup, is about –28 °C, highlighting its high flammability and the need for careful handling and storage.

MTBE is also notable for its relatively high solubility in water compared to other gasoline additives. Reported values range from 16.56 g/L (Aspen Plus) to 26 g/L (GESTIS Database) [14,15]. This high solubility contributes to MTBE's enhanced mobility in groundwater, raising environmental concerns regarding contamination and persistence in subsurface environments.

1.2. MTBE Application and Production Rate

1.2.1. Uses and Applications

MTBE was originally introduced as a replacement for tetraethyl lead in gasoline, and the fuel industry remains its largest consumer. It is typically blended with gasoline in concentrations ranging from 5% to 30% by volume to enhance octane ratings and reduce emissions of incomplete combustion products [16]. This results in improved engine performance, reduced maintenance needs, and lower levels of pollutants such as carbon monoxide and hydrocarbons.

Beyond its primary role in fuel formulation, MTBE is also used as a solvent in chemical industries and scientific research. It is particularly effective for high-throughput lipid extraction in biochemical analysis due to its compatibility with biological samples and reduced risk of protein denaturation [17]. In petroleum refining, MTBE is employed in dewaxing processes to remove oil paraffin deposits and improve wax quality [18]. Although MTBE has moderate solubility in water, it functions similarly to solvents like tetrahydrofuran (THF) and ethyl tert-butyl ether (ETBE), with the added advantage of not forming explosive peroxides in solution.

1.2.2. Selected Production Rate

This section presents an overview of the global and CIS market demand for methyl tertiary-butyl ether (MTBE), focusing on projections for 2029. To estimate the required production rate, an approach based on global demand growth was used. Detailed calculations for both methods are provided in Appendix A, Table A.3.

Global demand for MTBE is expected to increase steadily due to its continued use as an octane enhancer and anti-knocking agent in gasoline. In 2022, demand stood at 17.6 million tonnes, with forecasts indicating it could reach over 28 million tonnes by 2032, at an average compound annual growth rate (CAGR) of approximately 4.6% [19–21].

Using the CAGR method, projected global demand in 2029 is estimated to be 23.1 million tonnes. Based on Kazakhstan’s target market, a GDP-based production rate calculation method was applied by taking the ratio between GDPs of the Commonwealth of Independent States (CIS), excluding Russia and that of global. With the CIS region accounting for 0.666% of global GDP, the regional demand in 2029 is projected to be 154,000 tonnes/year. The objective of this project is to supply 25% of this demand, resulting in a target production rate of 38,500 tonnes/year.

Kazakhstan's domestic MTBE production landscape supports the feasibility of this target. Pavlodar Neftekhim increased its capacity from 20,000 to 30,000 tonnes/year between 2019 and 2021 [22, 23], and a new plant in Shymkent is expected to reach 57,000 tonnes/year [24]. The proposed rate of 38 500 tonnes/year is strategically positioned between these two capacities, ensuring realistic scalability and alignment with regional demand.

1.3. Review on the Selected Production Route

There are several industrial pathways for MTBE production, including direct etherification of isobutylene with methanol[25], production via tert-butyl alcohol (TBA)[26], and synthesis

from butane[27]. Each route differs in terms of feedstock availability, energy consumption, process complexity, and byproduct formation. A comparison of these methods is provided in Table in Appendix A, Table A.4.. Among them, the direct etherification of isobutylene with methanol stands out as the most widely adopted route due to its simplicity, moderate energy requirements, and high process efficiency. The raw materials for MTBE production include methanol, which is readily available from domestic suppliers in Kazakhstan, and isobutylene. By purchasing isobutylene directly instead of producing it via tert-butanol dehydration, the process simplifies operations, reduces energy consumption, and eliminates the need for additional reaction and separation steps.

To carry out the liquid-phase etherification of isobutylene with methanol, an appropriate catalyst is required to ensure high conversion, yield, and selectivity. Amberlyst-15 was selected for MTBE synthesis based on comparison between different commercially available catalysts. As shown in Appendix A, Table A.5., Amberlyst-15 exhibits superior performance at lower temperatures and higher methanol/isobutene ratios, which aligns well with our process configuration that includes methanol recycling. Amberlyst-15 achieved up to 94.5% isobutene conversion, 92.7% MTBE yield, and 98.1% selectivity, outperforming ZSM-5 and ZSM-11 under similar conditions [28].

Supporting literature further reinforces this choice. Nicolaides et al. [29] and Hatchings et al. [30] compared Amberlyst-15 to H-ZSM-5 and other zeolites, demonstrating Amberlyst-15's higher efficiency even at mild operating conditions. Although some studies, such as Chu and Kuhl [28], suggest that zeolites may be more advantageous at low methanol-to-isobutene ratios, this limitation is mitigated in our design due to efficient methanol recovery and recycling. Consequently, Amberlyst-15 provides the optimal balance between performance, process simplicity, and operational cost for the selected MTBE production route.

For the MTBE production process, appropriate thermodynamic and kinetic models were selected based on literature. The UNIFAC model was chosen to describe phase equilibria and activity coefficients in the MTBE system. This method provides a reliable estimation of activity coefficients for non-ideal liquid-phase systems, which is crucial for calculating reaction rates, separation, and component interactions in both the reactor and downstream units. The system exhibits non-ideal behavior, making UNIFAC a suitable choice for thermodynamic modeling.

This reaction proceeds via a Langmuir–Hinshelwood–Hougen–Watson (LHHW) mechanism, in which methanol and isobutylene are being absorbed onto the catalyst surface before reacting. The surface reaction between the adsorbed species is identified as the rate-limiting step. This approach is supported by the work of Zhang and Datta [31], who experimentally derived the model. The kinetic rate law incorporates the adsorption and surface saturation, and activity coefficients were determined using the UNIFAC method. The model assumes methanol dominates adsorption, which leads to strong inhibition effects at high methanol concentrations. All reaction rate expressions for each component and detailed kinetic parameters are provided in Appendix A.

For our project, Grade A MTBE, with a purity of at least 98%, was selected to optimize performance and comply with fuel quality requirements. The Table A.6 in Appendix A summarizes the grading and purity specifications of MTBE [32, 33].

Chapter 2: Process Summary

2.1. Process Flow Diagram

In Figure 2.1.1 a detailed process flow diagram is demonstrated. The product of this process is 98.4 wt% MTBE purity.

To sustain the process, three streams of inlet raw materials are present, with details in Table 2.1.1. Main reaction raw materials are introduced with streams 1 and 7.

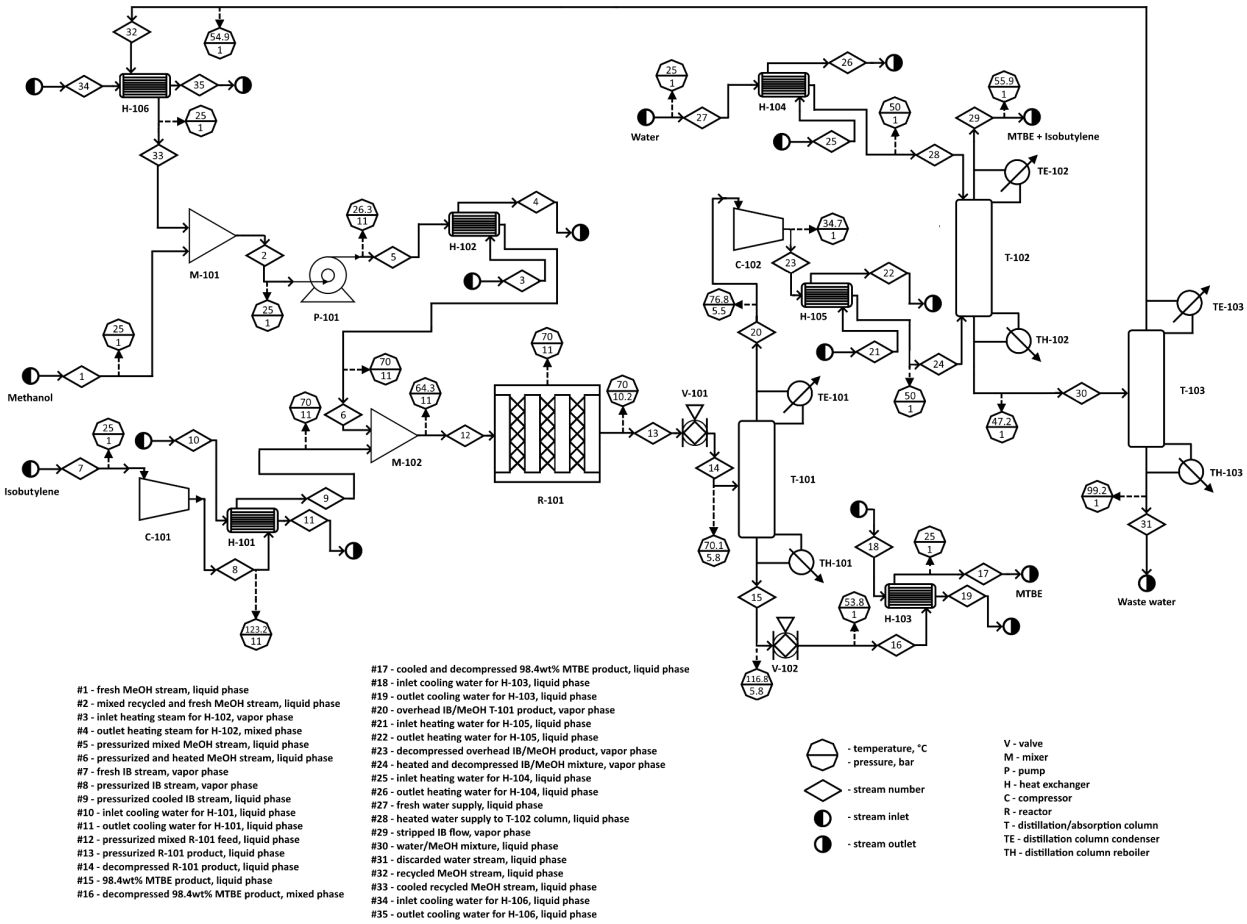

Figure 2.1.1. General process flow diagram

Table 2.1.1. Inlet raw materials

Stream ID	Streams	Temperature, °C	Pressure, bar	Phase
1	Methanol inlet	25	1	Liquid

7	Isobutylene inlet	25	1	Gas
27	Water inlet	25	1	Liquid

However, to maintain a specified reaction in the reactor, and to recycle process materials, the pre-processing manipulations over raw materials are required. This involves passing stream 7 through compressor C-101, and condensing resulting stream 8 in condenser H-101 to form reactor isobutylene feed stream 9. At the same time, in M-101 mixing of recycled methanol stream 33 from distillation column T-103 with fresh methanol supply from stream 1 takes place. Formed stream 2 is then pumped and heated through H-102 to feed reactor methanol via stream 6. Streams 6 and 9 are mixed in M-102 to form plug-flow reactor feed stream 12. Reaction is performed in reactor R-101. The conditions of outlet streams from mentioned blocks are specified in Table 2.1.2.

Table 2.1.2. Pre-processing raw materials

Unit ID	**Unit operation description**	**Unit outlet temperature, °C**	**Unit outlet pressure, bar**
C-101	Isobutylene compression	123	11
H-101	Isobutylene condensing	70	11
M-101	Recycled and fresh methanol mixing	25	1
P-101	Methanol feed pumping	26	11
H-102	Methanol feed heating	70	11
M-102	Reactor feed mixing	64	11
R-101	Plug-flow reactor with catalyst	70	10

After reaction takes place, the reactor product stream 13 is passed through valve V-101 to decrease pressure. Stream 14 from the valve reaches distillation column T-101, where high purity MTBE is separated from product mixture as stream 15 and expanded in V-102 to 1 bar and cooled down in H-103 to 25 °C in outlet stream 17. Rest of the product with unreacted materials in stream 20 is decompressed through C-102 and heated up by H-105 to reach the operating conditions of distillation column T-102 as stream 24. Corresponding unit outlet conditions are specified in Table 2.1.3.

Table 2.1.3. Separation of MTBE product

Unit ID	Unit operation description	Unit outlet temperature, °C	Unit outlet pressure, bar
V-102	Depressurizing reactor product stream	54	1
H-103	Cooling down reactor product	25	1
T-101	MTBE distillation	117	6
C-102	Depressurizing MTBE/IB/methanol mixture	35	1
H-105	Heating MTBE/IB/methanol mixture	50	1

Fresh water inlet stream 27 is passed through H-104 heater to yield a conditioned stream 28 for absorption column feed. Absorption column T-102 is supplied with streams 24 and 28 to produce IB/MTBE waste in stream 29, and the methanol is absorbed to yield methanol-water mixture in stream 30. It is then routed for water-methanol separation into distillation column T-103. The conditions of mentioned units' outlets are specified in Table 2.1.4.

Table 2.1.4. Separation of IB/MTBE unreacted mixture

Unit ID	Unit operation description	Unit outlet temperature, °C	Unit outlet pressure, bar
H-104	Heating water feed to the absorption column	50	1
T-102	Methanol absorber	56	1

Table 2.1.5 provides information on conditions of separating adsorbed methanol from water and recycling it. The methanol-water stream 30 is fed to distillation column T-103 to remove water into outlet stream 31 as hot liquid. The methanol hot liquid stream 32 is fed to cooler H-106 to cool down liquid to 25°C; cooled stream 33 is fed to mixer M-101.

Table 2.1.5. Separation of methanol-water mixture

Unit ID	Unit operation description	Unit outlet temperature, °C	Unit outlet pressure, bar
T-103	Methanol-water distillation	99	1
H-106	Methanol recycling cooler	25	1

Summarizing the information on PFD products, the Table 2.1.6 provides information on conditions of outlet streams.

Table 2.1.6. PFD outlets

Stream ID	Streams	Temperature, °C	Pressure, bar	Phase
17	High-purity MTBE outlet	25	1	Liquid
29	IB/MTBE waste outlet	56	1	Vapor
31	Waste water outlet	99	1	Liquid

2.2. Material Balance of MTBE Production

This chapter presents the material balance for the entire process of producing MTBE at a purity of 98.4 wt%. It includes material balance calculations for reactors, distillation columns, and mixers. All validations were conducted using Aspen Plus V14 and were cross-verified with both hand calculations and Excel calculations for accuracy.

The simulation was conducted with assumptions for a plant with a production capacity of 38.5 kton/oper-year. Given an on-stream factor of 90%, the simulation reflects a chemical plant designed to operate for 8000 hours per year. This annual runtime is based on 91.3% operational efficiency out of the total possible 8 760 hours per year, allowing for 8.7% downtime for scheduled maintenance and other necessary shutdowns. Kinetics is based on the paper by Zhang and Datta, from which values were used to calculate material balance for consistency [31]. First, the production rate was converted to a molar basis, then divided by the MTBE conversion rate, calculated to be 87.5% after constructing a PFR reactor with reactions in Aspen Plus V14. A 2% loss is considered in the MTBE plant to account for material losses from unavoidable factors, such as evaporation, incomplete reactions, and minor leaks during storage and handling. This allowance ensures realistic yield expectations and supports efficient operation planning. The molar ratio of methanol to isobutylene was set at 1.1, following the Zhang and Datta paper. The results from the feed calculations are given in Table 2.2.1.

Table 2.2.1. The inlet flow rates of raw reactants

Components	MeOH	IB
Mole Flow, kmol/oper-year	520552.79	472735.57

The flow summary table for streams between 1 and 12 provides detailed information on temperature, pressure, and mass flow rates of key components in the MTBE plant (Table 2.2.2). Inlet streams 1 and 7 enter at 25°C and 1 bar pressure, carrying 15.15 kton/oper-year of methanol. Stream 6 contains 15.72 kton/oper-year of methanol but at different conditions 70°C and 11 bar. Stream 7, at 25°C and 1 bar, introduces 29.21 kton/oper-year of IB. This isobutylene flow rate remains constant in Streams 8 and 9, both at 11 bar and temperatures of 123.20°C and

70°C, respectively. Stream 12, the combined output of methanol and isobutylene, flows at 11 bar and 64.28°C, with a total mass flow rate of 45.02 kton/oper-year, containing 15.72 kton/oper-year of methanol and 29.21 kton/oper-year of isobutylene.

Table 2.2.2. The flow summary of streams 1-12

Stream	**1**	**5**	**6**	**7**	**8**	**9**	**12**
Temperature	25.00	26.28	70.00	25.00	123.20	70.00	64.28
Pressure	1.00	11.00	11.00	1.00	11.00	11.00	11.00
Mass flow rate, kton/oper-year							
MEOH	15.15	15.72	15.72	0.00	0.00	0.00	15.72
IB	0.00	0.01	0.01	29.21	29.21	29.21	29.21
Water	0.00	0.02	0.02	0.00	0.00	0.00	0.02
DIB	0.00	1.33E-10	1.33E-10	0.00	0.00	0.00	1.33E-10
MTBE	0.00	0.06	0.06	0.00	0.00	0.00	0.06
Total	15.15	15.81	15.81	29.21	29.21	29.21	45.02

Stream 13 represents the material balance around the reactor. The results from kinetic calculations were taken to obtain conversion of MTBE. Taking into account the main and side reaction 87.5% of isobutylene converted to MTBE and a very small amount converted (6.47E-6%) to DIB. After adjusting the reactor with mole conversions the mass flow results were collected. Stream 13, at 70°C and 10.24 bar, has a total flow rate of 45.02 kton/oper-year, including 1.12 kton/oper-year of methanol, 3.64 kton/oper-year of isobutylene, and 40.24 kton/oper-year of MTBE. The pressure decreased to 5.8 bar after valve in Stream 14. Streams 14, 15, and 20 reflect the material balance around the distillation column with specific split fractions for different components. Stream 14 serves as the initial feed into the distillation column before component distribution. In Stream 15, 98.4 wt% of MTBE [34], isobutylene, and diisobutylene are directed here, along with 1.32 wt% of methanol, concentrating most of these components in the product stream. Stream 20 is mainly designated for isobutylene recovery, with 60.03 wt% of IB, 29.84 wt% of MTBE, and 10.13 wt% of methanol directed here. The summary of streams between 14 and 30 given in Table 2.2.3. The water comes from Stream 27, which is based on a 1.05:1 weight ratio of unreacted isobutylene to water [35].

Table 2.2.3. The flow summary of streams 14-30

Stream	**14**	**17**	**20**	**24**	**28**	**29**	**30**
Temperature	70.09	25.00	76.82	50.00	50.00	55.87	47.15
Pressure	5.80	1.00	5.50	1.02	1.00	1.00	1.00
Mass flow rate, kton/oper-year							

MEOH	1.12	0.52	0.60	0.60	0.00	0.01	0.59
IB	3.64	0.08	3.56	3.56	0.00	3.56	0.01
Water	0.02	0.02	0.00	0.00	3.73	0.29	3.44
DIB	4.71E-5	4.71E-5	1.13E-7	1.13E-7	0.00	1.13E-7	1.33E-10
MTBE	40.24	38.46	1.77	1.77	0.00	1.71	0.06
Total	45.02	39.08	5.94	5.94	3.73	5.57	4.10

In T-103, water has a split fraction of 0.99, indicating that this component is mostly directed to the bottom (Stream 31), while other components are directed entirely to the top. In Stream 32, methanol has a high split fraction, ensuring it exits at the top. Operating at temperature range between 54.85°C and 99.17°C and at 1 bar, Stream 32 shows methanol and water remaining at 0.58 kton/oper-year and 0.02 kton/oper-year, respectively, maintaining low-pressure conditions. Detailed data about the mass flow rate is given in the Table 2.2.4.

Table 2.2.4. The flow summary of streams 31-33

Stream	**31**	**32**	**33**
Temperature, ℃	99.17	54.85	25.00
Pressure, bar	1.00	1.00	1.00
Mass flow rate, kton/oper-year			
MEOH	0.02	0.58	0.58
IB	1.62E-11	0.01	0.01
Water	3.42	0.02	0.02
DIB	5.14E-18	1.67E-08	1.67E-08
MTBE	5.75E-09	0.06	0.06
Total	3.44	0.67	0.67

The material balance for the process, previously considered without recycling, from PFD should be updated to incorporate the recycling of Stream 33 to M-101. In that case the methanol flow rate is determined as the sum of the feed and the recycle stream, amounting to about 490720.79 kmol/oper-year.

The overall mass balance reveals equal inlet and outlet flows at 48.09 kton/oper-year, ensuring conservation within the MTBE process (Table 2.2.5). Key inlets include Stream 1 (15.15 kton/year) and Stream 7 (29.21 kton/year), while the outlets are Stream 17 (39.08 kton/year), Stream 29 (5.57 kton/year) and Stream 31 (3.44 kton/year). This balance confirms efficient material distribution in the system.

Table 2.2.5. The overall material balance

Overall mass balance			
Inlet		**Output**	
Stream	**Mass flow, kton/oper-year**	**Stream**	**Mass flow, kton/oper-year**
1	15.15	**17**	39.08
7	29.21	**29**	5.57
27	3.73	**31**	3.44
Total	48.09	**Total**	48.09

Temperatures and pressures for the streams were determined using Aspen software. The mass flow rates and mole flow rates obtained showed closely matching values in both Excel and Aspen.

2.3. Energy Balance of MTBE Production

In this section the energy balance is considered as well as materials balance for valves, compressors, and heat exchangers according to the PFD indicated above. Each unit has individual formulas to calculate heat duty of heat exchangers and power of compressors, valves, and a pump.

The equation to calculate the amount of heat energy (Q) needed to change the temperature of a substance without a phase change is provided below (Equation 2.3.1). It is useful for processes such as heating or cooling in heat exchangers, where temperature changes occur within a single phase.

$$Q = mC_p\Delta T \tag{2.3.1}$$

, where Q is a heat duty needed to change a substance's temperature without a phase change, m is the mass flow rate, Cp is the specific heat capacity, and is the temperature change.

$$Q = m\Delta H \tag{2.3.2}$$

The Equation 2.3.2 is particularly relevant for the calculation of heat energy when materials undergo phase changes, such as in the vaporization of water to steam in a boiler. The enthalpy term represents the energy required to overcome molecular bonds and transition to a different phase without a change in temperature.

$$W = \frac{m\Delta P}{\rho} \tag{2.3.3}$$

In practical applications, the Equation 2.3.3 is applied in gas compression or expansion processes where pressure changes are a primary concern.

Table 2.3.1. Energy balance for pressure changers

Pressure changers					
	P-101	**V-101**	**V-102**	**C-101**	**C-102**

Mass flow rate, kg/s	0.55	1.56	1.36	1.01	0.21
Density mix, kg/cum	793.03	674.50	625.81	2.31	12.11
Change in pressure, Pa	-1000000.00	443800.00	477000.00	-1000000.00	448000.00
Work, kW	2.34	0.00	0.00	156.55	-12.21

Table 2.3.2. Energy balance for temperature changers.

Temperature changers						
	H-101	**H-102**	**H-103**	**H-104**	**H-105**	**H-106**
Mole flow rate, kmole/s	0.018	0.017	0.016	0.007	0.004	0.001
CPmix, kJ/kmol-K	114.506	89.942	173.103	74.073	92.160	105.975
Change in temperature	53.20	-43.72	28.759	-25.00	-15.316	29.853
Q total, kW	411.613	74.838	303.893	13.463	5.103	2.062

Chapter 3: Major Equipment Design

6 major equipment were designed in this chapter including 1 reactor, 2 heat exchangers and 3 separation units. The design specifications and working principles of these 6 units were discussed below.

3.1. H-101 Heat Exchanger

After being compressed, the isobutylene stream vaporizes and leaves the compressor at $123.2^{\circ}C$. The inlet stream of isobutylene into the reactor should be at $70^{\circ}C$, meaning that it is required to condense the isobutylene vapor. In this section, the H-101 heat exchanger will be applied as a condenser and its design specifications will be explained.

3.1.1. Working Principles of H-101

Condenser is a heat exchanger equipment applied to convert a vapor into a liquid. A heat exchanger is designed to transfer heat fluids with varying temperatures. The fundamental principle is heat exchange between fluids without direct mixing. There are several types of heat exchangers like double pipe, plate and frame, shell and tube, plate-fin, spiral heat.

In condensers, heat is removed from a hot vapor, causing it to lose energy and transition into a liquid phase. This process is essential in power plants, refrigeration, and chemical industries. Heat exchangers, in general, consist of hot and cold fluids separated by a solid barrier that facilitates heat transfer. The effectiveness of heat exchange depends on factors such as

temperature difference, surface area, thermal conductivity of materials, and fluid flow rate. Common flow configurations include parallel flow, counterflow, and crossflow.

Condensers are designed as shell and tube exchangers, but with the condition of shell diameter, D_s, equal to baffle spacing l_B. There are 4 condenser types: horizontal with condensation in the shell, horizontal with condensation in the tubes, and vertical with condensation in the shell, vertical with condensation in the tubes. Horizontal exchangers with condensation in the shell side are the most widely used variety of the condenser [36]. Therefore, for the design of H-101 horizontal shell-side configuration was chosen.

Table 3.1.1. Information about stream results of the H-101 heat exchanger

Location	**Tube side**	**Shell side**
Chemical composition	H_2O	C_4H_8
Inlet temperature, ℃	23.00	123.20
Outlet temperature, ℃	42.77	70.70
Inlet pressure, bar	1.50	11.00
Outlet pressure, bar	1.24	10.96
Mass flow rate, kg/h	18000.00	3650.85
Total heat exchanged, kW	409.10	
Fouling resistance, m² ℃/W	0.00017	0.00020

The heat exchanger H-101 is applied to condense the isobutylene stream with the help of cold water. The cold water is sent to the tube side, while hot isobutylene stream goes through the shell side, where isobutylene temperature reaches approximately $70^{\circ}C$. The general information about inlet and outlet streams of condenser H-101 are indicated in Table 3.1.1.

The temperature curve, shown in Appendix B Figure B.1, provides a visual representation of how the hot and cold fluid temperatures vary as heat is transferred within the exchanger. Because the two lines maintain a relatively consistent separation, the temperature difference driving heat transfer remains sufficient across the entire exchanger. This prevents the occurrence of temperature cross-over, where the hot and cold curves would nearly intersect, signaling inadequate driving force for heat transfer. While the cold stream increases its temperature from $23^{\circ}C$ to $43^{\circ}C$ the hot stream decreases its temperature from 123°C to 70°C. At 75°C isobutylene condenses from vapor into liquid as it is the dew temperature of isobutylene, and till 70°C isobutylene liquid undergoes subcooling. Overall, the temperature curve plot confirms that the selected design effectively condenses the hot stream within the desired temperature range, without requiring excessive surface area or encountering problematic operational conditions.

3.1.2. Selection of Design Specifications

The selected heat exchanger design is based on standard engineering principles outlined in *Chemical Engineering Design* [36] and the Tubular Exchanger Manufacturers Association (TEMA) standards. The primary design considerations include tube dimensions, tube arrangement, pass configuration, baffle design, and material selection to optimize thermal performance, operational efficiency, to avoid vibrations, and to satisfy the appropriate values of parameters like velocity of fluids, pressure drop and overall heat exchanger coefficient [36]. The design specifications selected for heat exchanger design are presented in Table 3.1.2.

The heat exchanger consists of tubes with an outer diameter of 16 mm and an inner diameter of 11.8 mm, which are standard sizes for efficient heat transfer while maintaining structural strength. The tubing length of 4.88 meters allows for adequate heat transfer area within a compact design. Although shorter tube length would decrease pressure drop in the tube side, it would significantly decrease water velocity. The tubes are arranged in a 90-degree square pattern, a configuration known for its high thermal performance and ease of cleaning, as well as mechanical robustness under varying operational conditions.

The exchanger includes a two-pass tube configuration with a single shell pass. The two-pass arrangement enhances the heat transfer coefficient by increasing the velocity of the fluid within the tubes, promoting improved convective heat transfer. The single shell pass design ensures a straightforward flow path, reducing pressure drop and allowing for effective temperature control across the heat exchanger.

Baffles are included with a 35% cut to support the tubes, induce fluid turbulence, and minimize dead zones within the shell. The 35% cut is chosen to balance pressure drop and heat transfer enhancement, ensuring sufficient flow distribution while avoiding excessive pressure losses that could reduce system efficiency. The baffle spacing and arrangement are designed according to TEMA recommendations to prevent tube vibration and ensure operational longevity.

The material selected for the heat exchanger is stainless steel, a choice driven by its excellent corrosion resistance, high mechanical strength, and thermal conductivity. Stainless steel 316 is well-suited for applications involving aggressive fluids, high temperatures, and prolonged operational lifetimes, making it a preferred material in industrial heat exchanger applications.

The BEM type heat exchanger is commonly used for condenser applications due to its simple, cost-effective design and efficient performance for vapor-to-liquid heat transfer. With fixed tubesheets and a one-pass shell, it provides a large heat transfer surface within a compact footprint, making it ideal for condensing vapors like isobutylene using cooling media such as water.

Overall, the selected design ensures efficient heat exchange, mechanical reliability, and compliance with industry standards, making it a robust choice for industrial applications requiring durability and performance.

Table 3.1.2. Geometry of H-101 heat exchanger

Schematic representation of H-101		
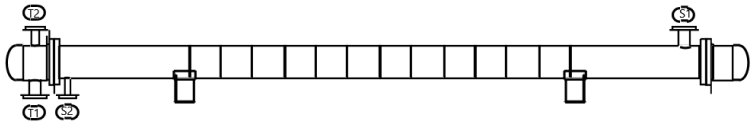		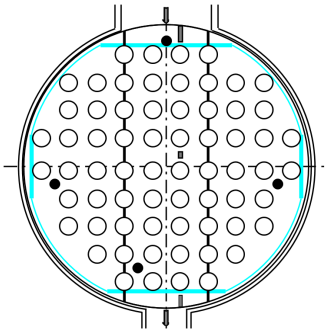
Location	Tube	Shell
Inner diameter of the tube, mm	11.80	248.65
Outer diameter of the tube, mm	16.00	255.46
Tube length, m	4.88	
Effective area, m^2	15.90	
Baffle spacing, mm	248.65	
Baffle cut, %	35.00	
Number of baffles	13.00	
Bundle diameter, mm	238.65	
Number of tubes	66.00	
Tube pitch diameter, mm	24.00	
Tube pattern	90° square pattern	
Tube passes	2.00	
Shell passes	1.00	
Shell in series	1.00	
Shell in parallel	1.00	
TEMA type	BEM	

Type of material	Stainless steel SS 316
Total cost, $	329 897.00

3.1.3. H-101 Design Calculations

Initially, it was necessary to calculate logarithmic mean temperature difference , ΔT_{lm}, and the correction factor, F_t, using the R and S ratios. For that, the equations below were applied.

$$\Delta T_{lm} = \frac{(T_1 - t_2) - (T_2 - t_1)}{ln\frac{(T_1 - t_2)}{(T_2 - t_1)}} \quad (3.1.1)$$

$$R = \frac{T_1 - T_2}{t_2 - t_1} \quad (3.1.2)$$

$$S = \frac{t_2 - t_1}{T_1 - t_1} \quad (3.1.3)$$

$$F_t = \frac{\sqrt{R^2+1} * ln\frac{1-S}{1-RS}}{(R-1) * ln\frac{2-S(R+1-\sqrt{R^2+1})}{2-S(R+1+\sqrt{R^2+1})}} \quad (3.1.4)$$

, where T_1-inlet hot stream temperature and T_2-outlet hot stream temperature, t_1 - inlet cold stream temperature and t_2- outlet cold stream temperature. True temperature difference, T_m, was calculated by multiplying the correction factor to the logarithmic mean temperature difference.

Further, heat exchanger area, A, area of 1 tube, $A_{1\,tube}$, and number of tubes, N_t, were calculated using the assumed overall heat transfer coefficient, U = 500 $W/m^{2\circ}C$, applying equations below.

$$A = \frac{Q}{UF_t T_m} \quad (3.1.5)$$

$$A_{1\,tube} = d_o * \pi * L \quad (3.1.6)$$

$$N_t = \frac{A}{A_{1-tube}} \quad (3.1.7)$$

, where Q is the heat duty of the reactor (calculations were done in Excel), L is the length of the tube, d_o is the outer diameter of the tube.

Further, bundle, D_b, and shell, D_s, diameters, and the number of tubes in the center row, $N_{r-center}$, were calculated using the formulas below. For that, pitch diameter, d_{pitch} was used. The square pitch arrangement with 2 tube passes was chosen to provide sufficient velocity of the fluid in the tube.

$$d_{pitch} = 1.5 d_o \quad (3.1.8)$$

$$D_b = d_{pitch}\left(\frac{N_t}{K_1}\right)^{1/n_1} \quad (3.1.9)$$

$$N_{r-center} = \frac{D_b}{d_{pitch}}\ center\ row \quad (3.1.10)$$

, where K_1 and n_1 are constants chosen on the basis of the square pitch arrangement [Appendix B Table B.1] and number of tube passes. Values were taken from the [36].

The physical properties of viscosity, density and thermal conductivity were chosen on the basis of mean temperature condensate calculated using the tube wall temperature. For that, the equations below were used.

$$T_{wall} = T_{shell} - \frac{(T_{shell} - T_{tube})*U}{h_c} \quad (3.1.11)$$

, where T_{wall} is the wall temperature, T_{shell} - average temperature in the shell, T_{tube} - average temperature in the tube, h_c - condensing coefficient, which was assumed to be 1200 $W/m^{2\circ}C$.

$$T_{condensate} = \frac{T_{shell} + T_{wall}}{2} \quad (3.1.12)$$

, where $T_{condensate}$ is the mean temperature condensate.

To check the assumption of the condensing coefficient, the following equations were used. Equations below involve viscosity, density, and thermal conductivity values, which were found using Aspen Plus V14.

$$h_c = 0.95 k_l \left(\frac{\rho_l(\rho_l - \rho_v)g}{\mu_L * \Gamma_h}\right)^{1/3} * N_r^{-1/6} \quad (3.1.13)$$

$$\Gamma_h = \frac{W_c}{LN_t} \quad (3.1.14)$$

$$N_r = \frac{2}{3} * N_{r-center} \quad (3.1.15)$$

, where W_c is the total condensate flow, N_r is the average number of tubes in a vertical tube row, ρ_l and ρ_v are liquid and vapor densities, respectively, g is the gravitational constant, μ_L is the liquid viscosity, k_l is the liquid thermal conductivity. For the calculations of condensing coefficient, average number of tubes in a vertical tube row was neglected as isobutylene is low viscosity condensate.

Tube side coefficient, h_i, was calculated using the equations provided further.

$$A_{cross-sectional} = \frac{\pi}{4} * \frac{d_i^2 * N_t}{2} \quad (3.1.16)$$

$$v_{tube} = \frac{W_c}{\rho} * \frac{1}{A} \quad (3.1.17)$$

$$h_i = \frac{4200*(1.35+0.02*T_{tube})*v_{tube}^{0.8}}{d_i^{0.2}} \quad (3.1.18)$$

, where $A_{cross-sectional}$ is the tube cross-sectional area, v_{tube} is the velocity in the tube, ρ water liquid density, and d_i is the inside diameter.

The overall heat transfer coefficient assumption was checked using the equation below.

$$\frac{1}{U_o} = \frac{1}{h_o} + \frac{1}{h_{od}} + \frac{d_o ln(\frac{d_o}{d_i})}{2k_w} + \frac{d_o}{d_i} \times \frac{1}{h_{id}} + \frac{d_o}{d_i} \times \frac{1}{h_i} \quad (3.1.19)$$

, where U_o is the calculated overall heat transfer coefficient, h_o is the outside fluid film coefficient, h_i is the inside fluid film coefficient, h_{od} and h_{id} are the outside and inside dirt coefficients, respectively, and k_w is the thermal conductivity of the tube wall temperature. Thermal conductivity of the SS 316 is 16.2 W/m·K. Stainless steel 316 was chosen as it can withstand the hot fluid temperatures, it is not corrosive and is cost efficient. The outside and inside dirt coefficients were chosen from Appendix B Table B.2. The overall heat transfer coefficient (U) presented by ASPEN is 566.5 W/m²·°C, which is higher than the assumed design value of 500 W/m²·°C. This indicates that the manual calculations align well with industry expectations.

Shell-side pressure drop

In order to calculate the shell side pressure drop, it is necessary to find the cross sectional area of the shell, mass velocity, equivalent diameter for flow, flow velocity inside the shell. All necessary formulas are presented below:

$$A_s = \frac{(d_{pitch} - d_o)*d_{shell-id}^2}{d_{pitch}} \quad (3.1.20)$$

$$M = \frac{W_c}{A_s} \quad (3.1.21)$$

$$d_{eq} = (d_{pitch}^2 - 0.785 * d_o^2) * \frac{1.27}{d_o} \quad (3.1.22)$$

$$Re = \frac{M*d_{eq}}{\mu} \quad (3.1.23)$$

$$u_s = \frac{M}{\rho_v} \quad (3.1.24)$$

$$\Delta P = \frac{8j_f \frac{d_{shell-id}}{d_{eq}} * \frac{L}{d_{shell-id}} * \frac{\rho_v u_s^2}{2}}{2} \quad (3.1.25)$$

where, A_s- cross section area of the shell, d_{pitch} pitch diameter, $d_{shell-id}$ inner diameter of the shell, M- mass flow rate per unit area, d_{eq}- equivalent diameter, μ- viscosity, Re- Reynolds number, u_s- velocity inside shell, ΔP - pressure drop, j_f- friction factor. Friction factor can be

obtained from shell-side friction factor graph or from tube-side friction factor graph [36].

For condensers, the pressure drop is calculated with the factor of 50%.

Tube side Pressure drop

$$\Delta P = N_p(8j_f(\frac{L}{d_i})(\frac{\mu}{\mu_w})^{-m} + 2.5)\frac{\rho u_t^2}{2} \quad (3.1.26)$$

where, N_p number of tube-side passes, μ viscosity at mean temperature, μ_w viscosity at wall temperature, m = 0.25 for laminar, m = 0.14 for turbulent flow, u_t - tube velocity.

The pressure drop calculations confirm the efficiency of the selected design. The shell-side pressure drop is calculated to be approximately 0.04 bar, while the tube-side pressure drop is 0.26 bar. These values are within acceptable limits, ensuring efficient fluid flow without excessive energy losses. The selected baffle cut and tube arrangement contribute to an optimized pressure drop, balancing flow distribution.

The minor discrepancy between the calculated and the Aspen Plus V14 simulation results is expected due to software-specific empirical correlations, numerical approximations, and assumed boundary conditions. However, the closeness of the values confirms the validity of the design approach and the accuracy of the applied methodologies.

Overall, the selected design ensures efficient heat exchange, mechanical reliability, and compliance with industry standards, making it a good choice for industrial applications requiring durability and performance.

3.2. Heat Exchanger H-102

Heat exchanger H-102 was used to heat recycled methanol with methanol feed from 26.3°C to 70°C, which will be sent to the reactor afterwards. Saturated steam at 1 bar and with temperature of 120.4°C was chosen as the heating medium. In order to determine the outlet temperature of steam, the shortcut model of heat exchanger was tested, and it was identified that the outlet temperature of steam is 99.63°C. All of the detailed calculations are presented in the Excel sheet.

Table 3.2.1. Information about stream results of the H-102 heat exchanger

Location	Inner tube	Annular space
Chemical composition	H_2O / steam	CH_3OH
Inlet temperature, °C	102.00	26.42
Outlet temperature, °C	99.63	70.00
Inlet pressure, bar	1.00	11.00
Outlet pressure, bar	1.00	11.00

Mass flow rate, kg/s	0.033	0.549

The next step in designing is to choose appropriate equipment sizing based on the standard reference data [37]. For this heat exchanger in order to satisfy parameters such as velocity, pressure drop, and overall heat transfer coefficient the following sizings were selected, as shown in Table 3.2.2.

Table 3.2.2. Basic geometry for H-102 unit

Parameters	**D_i**	**D_o**	**D_1**	**Length**
Value, m	0.0525	0.0603	0.0779	12.0000

Where, D_i - inside pipe inner diameter, D_o - inside pipe outer diameter, and D_1 - outside pipe inner diameter.

Based on inlet and outlet temperatures presented in Table 3.2.1 the LMTD temperature was calculated using Eq. 3.2.1. After that, based on Stainless steel SCH 40S tubes, the inside and outside diameters of inner pipe, and inside diameter of outside pipe were assumed. Using those diameters, A_f flow area and D_e equivalent diameters were calculated using Eqs. below:

Inner tube:

$$D_e = D_i \tag{3.2.1}$$

$$A_f = \pi D_i^2/4 \tag{3.2.2}$$

Annular space:

$$D_e = D_1 - D_o \tag{3.2.3}$$

$$A_f = \pi(D_1^2 - D_o^2)/4 \tag{3.2.4}$$

After which we find average temperature of inlet and outlet temperature for inner and annular space. Then make appropriate assumptions for film coefficients, after which T_{wall} is calculated using Eq. 3.2.5.

$$T_{wall} = \frac{h_i t_{ave} + h_o T_{ave} D_o/D_i}{h_i + h_o D_o/D_i} \tag{3.2.5}$$

Where, h_i and h_o are assumed film coefficients for inner and annular spaces respectively, t_{ave} and T_{ave} are average temperatures of inner and annular spaces, D_i - inside pipe inner diameter, D_o - inside pipe outer diameter.

The next step is to evaluate fluid properties (steam and methanol) at this wall temperature, specifically, density, viscosity, heat capacity and thermal conductivity.

Velocity, Reynolds number and Prandtl numbers are calculated using equations below:

$$V = \frac{W}{\rho A_f} \tag{3.2.6}$$

$$Re = \frac{D_e V \rho}{\mu} \tag{3.2.7}$$

$$Pr = \frac{C_p \mu}{k} \tag{3.2.8}$$

Where, W - mass flow rate in kg/s, ρ - density in kg/m^3, A_f - flow area in m^2, D_e - equivalent diameter in m, μ - viscosity in kg/m*s, C_p - heat capacity in J/kg*K, and k - thermal conductivity in W/m*K.

Fanning friction factor and Nusselt number are calculated using equations below:

$$f = (0.782\, ln(Re) - 1.51)^{-2} \tag{3.2.9}$$

$$Nu = \frac{(f/8)(Re-1000)Pr(1+D_e/L)^{2/3}}{1+12.7(f/8)^{0.5}(Pr^{2/3}-1)} \tag{3.2.10}$$

It is important to note that, for Equation 3.2.10 for L initially assumed L was used and the actual L is calculated at the end of all calculations.

Fanning friction factor and Nusselt number are calculated only for annular space, specifically for methanol being heater, because in inner tube steam is condensing and its calculations differ from single phase calculations. For annular space, heat transfer coefficient is calculated from Nusselt number using Eq. below:

$$h_o = \frac{Nu*k}{D_e} \tag{3.2.11}$$

Where, h_o- heat transfer coefficient of annular space, Nu-Nusselt number, k - thermal conductivity, D_e - equivalent diameter.

For inner tube, heat transfer for condensation in horizontal tube equation was used:

$$h_m = 0.555\left(\frac{g\rho_l(\rho_l-\rho_v)\lambda k^3}{\mu(T_v-T_w)D}\right)^{0.25} \tag{3.2.12}$$

Where, h_m- heat transfer coefficient for condensation, g - gravitational acceleration, ρ_l and ρ_v density of water and steam, λ - latent heat of vaporization, k_l - thermal conductivity of water, μ - viscosity of steam, T_v - vapor saturation temperature, T_w - wall temperature, D - equivalent diameter.

The next step is to assume a fouling factor for each tube based on used compounds and thermal conductivity of tube material. After obtaining all values overall heat transfer is calculated using Eq. 3.2.13.

$$1/U = \frac{D_o}{h_i D_i} + D_o \frac{ln(\frac{D_o}{D_i})}{2k} + \frac{1}{h_o} + \frac{R_i D_o}{D_i} + R_o \tag{3.2.13}$$

After finding the overall heat transfer calculation, it is possible to calculate heat duty and find the area of the heat exchanger.

$$Q = W_{hot} * \lambda \quad (3.2.14)$$

$$A = \frac{Q}{U*LMTD} \quad (3.2.15)$$

Where, W_{hot} - mass flow rate of steam, λ - latent heat of vaporization, U - overall heat transfer coefficient, LMDT - log mean temperature. From the area of the heat exchanger it is possible to find the actual length of the heat exchanger. Since it is a hairpin double pipe heat exchanger, its length is divided into two equal parts as an actual hairpin.

$$L = \frac{A}{\pi D_0} \quad (3.2.16)$$

$$N_{hairpin} = \frac{L}{2*L_{hairpin}} \quad (3.2.17)$$

Where, $N_{hairpin}$ - number of hairpins required, L - length of heat exchanger, $L_{hairpin}$ - length of hairpin.

Pressure drop calculation

Inner tube - Lockhart-Martinelli Model

This model suggests calculating pressure drop for each phase separately and through this approach find two-phase pressure drop. Initially mass flux was calculated using Eq. below:

$$G = \frac{W}{\pi(D_o)^2/4} \quad (3.2.18)$$

Where G - mass flux, W - mass flow rate of inner tube, D_o - outsider diameter of inner tube.

Then for each vapor and liquid phase, their Reynolds number, friction factor and pressure drop was calculated using equations below:

Liquid phase:

$$Re_l = \frac{GD_o}{\mu_l} \quad (3.2.19)$$

$$f_l = \frac{64}{Re_l} \quad (3.2.20)$$

$$\Delta P_l = f_l \frac{L}{D_o} \frac{G^2}{2\rho_l} \quad (3.2.21)$$

Vapor phase:

$$Re_v = \frac{GD_o}{v} \quad (3.2.22)$$

$$f_v = 0.079 Re_v^{-0.25} \quad (3.2.23)$$

$$\Delta P_v = f_v \frac{L}{D_o} \frac{G^2}{2\rho_v} \quad (3.2.24)$$

Then compute Lockhart-Martinelli Parameter (X):

$$X = \sqrt{\frac{\Delta P_l}{\Delta P_v}} \quad (3.2.25)$$

Determine Two-Phase Multiplier:

$$\phi_v^2 = 1 + 20/X + 1/X^2 \quad (3.2.26)$$

$$\Delta P_{two-phase} = \phi_v^2 * \Delta P_v \quad (3.2.27)$$

Where, $\Delta P_{two-phase}$ is the total pressure drop of the inner tube side in Pa.

Annular Space - Darcy-Weisbach approach with Hydraulic Diameter

Initially hydraulic diameter is calculated using Eq. below:

$$D_h = D_1 - D_o \quad (3.2.28)$$

Then calculate friction factor using Equation 3.2.19. and pressure drop is calculated using Equation below:

$$\Delta P = f \frac{L}{D_h} \frac{\rho_l V^2}{2} \quad (3.2.29)$$

Where, f - friction factor, D_h - hydraulic diameter, ρ_l- density of methanol, V - velocity of methanol.

All necessary calculations are presented in "Group 6, H102" Excel sheet in ESI.

Table 3.2.3. Geometry of H-102 heat exchanger

Schematic representation of H-102	
Type	Hairpin double pipe heat exchanger
Inner tube inner diameter, mm	52.5
Inner tube outer diameter, mm	60.33
Outside tube inner diameter,mm	77.92
Length, m	12

Length of hairpin, m	6
Number of hairpins	1
Area, m^2	2.27
Type of material	Stainless steel SS316
Cost (Aspen), $	6 428

Selection of material is based on the recommendations related to the feed composition, mechanical properties, and average material cost. Considering highly corrosive feed composition, it was decided to choose SS316, which is good for long-term reliability [38].

In Appendix C.1 it can be seen as a typical design of a double pipe heat exchanger. It is U-shaped and looks like a hairpin, in the Appendix is shown 1 hairpin.

3.3. PFR Reactor R-101

For the MTBE production process, a multitubular isothermal Plug Flow Reactor equipped with a cooling system using water was selected to manage the exothermic reaction between methanol and isobutylene. The multitubular design ensures efficient heat removal, preventing temperature fluctuations that could affect the catalyst activity or lead to undesirable side reactions. The isothermal operation enhances the reaction rate, providing a consistent environment for high conversion and selectivity towards MTBE. The use of water as a coolant helps maintain the optimal temperature, ensuring that the reaction conditions remain stable throughout the process and promoting maximum yield while reducing the formation of byproducts.

3.3.1. Review of Different Reactor Types

In the production of MTBE via the reaction between methanol and isobutylene, several reactor types were considered for their effectiveness and efficiency. The two main options were the Reactive Distillation (RD) reactor and the Plug Flow Reactor (PFR). Reactive Distillation offers several advantages, including simultaneous reaction and separation, leading to higher conversion rates and better control over the reaction equilibrium. However, it also comes with limitations, such as issues with large flow rates, liquid distribution, and residence time that could complicate the scale-up process [39]. Despite these benefits, the complexity and operational challenges of RD, especially when scaling up for large production capacities, led us to favor the PFR reactor for this project.

The PFR reactor offers a simpler, more controllable operation for continuous production, particularly in high-temperature and exothermic reactions like MTBE synthesis. Given the need for isothermic conditions to maintain optimal reaction rates and the robust temperature control offered by multitubular designs with water cooling, the PFR was chosen as the ideal reactor for our process. Additionally, the ease of temperature management, combined with the fact that we

could meet the required conversion levels through reactor volume and catalyst adjustments, makes the PFR a more reliable choice for consistent, large-scale MTBE production.

3.3.2. The Working Principle of Reactor

Mixed methanol and isobutylene are fed into the reactor. Both methanol and isobutylene are brought to the temperature of $70^{\circ}C$ and the pressure of around 11 bar. Under these conditions both of the reactants enter the reactor in the liquid phase. The reaction is facilitated with the help of an acid resin catalyst, Amberlyst-15. The primary reaction produces MTBE, with a minor by-product of diisobutene (DIB). The reactants are continuously consumed, and the product stream, containing MTBE, unreacted methanol, and isobutylene, exits the reactor. The unreacted components are then separated in downstream processes, ensuring maximum yield of MTBE. Table 3.3.1. contains three reactions taking place in the reactor.

Table 3.3.1. Main and side reactions

	Reaction	Product	Type of reaction
1	$CH_3OH + (CH_3)_2C = CH_2 \leftrightarrow (CH_3)_3COCH_3$	MTBE	main
2	$(CH_3)_3CCH_2C(CH_3) = CH_2 \leftrightarrow C_4H_8$	DIB	side
3	$(CH_3)_3CCH = C(CH_3)_2 \leftrightarrow C_4H_8$	DIB	side

As the reactants flow through the reactor in a plug flow pattern, the reaction proceeds according to the Langmuir-Hinshelwood-Hougen-Watson (LHHW) kinetic model adapted from Zhang et al., which describes the adsorption and surface reaction between methanol and isobutylene on the catalyst [31]. As it is an exothermic reaction the temperature of the product stream increases, which is an undesirable condition. Because of this, there is a necessity in the cooling system. Consequently, along with the overall reactor design, we performed the cooling system design using shell and tube heat exchanger specifications. The working principle of cooling is similar to that of heat exchanger indicated in section 3.1 without the condensation part. The inlet stream of excess methanol and isobutylene goes through the tube side, while the coolant fluid, water, circulates in the shell side to maintain the desired isothermal conditions.

3.3.3. Reactor Design Equations

Initially, it was necessary to determine the required volume of the reactor. For that it was required to find the volume of catalyst that will be used. To determine the weight of the catalyst, the Aspen Plus V14 simulation with specified kinetics and conversion reaching the maximum of 87.54% was used. The catalyst loading then was found to be 160 kg. The volume of the catalyst load was calculated using the bulk density of Amberlyst-15, which relates to bed voidage as shown in following equation:

$$V_{cat} = \frac{W_{cat}}{\rho_{part}(1-\epsilon)} \quad (3.3.1)$$

where W_{cat} is the catalyst weight, ρ_{part} is the particle density of the catalyst (1010 kg/m^3), and ϵ is the bed voidage (0.32). The catalyst volume was calculated to be 0.233 m^3.

To find out the required volume of the reactor, it is necessary to add 15% clearance to the volume of the catalyst. The equation is presented below.

$$V_r = 1.15 \times V_{cat} \quad (3.3.2)$$

By applying all formulas above and accounting for the volume of the catalyst bed, the required volume of reactor was determined to be 0.268 m^3.

316 stainless steel was chosen for the MTBE reactor due to its excellent resistance to corrosion, especially under the high temperatures (70°C) and pressures (11 bar). The reactor's content of methanol and isobutylene, can cause pitting and crevice corrosion, which SS316 resists due to its molybdenum content [40]. Additionally, the material's strength and resistance to stress corrosion cracking make it ideal for the water cooling system, which involves thermal cycling [41]. SS316 ensures durability and long-term reliability, minimizing maintenance and material degradation in the harsh reactor conditions.

3.3.4. Cooling System Design

Firstly, it was decided that cooling water temperature for the multitubular PFR will be supplied at 28°C because it strikes a practical balance for the MTBE reaction. The reaction runs at 70°C, and a 28°C inlet temperature provides enough of a temperature difference to effectively remove heat without overcooling the system. If the water temperature is lower, it might cool the reactor too much, slowing the reaction rate or requiring more energy to maintain the 70°C. The information about inlet and outlet streams are presented in Table 3.3.2.

Table 3.3.2. Information about stream results of the R-101

Location	**Tube side**	**Shell side**
Chemical composition	mixture of MEOH and IB	H_2O
Inlet temperature, ℃	70.00	28.00
Outlet temperature, ℃	70.00	45.54
Inlet pressure, bar	11.00	1.00
Outlet pressure, bar	10.24	1.00
Mass flow rate, kg/h	5627.44	30000.00

Total heat exchanged, kW	609.36	
Fouling resistance, m^2 ℃/W	0.00020	0.00017

Afterwards, to design the cooling system, shell and tube heat exchanger design specifications were used. Therefore, it was necessary to calculate sizing of the shell and choose the appropriate dimensions of the tube that would satisfy both volume requirement of the reactor and standard dimensions of TEMA (Tubular Exchanger Manufacturers Association) shown in Table B.3 in Appendix B. These dimensions were selected to optimize reactor performance while maintaining manufacturing and operational costs. The design specifications are presented in Table 3.3.3.

Table 3.3.3. Specification Sheet for R-101

Operating Conditions			
Temperature, °C		70.00	
Pressure, bar		11.00	
Isobutylene conversion, %		87.54	
Type and Sizing			
Type of Reactor	Multitubular isothermal plug flow reactor	**Number of Tubes**	195.00
Material	SS316	**Residence Time, s**	105.25
Orientation	Horizontal	**Volume of the Reactor, m^3**	0.28
Catalyst Type	Amberlyst-15	**Baffle cut, %**	35.00
Catalyst Loading, kg	160.00	**Tube passes**	6.00
Tube length, m	4.88	**Tube pattern**	90° square pattern
Outer Diameter of Tube, mm	25.00	**Shell passes**	1
Inner Diameter of Tube, mm	19.40	**Shell i.d., mm**	654.91
Effective area, m^2	75.25	**Bundle diameter, mm**	641.91
Schematic Diagram			

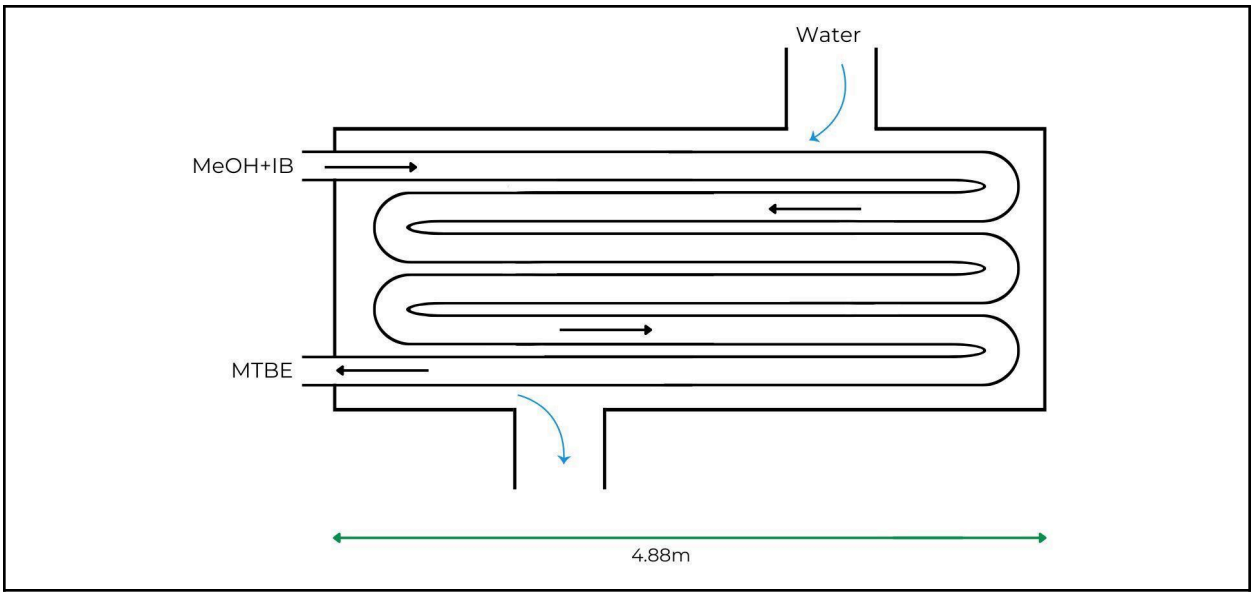

The length of 4.88 m is one of the commonly used tube lengths for heat exchangers. This length allows for efficient heat transfer and reaction time in the process. While shorter tubes would decrease pressure drop and pump work, the velocity of the streams in the tubes and shells would be significantly lower than the required velocity of 0.3 m/s. The outer diameter of 25 mm was chosen because it is a standard size commonly used in the industry for steel tubes. This diameter ensures a good balance between heat exchange efficiency and the structural integrity of the reactor [36]. The thickness of the tube wall, 2.8 mm, provides sufficient strength to withstand the internal pressures of the reactor and prevent deformation or failure.

The calculations to determine the shell diameter were made according to the heat exchanger calculations used in section 3.1. Calculations are presented in the Excel sheet (R-101) in ESI. The number of tubes was calculated using the ratio of the total heat transfer area required and the external surface area of a single tube. Therefore, the required number of tubes in the reactor unit is 196.

To determine heat transfer coefficient section 3.1 applied equations that are applicable for condensers. However, for general heat exchangers formulas vary. For both shell and tube side heat transfer coefficients were determined using the equation below.

$$\frac{h_i d_i}{k_f} = j_h RePr^{0.33}\left(\frac{\mu}{\mu_w}\right)^{0.14} \tag{3.3.3}$$

, where h_i is the heat transfer coefficient for the shell side, j_h is the heat transfer factor, μ_w and μ are viscosity of the fluid at wall temperature and at average tube side temperature. Viscosity correction was neglected. k_f is the thermal conductivity value and d_i is the inside tube diameter.

To find the Prandtl number, Pr, the equation below was applied.

$$Pr = \frac{C_p \mu}{k_f} \tag{3.3.4}$$

, where C_p is heat capacity. Other equations were the same as in the section for the heat exchanger.

In a multitubular reactor, turbulence minimizes back-mixing, which is essential for achieving high conversion and selectivity in reactions like those catalyzed by Amberlyst-15. For the heat exchanger design, turbulent flow on both the tube side (reaction fluid) and shell side (cooling water) increases the convective heat transfer coefficient, improving the removal of exothermic heat and preventing hotspots, thus maintaining stable operating conditions and optimizing the overall performance of the system.

Finally, to check whether selected design specifications are appropriate, pressure drop for both shell and tube sides were calculated. The shell side pressure drop was determined to be 0.36 Pa applying formula (3.1.26). The pressure drop of 0.80 bar for the tube side was calculated using expression (3.1.26), which ensures good contact between the fluid and catalyst for effective heat transfer and reaction, without overburdening the pumping system. As the next unit operates at 5.5 bar, the pressure drop in tubes is considered adequate and does not intervene with the following processes.

3.3.5. R-101 Unit Residence Time

Using the dimensions of the reactor tubes (length of 4.88 m and inner diameter of 19.4 mm), the volume of the reactor was calculated by determining the volume of each tube and multiplying it by the number of tubes. This calculation resulted in a total reactor volume of 0.281 m^3 which is slightly larger than the volume obtained from the catalyst weight and kinetics, as determined using Aspen Plus V14, accounting for the unloaded space in the reactor.

The residence time was calculated using the following expression:

$$\tau = \frac{V}{Q} \tag{3.3.5}$$

, where Q is the volumetric flow rate of the fluid. The residence time according to hand calculations is 110.58 s. The residence time obtained using Aspen Plus V14 is 105.25 s.

LHSV (Liquid Hourly Space Velocity) is an important parameter in reactor design which indicates how fast the reactants pass through the catalyst bed. It is defined by the following equation:

$$LHSV = \frac{Q}{V_{cat}} \tag{3.3.6}$$

The LHSV was calculated to be 39.33 h^{-1}. According to the DuPont datasheet [42], Amberlyst-15 typically operates within a space velocity 0.5 – 5 h^{-1}, so the calculated LHSV is above the recommended range. However, this is not a limitation for our design since conversion is primarily governed by the WHSV (Weight Hourly Space Velocity) as used in the LHHW kinetic model from Zhang et al. [31]. WHSV is calculated as:

$$WHSV = \frac{W_{feed}}{W_{cat}} \tag{3.3.7}$$

The calculated WHSV is 35.17h^{-1}. At 343K, the corresponding WHSV, the conversion reaches above 85%, which is consistent with Aspen Plus V14 result of 87.54%. Thus, despite high LHSV, our reactor operates realistically within the kinetic and thermal limits, and achieves the desired conversion.

3.4. MTBE Distillation Column T-101

The purpose of distillation column T-101 is to refine the MTBE from reactor products passed through depressurizing valve V-101. The feed conditions are adjusted to facilitate MTBE separation, with a temperature of 70.09°C and pressure of 5.8 bar. The column currently is designed to yield 98.426 wt% of MTBE with 0.013 wt% methanol, 0.002 wt% isobuthylene (IB) and 0.001 wt% water impurity at the bottom product. Distillate product is subject to further stripping and recovery in columns T-102 and T-103.

3.4.1. Working Principle

This distillation column functions based on the differences in relative volatilities of key feed components. The heavy key (HK) component, MTBE, is collected at the bottom, while the lighter, more volatile components, known as the light key (LK), are extracted as distillate. The reboiler heats the feed to just below the HK's boiling point at operating pressure, ensuring that volatile components transition into the vapor phase. A pressure drop occurs along the column from the reboiler to the condenser. As vapor rises through the packed sections, it interacts with the descending liquid feed in the rectifier section, establishing dynamic equilibrium [43]. This interaction enables volatile components to transition into the vapor phase while non-volatile components remain in the liquid phase. When designing this distillation column, it is important to consider the partial condenser, which condenses only a portion of the vapor, returning the liquid fraction as reflux while allowing the remaining uncondensed vapor to exit as the overhead product. This reflux improves separation efficiency, enabling the production of high-purity MTBE (>98 wt%) as the bottom product. Therefore, the separation process is optimized by controlling the reboiler and condenser temperatures, pressure drop, number of column stages, and reflux ratio to achieve efficient MTBE separation.

3.4.2. Relative Volatility of Components

The design of the distillation column begins with determining the saturation pressure for feed components in order to obtain their relative volatilities. Commonly used approach includes calculation of saturation pressure at reboiler and condenser temperatures via 3-coefficient Antoine equation as follows [43]:

$$P_{sat} = 10^{\left(A-\frac{B}{T+C}\right)} \tag{3.4.1}$$

Here, P_{sat} represents pressure in kPa, T is temperature in degrees Celsius and A, B and C are Antoine coefficients for kPa-Celsius dimensions (see Appendix D, Table D.1 for details). Consequently, relation of P_{sat} of lighter component i to P_{sat} of heavier component k provides relative volatility α_{ik} of component i with respect to component k as follows:

$$\alpha_{ik} = \frac{P_{sat,i}}{P_{sat,k}} \quad (3.4.2)$$

In order to account for relative volatility at every stage of the distillation column, a geometric mean of relative volatilities at reboiler (115.90 ℃, DSTWU-basis) and condenser (70.80 ℃, DSTWU-basis) temperatures are calculated. Table 3.4.1 provides final calculation results for T-101:

Table 3.4.1. P_{sat} and α_{ik} for column T-101 feed components

Component	Reboiler		Condenser		Geometric mean of relative volatilities
	Psat, kPa	α_{ik}	Psat, kPa	α_{ik}	
MTBE	3163.385	1.000	1172.647	1.000	1.000
Water	1309.489	0.414	241.378	0.206	0.292
MEOH	4294.599	1.358	969.149	0.826	1.059
IB	17674.509	5.587	7429.358	6.336	5.949

3.4.3. T-101 Column Theory

Theoretical layout of the distillation column is computed using a set of correlations from Fenske-Underwood-Gilliland-Kirkbridge (FUGK) method. Two-component Fenske equation was employed to calculate the theoretical minimum number of stages as follows [44]:

$$N_{min} = \frac{ln[\frac{(f_{i,D} \cdot f_{k,B})}{((1-f_{i,D})(1-f_{k,B}))}]}{ln(\alpha_{i,k})} \quad (3.4.3)$$

Here, N_{min} stands for minimum stages of distillation column; $f_{i,D}$ is for mole-fraction of LK component i in distillate; $f_{k,B}$ is for mole-fraction of HK component k in bottom product; α_{ik} is relative volatility of component i with respect to component k.

Afterwards, Underwood equations are used to determine the θ value and minimum reflux ratio. The q value is calculated from the enthalpy of flows (Eq. 3.4.4) and determined to be -0.53 for feed temperature of 70.09°C and pressure of 5.8 bar. Then, the θ value is obtained using the goal seek approach in Excel based on the Eq. 3.4.5. The reflux ratio is considered as 1.5 of a minimum reflux ratio of 8.03 calculated by the Eq. 3.4.6.

$$\frac{-h_f + h_l}{h_{ol} - h_{ov}} = q \quad (3.4.4)$$

Here, h_f and h_l is the enthalpy of feed and bottom product, respectively, while h_{ol} and h_{ov} are related to the enthalpy of distillate under total and partial condensation, considerably.

$$\sum \frac{\alpha_i x_{i,f}}{\alpha_i - \theta} = 1 - q \tag{3.4.5}$$

In this formula, α_i refers to the relative volatility of LK with respect to HK component; $x_{i,f}$ is mole-fraction of LK in the feed; θ value is correlation parameter; q is the quality of feed stream.

For simplicity, single θ value instead of component-bound is used to determine the minimum reflux ratio as follows:

$$\sum \frac{\alpha_i x_{i,D}}{\alpha_i - \theta} = R_{min} + 1 \tag{3.4.6}$$

Here, $x_{i,f}$ is mole-fraction of LK in the distillate; R_{min} is minimum reflux ratio.

According to Gilliland's correlation, the number of actual stages depends on the calculated minimum reflux ratio, reflux ratio and minimum required stages, it would require the general model to be tested over the range of reflux ratios. Through Aspen Plus V14 simulations 2.837 proved to be enough. In this work a subdivision form of Gilliland's correlation into X and Y terms is employed as follows:

$$Y = \frac{(N - N_{min})}{(N+1)};\ X = \frac{(R - R_{min})}{(R+1)};\ Y = 1 - exp\left[\frac{(1+54.4X)\cdot(X-1)}{(11+117.2X)\cdot\sqrt{X}}\right] \tag{3.4.7}$$

Here, N is the number of actual stages, N_{min} is the minimum required stages, R_{min} is the minimum reflux ratio, and R is the reflux ratio.

The theoretical values for N and N_f were determined to be 5.19 and 2.87, respectively, but through sensitivity analysis, 10 stages in total and the 5th feed stage are considered for more effective distillation. Also, considering the distillate rate of 12.09 kmol/hr in the DSTWU unit, the simulated rate-based Radfrac unit has a slightly higher rate of distillate leave of 12.8 kmol/hr due to the requirement of getting a high purity product. Pressure throughout the packed column is dropping by 0.03 bar from 5.5 bar in the condenser. Referring to Appendix D, Figure D.4 presents the pressure profile in the distillation column, whereas the temperature profile and composition profiles are given in Figure D.2 and D.3 in Appendix D, respectively.

Kirkbridge equation is used to calculate the ratio of stripping and rectifying regions as follows:

$$\frac{N_R}{N_S} = \left[\frac{[B]}{[D]} \cdot \frac{x_{i,f}}{x_{k,f}} \cdot \left(\frac{x_{i,b}}{x_{k,d}}\right)^2\right]^{0.206} \tag{3.4.8}$$

Here, N_R stands for rectifying stages (above the feed stage); N_S stands for stripping stages (below the feed stage); [B] is mole-flow rate of reboiler stream; [D] is the mole-flow rate of condenser stream; $x_{i,f}$ is mole-fraction of LK component in feed stream; $x_{k,f}$ is mole-fraction of HK component in feed stream; $x_{i,b}$ is mole-fraction of LK component in bottom flow; $x_{k,d}$ is mole-fraction of HK component in distillate flow.

3.4.4. T-101 Column Internals

In order to have a physical representation of the distillation column, it is necessary to model its internals. Overall, the column is represented by a single section between condenser and reboiler. Internal packing was chosen to be Sulzer MELLAPAK 250X sized packing for accounting and practical efficiency purposes [45]. Height of the packed section is 9.0 m (same as in theory), and the simulated diameter is 0.40 and 0.57 meters of rectifying and stripping sections, correspondingly. It exceeds the theoretically calculated one of 0.2144 m in order to prevent flooding.

In order to determine theoretically required column diameter, it is necessary to perform a series of calculations starting from the identification of flood pressure using following formula:

$$\Delta P_{flood} = 0.115 \cdot F_P^{0.7} \tag{3.4.9}$$

Here, ΔP_{flood} is flood pressure and F_P is packing factor (value is vendor-specific, provided in Table 3.4.2).

Table 3.4.2. Mellapak packing parameters

Structured Packing	**Material**	**Size**	**F_P, ft²/ft³**	**a, m²/m³**	**ε, m²/m³**
Mellapak	Stainless steel	250X	8.00	25.00	0.98

Second parameter needed is a flow parameter, defined as ratio between kinetic energies of liquid and vapor phase:

$$F_{LV} = \left(\frac{\dot{M}_L}{\dot{M}_V}\right) \cdot \left(\frac{\rho_V}{\rho_L}\right)^{0.5} \tag{3.4.10}$$

, where F_{LV} is the flow parameter; $\dot{M}_L$ is mass flow rate of liquid phase; $\dot{M}_V$ is mass flow rate of vapor phase; ρ_V is mass density of vapor phase; and ρ_L is mass density of liquid phase.

Calculated flood pressure and flow parameter are used in Sherwood-Eckert generalized pressure-drop correlation (GPDC) graph for structured packing. See Figure D.1 in Appendix D for details.

From the GPDC it is possible to obtain the empirical capacity factor that is later used to determine the superficial vapor velocity or estimated flooding velocity as follows:

$$u_{Vf} = \frac{F_C}{F_P^{0.5} \cdot \left(\frac{\rho_V}{\rho_L - \rho_V}\right)^{0.5} \cdot v_L^{0.05}} \tag{3.4.11}$$

,where u_{Vf} is superficial vapor velocity; F_C is empirical capacity factor; and v_L is kinematic viscosity of liquid phase.

Finally, obtained value can be used to determine the inside diameter of the packed tower as follows:

$$D_T = \left[\frac{4 \cdot \dot{M}_V}{f \cdot u_{Vf} \cdot \pi \cdot \rho_V}\right]^{0.5} \quad (3.4.12)$$

, here, D_T is packed tower internal diameter; and f is fraction of flooding (assumed as 0.5).

Subsequently, height of the packing column is based on packed-height equivalent to a theoretical stage (HETP), which is provided by Sulzer booklet [46].

3.4.5. T-101 Column Externals and Capital Cost

In order to have complete understanding of what unit is needed for the MTBE process, it is important to account for T-101 distillation column external dimensions and capital cost. This is done with pipe thickness equation as follows:

$$t_w = \frac{P_i \times D_i}{2 \times S \times E - P_i} \quad (3.4.13)$$

,where t_w is wall thickness; P_i is internal pressure; D_i is internal diameter; S is maximum allowable stress [47]; E is welded-joint efficiency, 1 for seamless pipe [47].

Subsequently, knowing the wall thickness it is possible to determine the shell mass as follows:

$$m_{shell} = \pi \cdot D_c \cdot L_c \cdot t_w \cdot \rho \quad (3.4.14)$$

,where D_c is column diameter; L_c is column length; ρ is material metal density.

The overall column length is determined by rule of thumb as adding 1.2 m for the condenser on the top and 1.8 m on the bottom for the reboiler [45]. So, having packing section length as 9.0 m, total distillation column length will be 12.0 m.

After that the capital cost of the unit could be calculated as follows [48]:

$$C_e = a + b \cdot S^n \quad (3.4.15)$$

Here, C_e is purchased equipment cost on a U.S. Gulf Coast basis for Jan. 2010; a, b are cost constants; S is size parameter in unit-bound units; n is sizing exponent for unit in question.

However, since the plant is being built in Kazakhstan in the 2020s, corrections need to be made [49]. For this purpose a CEPCI formula is used as follows:

$$C_f = C_e \times F_{location} \times \frac{CEPCI(2024)}{CEPCI\ (2020)} \quad (3.4.16)$$

Here, C_f is the final cost; $F_{location}$ is location factor (1.53 for Russia, assumed for Kazakhstan), CEPCI(year) is CEPCI at specific year. It is recommended to use the indexes 5 years apart [48].

Direct cost for the distillation column is not provided, instead it is advised to derive it component-wise [49]. For the case of T-101, kettle reboiler, condenser heat exchanger, pressure vessel and packing of 304 stainless steel (304 SS) are assumed to be major components of the distillation column. Theoretically, such a column would cost $165271 USD. However, due to its

practically larger diameter, the new cost is $193909 USD. Detailed calculations of capital cost are accessible in the “MTBE Distillation Cost” Excel file in ESI.

Table 3.4.3. T-101 column specification sheet

Unit	**T-101**	**Schematic Diagram**	
Height, m	12.00	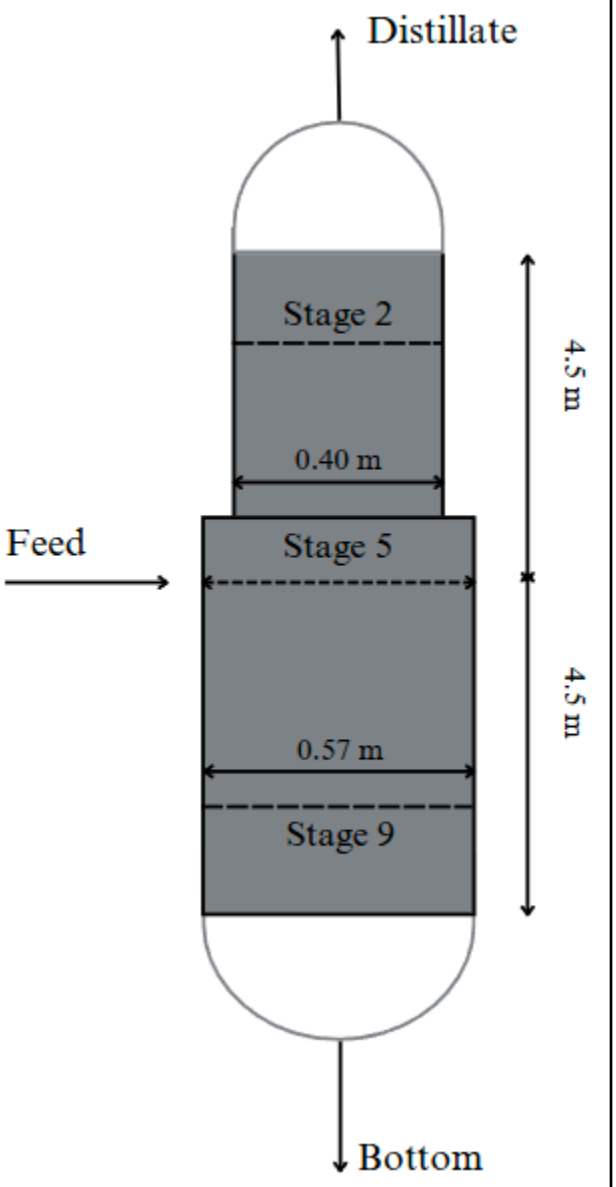	
Stages (Total/Feed)	10/5		
Reflux Ratio	2.84		
Inlet Conditions			
Temperature, ℃	70.09		
Pressure, bar	5.80		
Reboiler Conditions			
Type	Kettle		
Temperature, ℃	116.77		
Pressure, bar	5.77		
Condenser Conditions			
Type	Total		
Temperature, ℃	76.82		
Pressure, bar	5.50		
Mass Flow, kg/hr		**Internal design**	
Feed	5627.44	**Section**	CS-1
Distillate	742.11	**Packing type**	Sulzer Mellapak

Bottoms	4885.33	**Packing spacing, m**	9
Material	Stainless steel type 304	**Average Column Diameter, m**	0.48

3.5. T-102 Absorption Column

After T-101, the overhead stream containing methanol, water, isobutene, and trace amounts of MTBE is directed to the absorption column T-102. In this unit, water is used as the absorbent to recover methanol from the gas phase. The process enables selective absorption of methanol into the liquid phase while allowing unabsorbed hydrocarbons to exit the system. The top product consists mainly of isobutene and minor MTBE traces, while the bottom stream contains methanol-rich water.

3.5.1. T-102 Absorption Column Working Principle

Gas absorption is a process used to remove specific components from a gas or liquid mixture by dissolving them into a suitable liquid. This process involves the transfer of a solute between the gas and liquid phases when they come into close contact, eventually reaching equilibrium [50].

The primary objectives of gas absorption include separating components with economic value, serving as an intermediate step in the production of certain compounds, and eliminating unwanted components, such as pollutants. There are two main types of absorption: physical and chemical [50]. Physical absorption occurs when mass transfer takes place purely through diffusion, with the process governed by physical equilibrium. In contrast, chemical absorption involves a chemical reaction between the absorbed component and the liquid upon contact.

Various types of equipment are used in chemical industries for gas absorption, including packed columns, plate columns, centrifugal contactors, and bubble columns. These absorbers facilitate efficient mass transfer between phases, making them essential in industrial applications.

T-102 was designed as a packed random absorber due to the low gas flow rates and high liquid flow rates, making packed columns the optimal choice. Packed columns efficiently handle liquid absorption while maintaining a low pressure drop. Additionally, packed columns are better suited for foaming systems, provide cost-effective corrosion resistance, and offer simplified design and maintenance compared to plate columns. These factors collectively make the packed random absorber the ideal choice for methanol recovery in T-102.

3.5.2. Selection of Packing

For the methanol-water absorption column in the MTBE production process, 25 mm Pall Rings have been selected due to their superior performance characteristics. Pall Rings offer an open structure, which enhances gas-liquid contact by providing a large surface area, ensuring efficient mass transfer between phases. Their low pressure drop minimizes energy consumption, making them ideal for systems where pressure loss must be controlled. Additionally, Pall Rings have a high flooding point, allowing the column to handle variations in flow rates without

significant operational disruptions. Their high void fraction and large flow passages improve liquid distribution and reduce channeling, which is crucial for maintaining uniform absorption efficiency. Furthermore, Pall Rings are corrosion-resistant and lightweight, making them well-suited for methanol-water absorption. Given these advantages, 25 mm Pall Rings are an optimal choice for achieving effective and economical operation of the absorber.

3.5.3. Calculation of Design Parameters

The equilibrium line used in the absorber design was obtained using Aspen Plus by simulating the vapor–liquid equilibrium (VLE) behavior of the methanol–water system. Based on the simulation results, a linear approximation of the equilibrium relationship was derived in the form:

$$y^* = mx \tag{3.5.1}$$

where, y^* mole fraction of methanol in the gas phase at equilibrium, x mole fraction of methanol in the liquid phase, m -equilibrium line slope, and the calculated slope of the equilibrium line is 1.82.

For a dilute absorber with negligible heat of absorption and isothermal operation, the energy balance is automatically satisfied, allowing us to assume constant L and V. This ensures a straight operating line in the McCabe-Thiele diagram.

Applying a mass balance around the top of the column and assuming L and V are constant, we can write the solute B mass balance for constant L and V.

$$y_{j+1}V + x_0L = y_1V + x_jL \tag{3.5.2}$$

This linear equation defines the relationship between gas and liquid phase concentrations, forming the operating line for absorption.

To determine the number of equilibrium stages in the absorption column, the Kremsner and Eckert equation is used [51]. This equation accounts for the logarithmic mean driving force for mass transfer and is applicable under the assumption of a constant L/V ratio. It is given as:

$$N = \frac{ln(\frac{y_{N+1}-y^*_{N+1}}{y_1-y^*_1})}{ln(\frac{L}{mV})} \tag{3.5.3}$$

, where N is the number of equilibrium stages, m is the equilibrium slope, L and V are the liquid and vapor molar flow rates,

$$y^*_{N+1} = mx_N + b \text{ and } y^*_1 = mx_0 + b \tag{3.5.4}$$

Table 3.5.1.The values of the adsorption equilibria

Operating line			
L	V	Slope	Intercept

25.89	12.8	2.02	0.003
N		19.00	

Based on the given equilibrium and operating line data, the number of theoretical stages required for the absorption process is **19.**

3.5.4. T-102 Absorption Column Sizing

The capacity of a packed column depends on its cross-sectional area, with design typically aiming for the highest economical pressure drop to ensure proper liquid and gas distribution. For the packed column design, a pressure drop of 20 mm water per meter of packing height was assumed. Figure E.1 in Appendix E correlates liquid and vapor flow rates, system physical properties, and packing characteristics using the gas mass flow rate per unit column cross-sectional area, with lines representing constant pressure drop as a parameter. The flow factor F_{LV} provided in Figure E.1 in Appendix E covers a range that generally ensures satisfactory column performance [52].

$$F_{LV} = \frac{L}{V}\sqrt{\frac{\rho_v}{\rho_L}} \tag{3.5.5}$$

Gas mass flow rate per unit column cross-sectional area can be calculated as follows:

$$V_w = \left[\frac{K_4 \rho_v (\rho_L - \rho_v)}{13.1 F_p \left(\frac{\mu_L}{\rho_L}\right)^{0.1}}\right]^{1/2} \tag{3.5.6}$$

, where F_p is the packing factor that depends on the size and type of packing, μ_L is the liquid viscosity, and ρ_L and ρ_v are the liquid and vapor densities, respectively.

For the design of the packed column, the correlation for organic and hydrocarbon systems with low surface tension (< 25 mN/m) was applied. Given a packing diameter of $D_p = 25mm$, the height equivalent to a theoretical plate (HETP) was estimated using the relationship[52]:

$$HETP \simeq 18 D_p \tag{3.5.7}$$

Table 3.5.2. Specification table for T-102

Process data			
Gas flow rate, kg/h		**Liquid flow rate, kg/h**	
in	**out**	**in**	**out**
742.109	696.019	466.443	512.532

Column sizing	
Diameter,m	0.37
Height,m	9.00
HETP, m	0.45
Packing parameter	
Name	Pall rings
Type	Random
Size of packing,mm	25.00
Material of packing	Metal
Construction material	SS304
Shell thickness,mm	1.23
Cost, $	46 196
Operating conditions	
Temperature, ℃	50.00
Pressure, bar	1.00

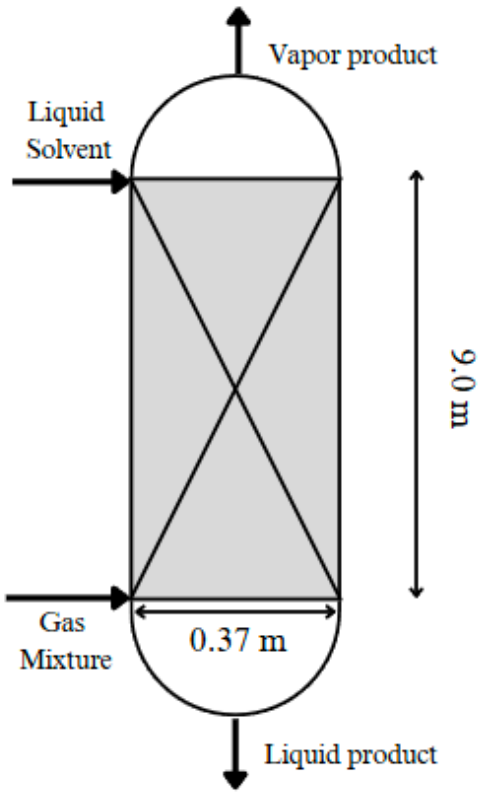

The shell thickness was determined for 304 SS using the given equation. The resulting shell thickness was found to be approximately 1.23 mm. The temperature profile (Figure E.2) given in the Appendix E. All hand calculations given in ESI Absorber excel sheet.

The calculated absorber diameter of 0.58 m closely aligns with the Aspen Plus V14 simulation results, which yielded a diameter of 0.37 m. However, the simulated diameter is higher than the theoretical one due to higher efficiency of methanol absorption found through sensitivity analysis. Also, the slight variation between these values can be attributed to differences in software-specific empirical correlations, numerical approximations, and assumed boundary conditions. Nevertheless, the strong agreement between the results validates the design methodology and the accuracy of the applied calculations.

3.6. Methanol Distillation Column T-103

The purpose of distillation column T-103 is to separate methanol from water in the bottom product of the T-102 methanol absorption column, facilitating the recycling of methanol back into the system. The feed conditions are directly derived from the T-102 bottom product, with a

temperature of 47.17 °C and pressure of 1 bar. The column is designed to remove local (T-102 bottom product basis) 97.38 wt%, while the remaining MTBE and IB recycles almost completely (>99.99 wt%). At the end of the distillation process in T-103, the resulting 0.45 wt% methanol-water mixture, containing trace amounts of MTBE and other components, is discarded.

3.6.1. Working Principle

This distillation column operates based on the principle of relative volatilities between key components in the feed. The HK component, water, exits the column at the bottom, while the more volatile components are removed as distillate. The basic principle is the same as in the T-101 distillation column, and the only difference between them is the total condenser, where vapours are totally condensed resulting in liquid distillate.

3.6.2. Relative Volatility of Components

The design of the distillation column begins with determining the saturation pressure for feed components in order to obtain their relative volatilities, as it was done in Eq. 3.4.1 and 3.4.2. To account for relative volatility at every stage of the distillation column, a geometric mean of relative volatilities at reboiler (99.00 ℃, DSTWU-basis) and condenser (50.86 ℃, DSTWU-basis) temperatures are calculated. Table 3.6.1 provides final calculation results:

Table 3.6.1. P_{sat} and α_{ik} for column T-103 feed components

Component	**Reboiler**		**Condenser**		**Geometric mean of relative volatilities**
	Psat, kPa	**α_{ik}**	**Psat, kPa**	**α_{ik}**	
MTBE	2264.738	3.088	668.248	6.937	4.629
Water	733.350	1.000	96.328	1.000	1.000
MEOH	2575.896	3.513	432.922	4.494	3.973
IB	13124.059	17.896	4648.852	48.260	29.388

3.6.3. T-103 Column Theory

Theoretical layout of the distillation column is computed using a set of correlations from FUGK method same to the calculation procedure for the T-101 distillation column (Eq. 3.4.3 - 3.4.7). The feed quality q for feed temperature of 43.79°C and pressure of 1 bar is 0.028. Performing the calculations further, the minimum number of stages is computed as 6.994, θ value as 3.469, minimum reflux ratio as 6.118, and the reflux ratio as 9.176. Theoretical values of N and N_f have been determined to be 11.90 and 6.99, while the distillate rate is 2.189 kmol/hr. Further information related to temperature and composition profiles is presented in Appendix F.

3.6.4. T-103 Column Internals and Capital Cost

To physically represent the distillation column, its internals must be modeled. The column is generally depicted as a single section between the condenser and reboiler. Sulzer MELLAPAK 250X packing was selected for its efficiency and practicality, consistent with its use in T-101. The packed section has a height of 11.6 m, exceeding the theoretical value, while the total height of the T-103 column is 14.6 m, according to the thumb rule. Putting all of the calculated values to the Aspen Plus V14 simulated distillation column, the model yields inconclusive results determined by the operating point deviating below the flooding pressure. Therefore the sensitivity analysis was performed and the diameter was adjusted to 0.21 m which prevents the flooding in the column. Regarding the capital cost of T-103 column, it is forecasted to be $166991 USD by Eq. 3.4.12 - 3.4.14, whereas the detailed calculations can be found in the "MeOH Recovery" Excel file in ESI.

3.6.5. T-103 Column Specification Sheet

Table 3.6.2. T-103 column specification sheet

Unit	**T-103**	**Schematic Diagram**

Height, m	14.6	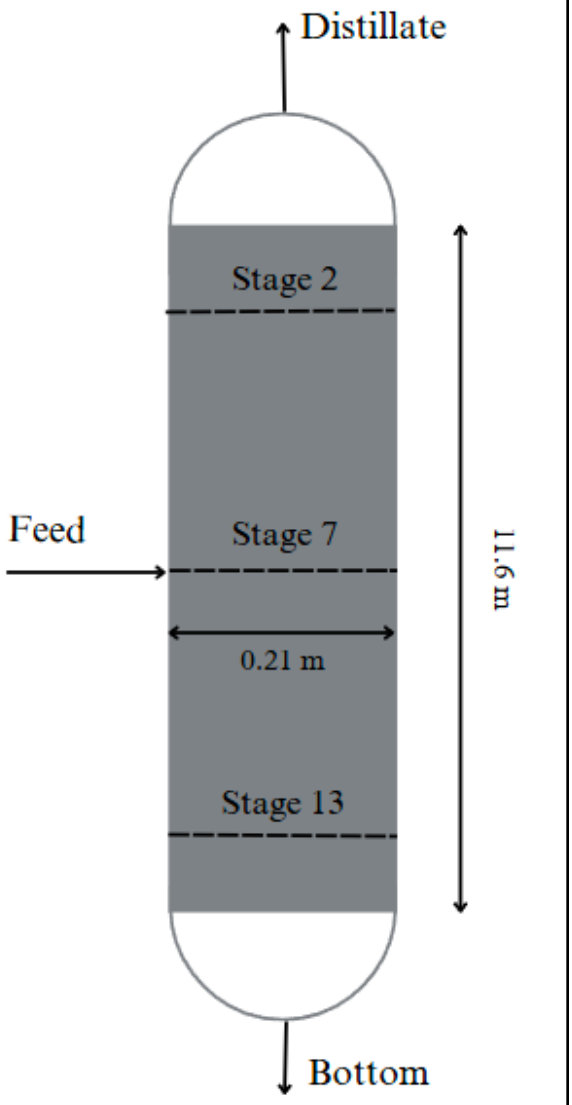	
Stages (Total/Feed)	14/7		
Reflux Ratio	3.16		
Inlet Conditions			
Temperature, ℃	44.15		
Pressure, bar	1.00		
Reboiler Conditions			
Type	Kettle		
Temperature, ℃	99.17		
Pressure, bar	1.00		
Condenser Conditions			
Type	Total		
Temperature, ℃	54.85		
Pressure, bar	1.00		
Mass Flow, kg/hr		**Internal design**	
Feed	512.674	**Section**	CS-1
Distillate	83.141	**Packing type**	Sulzer Mellapak
Bottoms	429.533	**Packing spacing, m**	11.600
Material	Stainless steel type 304	**Column Diameter, m**	0.208

Chapter 4: Minor Equipment Design

4.1. Temperature Changers

It is essential to adjust the process fluid temperatures to the required levels to ensure the main production proceeds efficiently. The heat duty can be calculated using the following formula:

$$Q = mC_p\Delta T \quad (4.1.1)$$

,where Q is a heat duty needed to change a substance's temperature without a phase change, m is the mass flow rate, Cp is the specific heat capacity, and ΔT is the temperature change.

4.1.1. Coolers Design

This process includes 3 coolers, all of them are taken as heat exchangers. H-101 is designed to cool the raw isobutylene stream to meet necessary conditions for the reactor. To reduce temperature in the recycle stream H-106 is used, while H-103 cools down the MTBE product. The heat duty values, along with the corresponding inlet and outlet temperatures for each cooler, are summarized in Table 4.1.1 below.

Table 4.1.1. The design values of the coolers

	H-103	**H-106**
Inlet temperature, ℃	53.76	54.85
Outlet temperature, ℃	25.00	25.00
Heat duty, kW	303.89	2.06

4.1.2. Heaters Design

This process primarily includes heat exchangers H-104 and H-105, whereas H-102 is designed as major equipment. H-104 increases the temperature of the inlet water before it enters the T-102 absorber, while H-105 heats the methanol-IB gas mixture prior to entering the methanol absorption column. All the details of H-102, which is responsible for methanol heating before the reactor, design are provided above. The heat duty values for heaters, along with its inlet and outlet temperatures, are provided in Table 4.1.2.

Table 4.1.2. The design values of the heaters

	H-104	**H-105**
Inlet temperature, ℃	25.00	34.68
Outlet temperature, ℃	50.00	50.00

Heat duty, kW	13.46	5.10

4.2. Pressure Changers

In this process, pressure-changing units are required to regulate the pressure of liquid and gas phase process streams to meet the operational conditions of downstream equipment.

$$W = V\Delta P \tag{4.2.1}$$

where, W is the power of the pump, V is the volumetric flow rate and ΔP is the change in pressure related to the operating stream.

4.2.1. Gas Phase Pressure Changers Design

To calculate the work can be calculated by:

$$W = \frac{(P_2V_2 - P_1V_1)}{1-\gamma} \tag{4.2.2}$$

, where W is the power of the compressing unit, P_1 and P_2 the pressure at the outlet and inlet of the stream respectively, V_1 and V_2 the outlet and inlet volumetric flow rates respectively, γ is the specific heat ratio of the component to be compressed.

In this process, compression units are required to change the pressure of process gases to meet operational conditions. The system includes two compressors: C-101 and C-102. C-101 is responsible for compressing isobutylene to the necessary pressure for the reactor, ensuring optimal reaction conditions. C-102, on the other hand, is used to expand the gas mixture before it enters the absorption column, allowing for efficient gas-liquid interaction.

Table 4.2.1. The design values of the compressor

	C-101	**C-102**
Inlet pressure, bar	1.00	5.50
Outlet pressure, bar	11.00	1.02
Net work, kW	156.55	-12.21

4.2.2. Liquid Phase Pressure Changers Design

The design includes P-101, V-101, and V-102. P-101 is responsible for increasing the pressure of the methanol liquid stream ensuring it reaches the required pressure for further reaction. On the other hand, V-101 and V-102 function as a pressure-reducing valve, lowering the pressure of the liquid stream after the reactor to match the conditions necessary for the T-101 and decompressing the MTBE product, respectively.

Table 4.2.2. The design values of the pump and valve

	P-101	V-101	V-102
Inlet pressure, bar	1.00	10.24	5.77
Outlet pressure, bar	11.00	5.80	1.00
Net work, kW	2.34	0.00	0.00

4.3. Storage Tanks

In this process, storage tanks are utilized for storing raw materials, final products, and waste streams. Specifically, TK-101 and TK-102 are used to store the feed materials methanol and isobutylene, respectively. Methanol is stored in liquid form at 25 °C in TK-101, while isobutylene is stored as vapor under the same conditions in TK-102. These tanks serve as the initial storage units before the reactants are introduced into the MTBE synthesis process. TK-104 is used for storing the final product, MTBE, as a liquid at 25 °C. It ensures buffer storage before the product is sent to further handling or shipment. TK-105 and TK-106 are designated for storing waste streams: TK-105 handles liquid wastewater at 99.17 °C, and TK-106 stores the MTBE+IB vapor mixture at 55.87 °C. Water is stored in TK-103. The volume of each tank was calculated using the relation:

$$V = Qt \tag{4.3.1}$$

, where V is the required volume, Q is the inlet flow rate, and t is the storage time.

The selection of SS316 stainless steel for the tanks ensures compatibility with chemicals and high corrosion resistance.

Table 4.3.1. Storage tanks design values

Storage tank	**TK-101**	**TK-102**	**TK-103**	**TK-104**	**TK-105**	**TK-106**
Stored material	Methanol	IB	Water	MTBE	Waste water	MTBE+IB
State	Liquid	Vapor	Liquid	Liquid	Liquid	Vapor
Temperature, ℃	25.00	25.00	25.00	25.00	99.17	55.87
Pressure, bar	1.00	1.00	1.00	1.00	1.00	1.00
Flow rate, m3 /year	20932.53	1.38E7	4113.67	57923.99	4102.18	2.9E6
Storage time,	6.00 [53]	0.25[54]	6.00 [55]	12.00 [56]	1.00 [57]	1.00 [53]

months						
Volume, m3	10466.27	6.90E+06	2056.84	57923.99	341.85	1.45E+06
Volume of 1 tank, m3	5000.00 [58]	50000.00 [59]	2000.00 [60]	30000.00 [61]	400.00 [62]	50000.00 [59]
Number of tanks	2.00	6.00	1.00	2.00	1.00	5.00
Material of tank	SS316 [63]	SS316 [64]	SS316 [55]	SS316 [56]	SS316 [57]	SS316 [63]
Total net weight, kg	123428.00 [58]	994285.00 [59]	58735.00 [60]	595398.00 [61]	19008.00 [62]	994285.00 [59]

Chapter 5: Plant Location and Layout

Choosing the location for a plant and planning its layout are important aspects in industrial plant design. These considerations affect process efficiency, the overall profitability of the plant, and future development. This chapter analyses key factors in selecting a plant location and determines suitable layout configuration.

5.1. Plant Site Location

While considering future MTBE plant location, the focus is on various factors such as availability of raw materials, utility costs, and market opportunities. Additionally, tax exemption would allow for more sustainable income in the beginning of operation. As of the date, there are 13 special economic zones (SEZs) in Kazakhstan. Out of them “Chemical Park Taraz”, “Pavlodar”, “National Industrial Petrochemical Park” and “Seaport Aktau” are of particular interest. Table 5.1.1 demonstrates the highlights of these economic areas

Table 5.1.1. Economic areas suitable for plant location

SEZ	**Chemical Park Taraz [65]**	**Pavlodar [66]**	**National Industrial Petrochemical Park [67]**	**Seaport Aktau [68]**
Location	Taraz (Jambyl region)	Pavlodar (Pavlodar region)	Atyrau (Atyrau region)	Aktau (Mangystau region)
Expiration	2037	2036	2032	2028
Related infrastructure	Taraz Khimprom	Pavlodar Petrochemical	1. Atyrau Oil Refinery (ANPZ)	1. KazTransOil 2. KarakudukMunay

industries nearby		Plant (PNHZ)	2. Tengizchevroil 3. Atyrauneftemash 4. JSC Embamunaigas 5. Chevron Munaigas Inc	
Specialization	Chemistry	Petrochemistry	Petrochemistry	Sea trade
Availability of water	Talas river	Irtysh river	Ural river	Distilling from sea
Methanol suppliers	Import only	Import only	Zhaik Petroleum, import	Import only
Isobutylene suppliers	Import only	Import only	Import only (upcoming Butadiene plant)	Import only

The National Industrial Petrochemical Park is selected due to its proximity to large industrial facilities like ANPZ, Tengizchevroil, and Atyrauneftemash, which support petrochemical operations. It specializes in petrochemistry, has access to the Ural River for water, and has major companies such as JSC Embamunaigas and Chevron, opening a door to collaborative business environments. Although methanol and isobutylene are currently imported, the future Butadiene plant is considered as a prospective local supply of isobutylene since 85 kilotons of isobutane-isobutylene fraction are planned to be produced there [69]. These factors make it the most strategic SEZ for the intended operations. In Figure 5.1.1 an adapted layout of SEZ with two possible MTBE plant locations is depicted [70]. Although Location II provides direct access to gas separation plant by local company, Location I is chosen due to access to city infrastructure and known interaction streamline with businesses and global railroad connection.

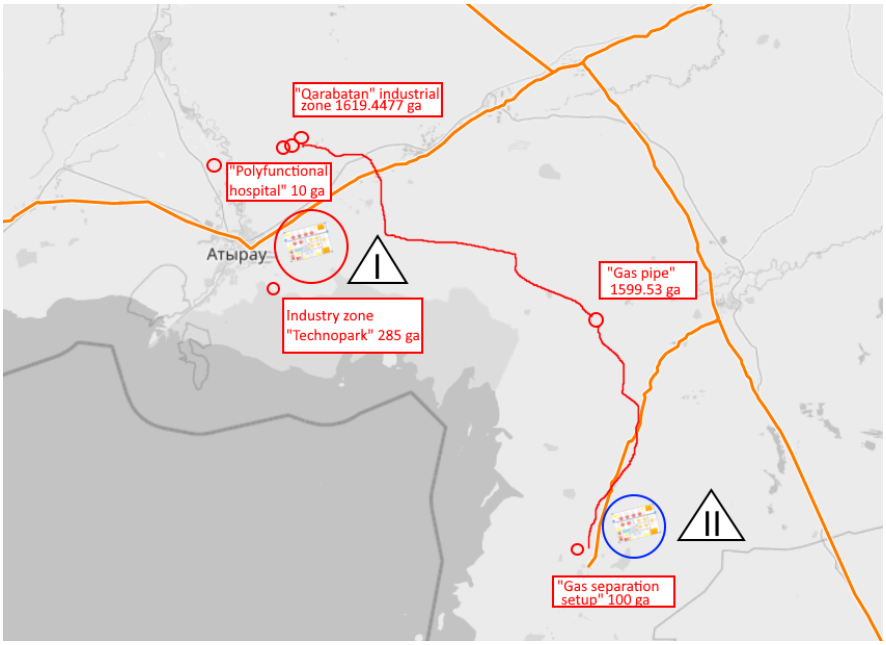

Figure 5.1.1. MTBE plant industrial section layout

5.1.1. Market Proximity

Proximity to consumers is an essential factor in selecting a production site, particularly for high-demand chemical products such as MTBE, and especially considering the fact that three LPPs are producing MTBE in Kazakhstan. In the Atyrau city there is oil processing plant ANPZ that manufactures a variety of fuels including MTBE-doped petrol. It is known that demand for MTBE as of 2021 was around 80 kilotons in Kazakhstan, with expected increase in future, while regional demand is 154 kilotons [71]. Despite already mentioned LPP “Pavlodar NefteChem” and LPP “Shymkent Chemical Company” plants manufacturing 77-87 kilotons of MTBE, and upcoming LPP “Butadiene” plant planning to product up to 40 kilotons per year [72], it is apparent that proximity of ANPZ would be beneficial for selling product.

Atyrau’s geographical position in western Kazakhstan offers logistical connection not only to key domestic consumers, but also to nearby countries in the CIS region, including Russia, Uzbekistan, and Turkmenistan. These countries, which maintain growing automotive and refining industries, have increasing demand for high-octane fuel components and additives like MTBE [73]. Kazakhstan's membership in the Eurasian Economic Union (EAEU) makes it easy to go through customs procedures, enabling export of MTBE within this region. In addition to overland routes, Atyrau’s proximity to the Caspian Sea offers a maritime link to other regional markets, including Azerbaijan and Iran, through the ports of Aktau (Kazakhstan) and Baku (Azerbaijan), as well as access to the wider Middle Eastern market via Iranian ports. This maritime logistics allows our product to compete outside of Kazakhstan by affordable pricing and access to a broader customer base. This makes Atyrau a compelling location for MTBE-related production.

5.1.2. Availability and Cost of Utilities

Following the selection of Atyrau as the preferred plant location, the next step is to check the availability and cost of essential utilities. The presence of large-scale facilities and the region's economy based on industrial petrochemical plants ensure access to core utilities, including electricity, water, transportation, and waste management services. Electricity can be purchased from local Atyrau Combined Heat and Power Plant (CHPP). Official tariffs state that for industrial consumers energy is priced as 45.02 KZT/kWh with VAT [74]. Although this rate is higher than in some other regions, it might be mitigated by installation of solar panels and wind turbines, which would reduce expenses and improve environmental sustainability. Water is provided from the Ural (Jaiyk) river by local "Atyrau Su Arnasy" company and priced as 410.68 KZT/m^3 for non-residential consumers with VAT [75]. Same company accepts wastewater for treatment from non-residential consumers for 232.16 KZT/m^3, including VAT [75]. The availability of a reliable water source is beneficial for this chemical process that involves 3.73 kton/oper-year water use for methanol absorption, and more than 10 kton/oper-year for cooling in heat exchangers. In summary, the Atyrau region provides all the needed utilities required for establishing a chemical production facility.

5.1.3. Proximity to Raw Materials

The production of MTBE requires isobutylene and methanol as primary raw materials. Most of isobutylene is planned to be obtained from Russian SIBUR Khimprom [76, 77], the upcoming Butadiene plant is planning to provide up to 85 kilotons of isobutane-isobutylene fraction, which allows for decreased costs on transportation [78]. Apart from that, there is decent railroad connection with overseas manufacturers. In terms of methanol supply, Zhaik Petroleum offers industrial quantities of methanol for sale domestically [79].

5.1.4. Transportation

Railroad connection with other regions of Kazakhstan is a main way of transportation of both feed and product chemicals, and it is maintained by "KTZ-Freight Transportation" JSC. Atyrau's railway network connects it to major regions within Kazakhstan and extends to neighboring countries, including Russia and China. This connectivity is crucial for enterprises like SIBUR Khimprom, Zhaik Petroleum and Butadiene LLP, enabling them to distribute their products effectively in CIS. Therefore, the MTBE plant could take advantage of developed transport infrastructure.

Incoming raw materials and MTBE sold for customers in other regions are required to be transported in tank cars, with an amount no less than 30 tons [80]. Tariffs for storage and transportation of dangerous goods as of 2025 are 7 tenge per hour per 1 ton in covered warehouses; 3 tenge per hour per 1 ton in open areas; and 7 tenge per hour per 1 ton in containers idle on station tracks [81]. These logistics capabilities further support the feasibility of locating the MTBE production facility in Atyrau.

5.1.5. Business Environment

The business environment of the Atyrau region is evaluated through key indicators such as taxation, labor availability, and labor cost. One of the significant advantages of locating the MTBE plant in this region is the opportunity to become a resident of the SEZ. Major advantage of SEZ residence is having corporate income, value added, land and property taxes of 0%.

Labour resources are based on 199 610 men and 194 592 women of working age in Atyrau region according to state statistics [82]. 95 100 of them are employed in industry and construction fields [82]. Given that the expected workforce requirement for a plant of this scale is in the range of no more than hundred employees, the region demonstrates sufficient labor capacity to support operations. As of the end of 2024, average salary of Atyrau workers was 640 938 KZT, while industry and construction specific workers had an average of 348 807 KZT [83, 84]. While this salary level is higher than the national average, it reflects the region's specialization in oil and gas industries, which reflects the availability of experienced individuals.

Considering the SEZ benefits and the availability of skilled labor, Atyrau presents an attractive business environment for establishing the MTBE production facility.

5.1.6. Environmental Risk and Climate

Public reports indicate that Atyrau's main ecological problems are related to the detrimental effect of industry on Jayik (Ural) river [85]. Air quality in the city is worsened by 1.6 times higher than the allowable presence of sub-2.5 μm particles, according to the US Air Quality Index [86]. State Ecology Department reports that ANPZ, Tengizchevroil LLP, "North Caspian Operating Company" N.V., Atyrau CHPP, Embamunaigas JSC, "West Dala" LLP and number of polygons contribute to pollution of air by hydrogen sulfide, ammonia, zinc, particles, nitrogen, sulfur and carbon oxides [87]. Water resources are characterized by increased levels of pollution from petroleum products and magnesium with heavy metals. These are detrimental both to human resources and equipment [88].

While the climate is semi-arid with a tendency to have high temperatures at summer and low temperatures at winter, which accelerates material degradation, the main problem still comes from pollution changing it. Heightened levels of hydrogen sulfide and nitrogen/sulfur/carbon oxides cause acidification of rain which corrodes equipment and buildings. This is somewhat mitigated by lower average annual precipitation of about 190 mm. Salinated ground water compromises structural integrity of plant buildings and health of personnel. To manage the ecological situation the state imposes some regulations on usage of filtering systems and maintaining sustainable processes in industries [89].

Movement of air masses is defined by predominantly north-western winds at summer and south-western winds at winter, speeding from 1.6 to 5.4 m/s and averaging around 3-4 m/s [90]. This should be taken into account when placing industrial and storage units on plant territory, since it affects the direction where air pollutants are going. When done properly, it allows for maintaining personnel well-being.

5.2. Plant Layout

In addition to the theoretical design of the process, it is essential to consider the physical layout of the MTBE production facility, focusing on optimization of operational efficiency and safety concerns.

5.2.1. Plant Layout Design

The MTBE production plant layout (Figure 5.2.1) is organized to ensure operational efficiency, safety, and regulatory compliance. It consists of multiple control zones, each dedicated to specific process stages such as feed preparation, reaction, purification, and recycling. The top section includes compressor (C-101), pump (P-101), mixer (M-101), and heat exchangers (H-101, H-102, H-106) units, for MeOH and IB feed handling for reactor conditions. The central left area features the main reactor (R-101) along with high pressure valve and MTBE distillation column (V-101, T-101), indicating the core reaction zone and the removal of 98.4wt% MTBE product. A separate lower zone with heat exchanger (H-103) and pressure valve (V-102) serves for conditioning ready high-purity MTBE for storage. On the central right, equipment such as IB absorption column (T-102), compressor (C-102), and heat exchangers (H-104, H-105) are for post-reaction treatment of low-purity product and methanol absorption for future processing in distillation column (T-103). Supporting utilities in frame include the Waste Water Tank (TK-105) to collect and manage waste from T-103; and Water Absorber Feed Tank (TK-103), facilitating the operation of T-102 column. The plant includes an Emergency Leak Fallback Pool for safety and containment in case of hazardous spills in reactor building with channels. Color-coded pipelines roughly distinguish process fluids: red color is for IB-containing stream, blue color for methanol stream, their mixture averages at purple. Then pale blue MTBE flow is separated, while the rest of low purity product is separated into yellow (IB+MTBE), green (recycled methanol) and blue (wastewater) streams. A central road connects all zones for streamlined operation, allowing for access of transport. The presence of vegetation units (represented by green symbols) is a common requirement in building codes, discussed in part 5.2.2. Additionally, pumping specialists recommend having maintenance space around pumps [91], while ANSI codes specify distance from 1 to 3 meters around equipment and, for hazardous equipment like reactors or high-pressure columns, increased free distance of 5-30 m [92]. That is why Figure 5.2.1 displays a yellow zone of minimal spacing and pale red zone of safety distance on the technological axis.

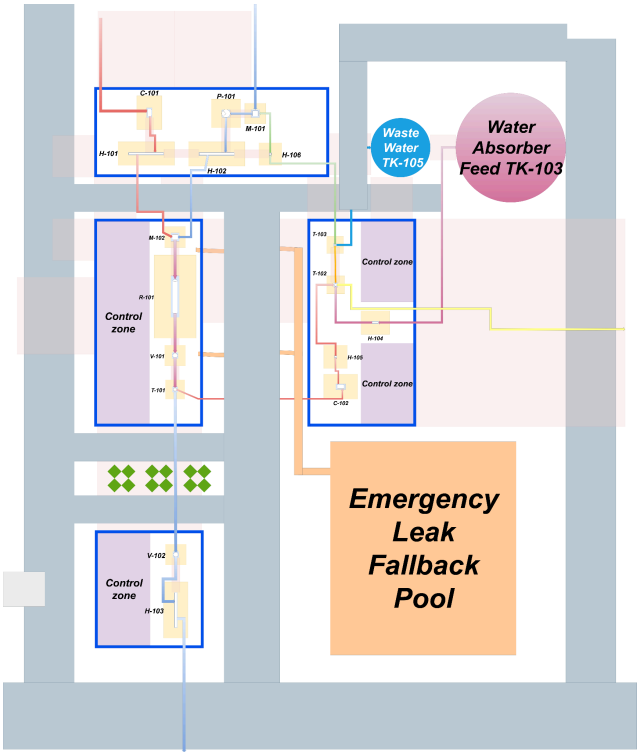

Figure 5.2.1. MTBE plant industrial section layout

5.2.2. Plant Layout Considerations

However, a chemical plant is not defined by equipment only. Its overall territory often includes occupation personnel buildings, safety points, and, most importantly, storage of products and raw materials. Therefore, a detailed MTBE plant facility was designed and shown in Figure 5.2.2. When designing flammable raw material and product storage, several regulations take place. General fire safety rules apply for administrative and housing objects of the plant: maintaining short distance between buildings and roads for better firefighter access (no more than 10-12 m), and maintaining distance of at least 6 meters between buildings [93]. For petrochemical objects it is recommended to increase such distance to 10 m and more. For fuel reservoirs it is recommended to increase further to at least 50 m [94]. If wastewater contains flammable compounds (methanol in case of T-103 waste stream, and MTBE+IB+MeOH in case of T-102 abs), its reservoir must stay 20 m away from other manufacturing facilities and 100 m away from residential buildings [95]. For petrochemical reservoirs of large volume there are additional limitations in action: for 50000 m^3 sized cylinders with floating roof, it is prohibited to go above 200000 m^3 group total and to have distance below 30 m. If volumed below 50000 m, then not closer than 0.5 of the radius of the tank [94]. This is why in Figure 5.2.2 translucent red squares are present, labelled “fire safety zones”. Largest ones define 1 diameter distance to surrounding buildings, while squares in between are maintaining safe distance between tanks in one group. If the number of tanks exceeds the group storage limit, like TK-102 and TK-106 do, excess tanks are put at slightly increased distance. Additionally, there are roads of at least 6

meters up to 15 meters between reservoirs and facility buildings. This allows for safe operation of the plant and for performant maintenance when heavy machinery is required.

On the territory of the plant there are also residential buildings present, and some regulations specify the presence of vegetation between industrial and residential buildings in order to mitigate harm to workers [96].

Finally, considering the mapping of wind in Atyrau, MTBE plant is to be placed such that industrial and storage buildings are from the eastern and north-eastern part of the complex, in accordance with wind data from part 5.1.6.

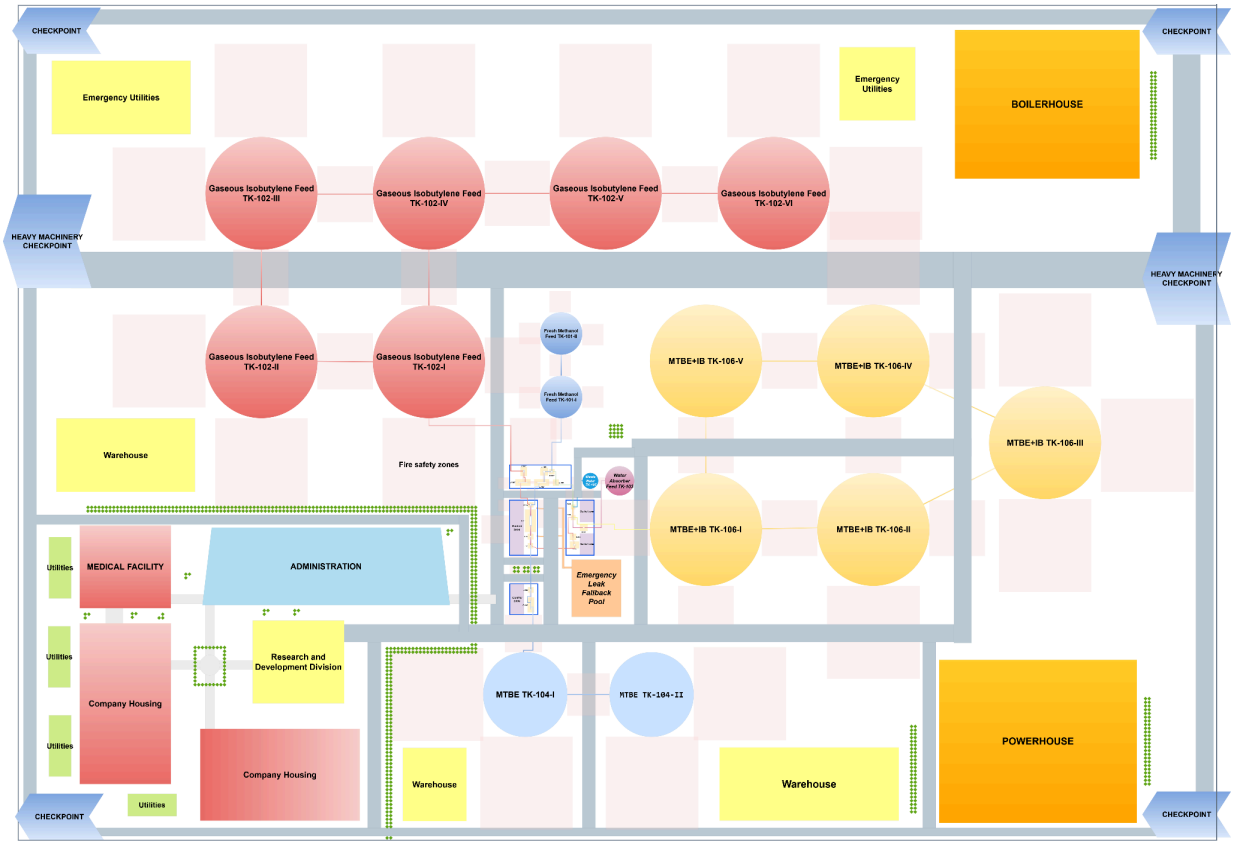

Figure 5.2.2. General MTBE plant territory layout

Chapter 6: Environment and Waste Streams

Environmental sustainability is a critical component of modern chemical and process engineering. This chapter evaluates the various waste streams generated by the process and outlines appropriate treatment processes. Each waste stream is examined in terms of its source, composition and flow rate. Based on this assessment, required treatment units are identified to ensure safe disposal and reuse of byproducts.

MTBE and isobutylene are volatile organic compounds that pose significant health and environmental risks due to their toxicity and potential air contamination. They are known to have adverse effects on human health, particularly through inhalation exposure in occupational settings. Therefore it is important to control concentration of those compounds in the working

area for ensuring safety of human health and ecosystem around. For MTBE exposure limit is 50 ppm [97] for isobutylene 250 ppm [98] and for methanol is 200 ppm [99] as an 8 hour time weighted average.

From the process flow diagram of Aspen, it can be seen that the top product of T-102 column (Stream 29) produces MTBE-isobutylene-methanol-water vapor mixture and it is required to consider its treatment process due to environmental/health regulations and economic reasons. Composition of this stream by mass and mass flow rate is summarized in Table 6.1.

Table 6.1. Composition of Stream 29

Component	**MTBE**	**Water**	**Methanol**	**IB**	**1-DIB**	**2-DIB**	**Total**
Mass fraction	0.31	0.05	1.70E-02	0.64	1.90E-8	1.40E-9	1.00
Mass flow, kg/hr	213.90	36.10	1.16	444.65	1.31E-5	9.90E-7	695.88

Due to the significant amount of MTBE and isobutylene present in this stream, a 2-step waste treatment process was suggested. First step is two stage partial condensation. Stage 1 is MTBE and methanol condensation. The vapor mixture is cooled to approximately 30-40 C under 3-5 bar pressure. The condensed liquids are collected in a two-phase separator, while isobutylene remains in the vapor phase. The next stage is isobutylene condensation to around -10 C under 2-5 bars and condensed isobutylene is collected. Second step is to separate MTBE from methanol. Since they form azeotrope and they are in liquid phase, it was suggested to use LLE using water. After this pure MTBE is ready for storage, while methanol rich water is sent to methanol recovery.

The next waste stream identified in this process is Stream 31 and its composition is presented in the Table 6.2. below.

Table 6.2. Composition of Stream 31

Component	**MTBE**	**Water**	**Methanol**	**IB**	**1-DIB**	**2-DIB**	**Total**
Mass fraction	1.34E-11	0.99	4.5E-03	3.77E-14	5.02E-22	2.06E-21	1.00
Mass flow, kg/hr	5.75E-9	427.58	1.94	1.62E-11	2.15E-19	8.87E-19	429.53

Due to the negligible amount of MTBE, isobutylene, 1-DIB, and 2-DIB presented in this stream, their presence will be neglected, and the treatment process will be focused on water treatment from methanol. To separate water from methanol it was decided to use an activated sludge method. Highly concentrated microorganisms would be used to degrade methanol and to take pure water for reuse. This method was chosen because of cost efficiency and due to low concentration of methanol in water-methanol mixture.

Chapter 7: Total Investment and Profitability

7.1. Price of Raw Materials and Final Products

As previously mentioned, there are two feeds to the reactor: methanol and isobutylene. One of the feed materials - methanol can be purchased directly in Kazakhstan. The first company Crystal IG is located in Astana and sells methanol for $200/MT[100]. The second company from Uralsk named KazNefteHim Operating set the price at approximately $500/MT[101]. The choice depends on plant location to decrease the transportation cost. The second feed material, isobutylene with purity 99.9% can be purchased for $2-5/kg from Russian SIBUR Khimprom[76].

To establish the selling price of MTBE it is needed to compare it with competitors' markets. According to IMARC Group data, during March 2024 the lowest price of MTBE was in China, while in the USA it reached $1081/MT (Table 7.1.1.)[102]. Dongying City Longxing Chemical Co., Ltd. company in China produces MTBE with purity 99.8% and selling price ranges between $1000-1200/MT[103]. Other companies in China sell MTBE at high prices from $1000/MT to $1600/MT but their purity reaches 99.9%[104]. There is a local company KazNefteHim Operating which sells MTBE with max 98 wt% at 500 tg/kg which is approximately $1000/MT[105]. The designed plant will produce MTBE with 98% purity like KazNefteHim Operating so the selling price should be about $1000/MT.

Table 7.1.1. Methyl Tert-Butyl Ether Prices March 2024 [102]

Product	Region	Price
MTBE	USA	1081 USD/MT
	China	937 USD/MT
	MEA	1041 USD/MT

7.2. Cost of Equipment and Storage Tanks

The cost of individual equipment components is commonly estimated using the Cost Curve for Purchased Equipment, which is typically based on the assumption that the material of construction is stainless steel.

$$C_e = a + bS^n \tag{7.2.1}$$

a,b - cost coefficients; S - size parameter, specific to equipment; n - exponent, specific to equipment. For heat exchangers and reactors, the size parameter S was defined as the surface area of the unit, calculated using standard geometric relations for cylindrical equipment.

For distillation columns, the size parameter was based on the shell mass, which was determined using the following equation:

$$Shell\ mass = \pi D_c L_c t_w \rho \tag{7.2.2}$$

where is the D_c column diameter, L_c is the column height, t_w is the wall thickness, and ρ is the density of the construction material. This approach allows for a more accurate representation of the equipment size and subsequently its cost. The Chemical Engineering Plant Cost Index (CEPCI) used for updating equipment costs was calculated by dividing the 2024 index value (798.8) by the 2010 base year index (532.9). This ratio served as a scaling factor to adjust historical cost data to present-day values, ensuring the capital cost estimates reflect current economic conditions and inflation trends in the chemical industry. Material cost factors were also incorporated based on the type of stainless steel selected, such as SS 304 or SS 316, to account for differences in material expenses. In addition, installation factors were applied to estimate the full installed cost of each equipment unit. These factors vary depending on the complexity and nature of the equipment: a value of 3.5 was used for heat exchangers, 2.5 for compressors, pumps, and tanks, and 4.0 for distillation columns.

To account for regional cost differences, Russia is used as the reference location with a location factor of 1.53. The nearest industrial center in Russia is situated in the Chuvashia Republic. Since the plant is planned to be established in SEZ "NINT" , the location factor for this site is adjusted by adding 10% for every 1000 miles of distance from Chuvashia, in accordance with the method outlined by Alkayat and Gerrard [36]. Given that the distance between Atyrau and Chuvashia is approximately 753 miles, a proportional adjustment is made to reflect this difference. The results of ISBL estimation are collected in Table 7.2.1 and all calculations can be retrieved from the Excel file "Economic Analysis".

$$LF_{Atyrau} = 1.53 \times 1.1^{\frac{753}{1000}} = 1.64 \quad (7.2.3)$$

The cost of storage tanks were calculated on the basis of the required net weight of storage tanks and the cost of material per tonne as shown in the equation below.

$$C_{storage\ tanks} = W_{storage\ tanks} \times P_{material} \quad (7.2.4)$$

, where $C_{storage\ tanks}$ - total cost of all storage tanks, $W_{storage\ tanks}$ - total weight of all storage, $P_{material}$ - price of SS316 per tonne, which was taken to be 20000 KZT/tonne [106]. Accounting for location, material cost, installation factors and CEPCI index the estimated cost of all storage tanks were taken to be $1 125 671.

Table 7.2.1. Cost of equipment

Unit	ID	Equipment cost, $	ISBL
Reactor	R-101	37 643	421 046
	H-101	29 494	329 897
	H-102	6 428	71 901
	H-103	29 003	324 406

Heater/Cooler

	H-105	2 751	30 765
	H-104	4 316	48 274
	H-106	2 682	30 000
Compressor	C-101	1 072 000	11 200 048
	C-102	120 500	1 258 961
Pump	P-101	20 800	217 314
Distillation column	T-101	945 934	1209208
	T-103	814 612	260336
Absorption	T-102	192 322	61462
Storage tank	all TKs	107 742	1 125 671

7.3. Capital Investment Estimation

The Outside Battery Limits (OSBL) cost, which accounts for the additional infrastructure such as utilities, buildings, and site preparation and this value corresponds to roughly 40% of the ISBL, aligning with standard industrial practice.

Engineering costs, covering detailed design, project management, and engineering services, were calculated using the rule of thumb that suggests 30% of the sum ISBL and OSBL values. This yielded a total engineering cost of approximately $7 000 000.

To account for potential uncertainties such as market price fluctuations or unforeseen changes during the project, contingency charges were also included. These were estimated at 10% of the combined ISBL and OSBL, resulting in a value of $2 340 000. The total capital investment, which is the sum of ISBL, OSBL, engineering costs, and contingency charges.

Table 7.3.1. Capital investment calculations

Components	Cost, USD/year
ISBL	16 687 289
OSBL	6 674 593
Engineering cost	7 008 322
Contingency charges	2 336 107
Capital Investment	32 707 087

7.4. Fixed Costs

The estimation of operating labor requirements for the plant was carried out using the method proposed by Alkayat and Gerrard [36], which is based on data collected from five chemical companies. This method calculates the number of operators required per shift using equation 7.4.1, where the total number of processing steps is divided into two categories:

particulate handling steps P and non-particulate processing steps N_{np}. Particulate steps include operations such as transportation, size control, and removal of solids, while non-particulate steps include compression, heating, cooling, mixing, and reaction processes.

$$N_{OL} = (6.29 + 31.7P^2 + 0.23N_{np})^{0.5} \quad (7.4.1)$$

$$N_{np} = \sum Equipment \quad (7.4.2)$$

This process does not involve particulate solids (i.e., P = 0), and the value of was N_{np} determined by summing all relevant unit operations (such as compressors, towers, reactors, and heat exchangers). Applying this method yielded a value of 3.01, representing the number of operators needed per shift. Since a chemical plant operates continuously (24/7), this value was multiplied by the standard operator coverage factor to estimate the total number of operators required. As a result, the total number of operators needed for plant operation was rounded to 14.

The value of N_{OL} in Equation 7.4.1 represents the number of operators required to staff the process unit for each shift. On average, one operator works 245 shifts per year, considering a 48-week work year with five 8-hour shifts per week. Since a typical chemical plant operates continuously (24/7), it requires 1095 shifts annually (365 days × 3 shifts per day). Therefore, to cover these shifts, approximately 4.46 operators are needed for every operator position on a shift, calculated as 1095 divided by 245. This ensures continuous coverage but does not include supervisory or support personnel. To calculate the operating labor the following equation used:

$$Operating\ labor = N_{OL} \cdot N_{np} \quad (7.4.3)$$

For the purpose of this analysis, we used the highest average monthly salary of a chemical engineer in Kazakhstan for the year 2025, which was rounded to 593,000 KZT. This value serves as the basis for estimating the operating labor cost. [106]

$$C_{OL} = Operating\ Labor \cdot Average\ Salary \quad (7.4.4)$$

The annual cost of operating labor was estimated as 192 696 USD.

The total labor cost includes not only the base wages of operating personnel but also additional components such as supervision and direct salary overhead. These fixed costs are calculated using standard assumptions for average expenses. Supervision is estimated at 25% of the operating labor cost, while the direct salary overhead is calculated as 40% of operating labor plus supervision. Beyond labor, the plant incurs a maintenance cost which represents approximately 3% of the ISBL. Property tax and insurance are estimated at 1% of the ISBL, and environmental charges are calculated as 1% of ISBL plus OSBL costs. Additionally, general and administrative costs are estimated at 65% of the total labor plus supervision and direct salary overhead. A detailed breakdown of these fixed costs is provided in Table 7.4.1, and the full calculations can be found in the Excel file “Economic Analysis” available in the ESI.

Table 7.4.1. Fixed cost estimation

Components	Cost, USD/year
Labor cost	192 696
Supervision	48 174
Direct Salary Overhead	125 252
Maintenance	500 619
Insurance	166 872
General and administrative costs	298 679
Environmental	6 841 788
Total cost	8 174 081

7.5. Variable Cost of Production

7.5.1. Cost of Raw Materials

The total annual cost of raw materials for the process was calculated based on the flow rates and unit prices of methanol and isobutylene. The flow rate of methanol was estimated at 16 598 tonnes per year, with a unit cost of $500 per tonne, resulting in a total annual cost of approximately $8 298 919. Similarly, the flow rate of isobutylene was determined to be 32 003 tonnes per year, with a unit cost of $200 per tonne, leading to an annual cost of approximately $6 400 698, the price of water not taken into account. Therefore, the total cost of raw materials amounts to $14 699 617 per year.

7.5.2. Cost of Utilities

The annual utility cost for the process was estimated to be approximately $299 680 based on simulation results obtained from ASPEN Plus. This value encompasses the expenses associated with utilities essential for plant operation, including electricity, cooling water, steam, and other process-related services. The estimate reflects the energy requirements determined through the simulation of the plant's operation under steady-state conditions.

7.5.3. Cost of waste treatment from T-102

The first step consists of two stage condensation, in which we initially condensate MTBE and methanol and then isobutylene. Setup consists of a simple heat exchanger, cryogenic heat exchanger, refrigeration unit, 2 storage tanks, pipings, valves, and controllers. Second step consists of a liquid-liquid extraction system, which consists of a mixer-settler unit, water circulation and injection system, storage tank, pipings and valves. Rough cost estimation of those units were summarized in Table 7.5.1 below.

Table 7.5.1. Capital cost for waste treatment

Stage & Equipment	Cost estimate, $

Stage 1- Condensation system	
Primary condenser for MTBE/methanol	8 000
Cryo-condenser for isobutylene	12 000
Refrigeration Unit	15 000
Storage tank (2x)	6 000
Pipings, Valves, Controllers	5 000
Stage 2 - LLE system	
Mixer - Settler	10 000
Water circulation + injection unit	2 000
Storage tank	3 500
Pipings, Valves, Controllers	3 500
Total	65 000

Rough estimation of operating cost including electricity, water consumption, maintenance, and labor gives an annual cost of $30 000.

7.5.4. Cost of waste treatment from T-103

According to [107] and [108], theoretical chemical oxygen demand (COD) of methanol is 1.5 kg/kg of methanol and sludge yield of methanol is 0.2 kg biomass/kg of COD. Simple multiplication of those values with mass flow rate of methanol gives 0.5836 kg biomass per hour, which is 14 kg per day. Removing 99% water content from this sludge and 50% of this dry mass is bacterias, resulting in 0.07 kg per day bacterias, which is 25.55 kg per year. According to [109], the average price of bacteria is $20 per kg. Therefore it gives $511/year.

Rough estimation of capital cost including aeration tank, blower, diffusers, settler, pipes, controllers result in $33000. Similarly, a rough estimation of operating cost is around $6600, which includes electricity, microorganisms, sludge disposal, labor and maintenance. Total capital cost of waste treatment is $98,000 and annual operating cost is $36 600. All of the capital costs were estimated using Alibaba's website.

The waste treatment installation was taken to be approximately $98 000, which was accounted as a part of equipment cost in ISBL calculations. Moreover, the annual work of waste equipment was taken to be $36 600, which was summed to the variable cost.

Table 7.5.2. Variable cost estimation

Components	Cost, USD/year
Utility cost	299 680

Waste treatment installation	98 000
Waste treatment work	36 600
Variable cost	15 035 897

7.6. Economic Analysis

7.6.1. Profits

The selling price of MTBE was taken to be 1000 USD/MT. The overall production rate of MTBE is 38500 tonnes of MTBE per year, meaning that the annual revenue is equal to $38500000 million. The inflation is neglected in these calculations. According to [36] many companies operate under the assumption that while inflation may affect prices, profit margins, as well as cash flows, remain largely unaffected. As a result, inflation is often disregarded when evaluating economic performance of projects.

To determine the profit of the project, it is necessary to determine the cash cost of production (CCOP) which is taken as the summation of fixed and variable production costs as shown in Equation 7.6.1.

$$CCOP = VCOP + FCOP \quad (7.6.1)$$

, where VCOP - sum of all variable costs of production minus by-product revenues and FCOP is the sum of the fixed costs of production. As our project does not produce the by-product revenues VCOP is taken as a sum of variable costs.

The gross profit is calculated using the equation that considers the main product revenues and CCOP as shown below.

$$\text{Gross profit} = \text{Main product revenues} - CCOP \quad (7.6.2)$$

The depreciation value is calculated using the straight-line depreciation method according to the equation below.

$$D = \frac{C}{n} \quad (7.6.3)$$

, where D is the depreciation value, C - is the fixed capital investment and n - amount of year C is depreciated over, which was taken as 15 years.

7.6.2. Profitability

The cash flow is calculated according to the production schedule indicated in Table 7.6.1.

Table 7.6.1. Production schedule

Year	**Costs**	**Revenues ($/year)**	**Explanation**
0	30% of capital investment	0	Engineering + long lead-time items
1	70% of capital investment	0	Remaining

			construction
2+	VCOP and FCOP	38 500 000	Production

As indicated above the first two years will be used to buy the capital like equipment, engineering cost, contingency charges etc. Therefore, the first two years the cash flow will be negative. Starting from year 2 the production will start with annual revenue of 38500000$. After determining the gross profit, taxable income can be taken as gross profit minus the depreciation. However, as the annual income neglects taxes due to the fact that the production unit is placed on the territory of a special economic zone (SEZ), the final annual cash flow will be taken as just annual gross profit.

In Figure 7.6.1, it is shown how cumulative cash flow varies by year for the next 10 years.

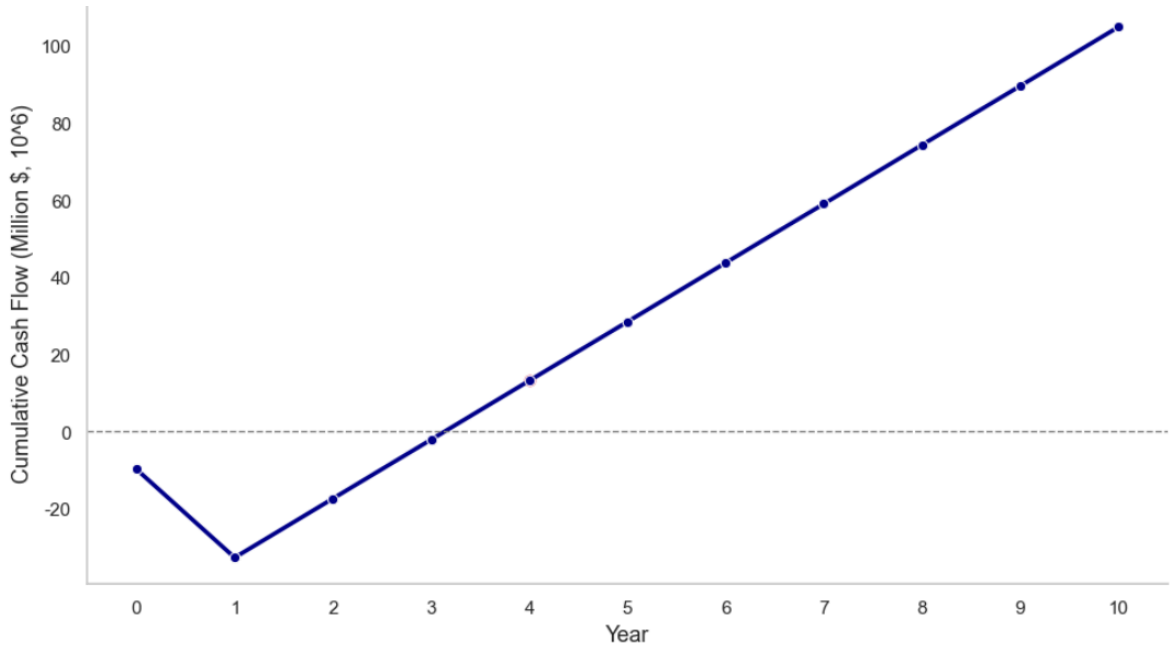

Figure 7.6.1. Cumulative cash flow over 10 years

As shown in Figure 7.6.1 the cumulative cash flow increases linearly with the start of the production. The trend of cumulative cash flow over the years is applied to determine the payback period as payback period is taken to be the time when the cumulative cash flow will be equal to 0. Cumulative cash flow in year 3 is $-2.13 mln and in year 4 it is $13.16 mln. The exact payback period is determined below.

$$Payback\ period = 3 + \frac{-(-2.13)}{13.16-(-2.13)} = 3.14\ years \qquad (7.6.4)$$

The net present value is taken to be the sum of present value over the years, which is calculated using the Equation 7.6.4. The Internal Rate of Return (IRR) is calculated using the Excel spreadsheet formula.

$$PV = \frac{Cash\ flow}{(1+i)^{year}} \tag{7.6.5}$$

, where PV - present value, i - discount rate, which is taken to be 12%.

Taking the sum of present value, net present value was calculated to be $42.49 mln and the IRR was determined to be 39.7%. IRR is also indicated in Figure 7.6.2, where it is shown at a point where NPV intersects the value of 0.

The Return on Investment (ROI), taken as the inverse of the payback period, is 31.9%, further highlighting the efficiency of capital usage. ROI is a measure of how effectively the initial capital investment is used to generate profit. A 31.9% ROI means that for every dollar invested, the project returns 30 cents in profit annually after payback. This is a high return by industrial standards and suggests strong capital efficiency. Alongside a Net Present Value (NPV) of $42.49 million and an Internal Rate of Return (IRR) of 39.7%, the high ROI confirms that the project not only recovers its initial investment quickly but also delivers substantial profits over time, making it an economically sound and attractive investment. Overall, the data suggests that the MTBE production plant is a sound investment with a quick return period and strong long-term profitability. More detailed calculations are presented in ESI "Economic Analysis" Excel spreadsheet.

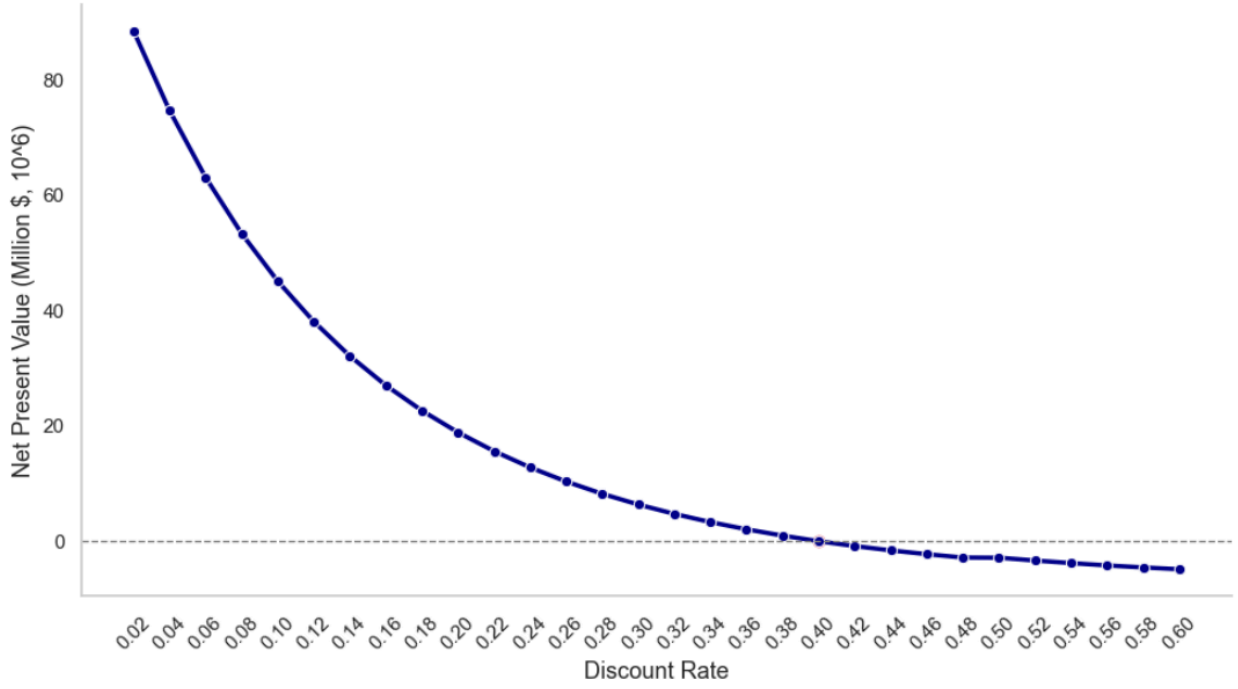

Figure 7.6.2. Variation of NPV based on discount rate

Chapter 8: Conclusions and Future Work

8.1. Conclusion

In conclusion, this project successfully developed a comprehensive design for an industrial-scale methyl tertiary-butyl ether (MTBE) production plant in Kazakhstan, targeting an output of 38,500 tonnes per year of Grade A MTBE with a purity of 98.4 wt%. The direct liquid-phase etherification of methanol and isobutylene over Amberlyst-15 was selected as the optimal route, due to its high conversion efficiency, operational simplicity, and catalyst performance under moderate conditions. The kinetic model based on the Langmuir–Hinshelwood–Hougen–Watson mechanism that was validated using literature data and simulated in Aspen Plus V14 yielded an isobutylene conversion of 87.5%.

The design of major and minor equipment for the MTBE production plant was carried out with a focus on process efficiency and conversion. Major equipment includes two shell-and-tube heat exchangers (H-101, H-102), the multitubular isothermal PFR reactor (R-101) with shell and tube cooling system, three distillation columns (T-101, T-102, T-103). Each unit was designed using both hand calculations and Aspen Plus simulations to compare and ensure the units were of accurate sizing, optimal operating conditions, and thermal performance. SS316 stainless steel was selected as the primary construction material for most of the units which had high-temperature and corrosive environments, particularly in the reactor and heat exchangers. Minor equipment such as pumps, coolers, heaters, compressors, and storage tanks were also designed to support continuous operation, manage phase transitions, and maintain system pressure and temperature stability. It was important to ensure that all the equipment could handle the flow rates and that pressure drops remained within allowable limits. The PFD incorporates all the units and streams and was used for efficient layout planning.

The selection of Atyrau as the site for the MTBE production plant was based on availability of and proximity to raw materials, utility and infrastructure costs and economic profitability. The location ensures not only the connection to domestic consumers, but also the logistical connection with the nearby countries where the demand for MTBE is projected to increase. Moreover, Atyrau's proximity to the Caspian Sea contributes to an access to a broader customer base outside of the country. The plant layout was designed in accordance with safety regulations and optimized for space efficiency, process flow, and accessibility. Critical units such as the reactor, distillation columns, and storage tanks were arranged to minimize pressure losses, streamline material handling, and include a separate area in case of hazardous spills. The streamlines were colored appropriately for convenience and flammable raw material storage tanks locations were designed according to safety requirements.

In terms of environmental management, the project addresses all major waste streams resulting from the MTBE synthesis process. Wastewater, unreacted hydrocarbons, and trace amounts of byproducts are handled through appropriate separation, neutralization, and disposal mechanisms. However, current treatment strategies for the IB/MTBE and methanol-water waste streams still present room for improvement. While most waste is separated in dedicated units like T-102 and T-103, the final outlet streams lack full resource recovery. Future improvements

should focus on integrating recovery systems for methanol and isobutylene to reduce environmental load and operating costs. In addition, emissions from flare systems, potential groundwater contamination from storage, and the flammability of MTBE require robust containment, monitoring, and emergency response infrastructure, all of which have been incorporated into the plant design. Overall, the environmental impact has been minimized through material selection, closed-loop recycling, and energy integration, supporting Kazakhstan's broader sustainability targets.

In terms of environmental management, the project addresses all major waste streams resulting from the MTBE synthesis process. However, current treatment strategies for the IB/MTBE and methanol-water waste streams still present room for improvement. While most waste is separated in dedicated units like T-102 and T-103, the final outlet streams lack full resource recovery. Future improvements should focus on integrating recovery systems for methanol and isobutylene to reduce environmental load and operating costs. In addition, emissions from flare systems, potential groundwater contamination from storage, and the flammability of MTBE require robust containment, monitoring, and emergency response infrastructure, all of which have been incorporated into the plant design. Overall, the environmental impact has been minimized through material selection, closed-loop recycling, and energy integration, supporting Kazakhstan's broader sustainability targets.

The total investment and profitability analysis of the MTBE production plant confirms its economic feasibility and strong return potential. Capital expenditures were calculated based on the cost of major and minor equipment, installation, utilities, and infrastructure, using the ISBL and OSBL method, along with Engineering and Contingency costs. The estimated total capital investment aligns with industry benchmarks for medium-scale chemical plants. Fixed and variable operating costs including raw materials, utilities, labor, and waste treatment were calculated annually, resulting in a competitive cost structure. Revenue projections were based on market prices of MTBE and regional demand forecasts, resulting in a net present value (NPV) of $42.49 million, an internal rate of return (IRR) of 39.7%, and a payback period of just 3.14 years. These indicators demonstrate that the project is financially attractive and resilient to market fluctuations. Moreover, optimization of waste recovery and process integration could further improve the plant's long-term profitability and environmental performance.

8.2. Future Work

- Conduct pilot-scale experiments to validate simulation results, reactor conversion, and product purity under industrial operating conditions. This includes verifying kinetics, heat transfer coefficients, and pressure drops.
- Develop a dynamic model to simulate plant behavior during startups, shutdowns, and feed fluctuations. Implement advanced control strategies (e.g., PID, MPC) to maintain optimal operation. Optimization of catalyst utilization and regeneration cycles is also crucial for maintaining long-term performance
- Future work should focus on integrating advanced separation technologies such as pervaporation, membrane separation, or extractive distillation to recover unreacted feed

components from waste streams. Recycling of isobutylene and methanol via these methods could significantly reduce raw material costs and emissions. Additionally, the system could be extended to co-produce tert-butanol (TBA) or ethylene glycol from side reactions if proper catalyst and reactor tuning is implemented.

- Further research may explore reactive distillation, which combines reaction and separation in a single unit, as a process intensification alternative.
- Evaluate the possibility of integrating the MTBE unit into existing refinery infrastructure in Atyrau or Shymkent to reduce utility demands and logistic costs.
- Explore greener alternatives such as bio-based isobutylene and ETBE or bio-MTBE. Assess feasibility of replacing Amberlyst-15 with biodegradable or metal-organic framework catalysts.

References

[1] Interfax, "Oil production at Kazakhstan's Kashagan field reaches full capacity after overhaul - Energy Ministry," Nov. 5, 2024. [Online]. Available: https://interfax.com/newsroom/top-stories/107358/

[2] Reuters, "Kazakhstan's oilfields, disputes and settlements with oil majors," Jan. 28, 2025. [Online]. Available: https://www.reuters.com/markets/asia/kazakhstans-oilfields-disputes-settlements-with-oil-majors-2025-01-28/

[3] Wikipedia, "List of countries by coal production," [Online]. Available: https://en.wikipedia.org/wiki/List_of_countries_by_coal_production

[4] Emission Index, "Greenhouse Gas Emissions in Kazakhstan," Jul. 16, 2024. [Online]. Available: https://www.emission-index.com/countries/kazakhstan

[5] H. Hamid and Mohammed Ashraf Ali, Handbook of MTBE and Other Gasoline Oxygenates. CRC Press, 2004.

[6] K. R. Green and W. A. Lowenbach, "MTBE Contamination: Environmental, Legal, and Public Policy Challenges," Environmental Forensics, vol. 2, no. 1, pp. 3–6, 2001, doi: https://doi.org/10.1080/15275920127930.

[7] Gaston Casillas, Mike Fay, Jennifer Przybyla, Kimberly Zaccaria, Mario Citra, Lisa Ingerman, Sabah Tariq and David W. Wohlers, HEALTH EFFECTS Toxicological Profile for Methyl tert-Butyl Ether (MTBE). Atlanta (GA): Agency for Toxic Substances and Disease Registry (US), 2023, URL: https://www.ncbi.nlm.nih.gov/books/NBK601205/.

[8] H. Kazemi Shariat Panahi, M. Dehhaghi, M. Aghbashlo, K. Karimi, and M. Tabatabaei, "Conversion of residues from agro-food industry into bioethanol in Iran: An under-valued biofuel additive to phase out MTBE in gasoline," Renewable Energy, vol. 145, pp. 699–710, Jan. 2020, doi: https://doi.org/10.1016/j.renene.2019.06.081.

[9] B. Li et al., "Preliminary Study of Biological Activated Carbon Treatment for Removing MTBE from Groundwater," International Conference on Bioinformatics and Biomedical Engineering, Jun. 2010, doi: https://doi.org/10.1109/icbbe.2010.5517277.

[10] R. Gonzalez-Olmos, Frank-Dieter Kopinke, K. Mackenzie, and A. Georgi, "Hydrophobic Fe Zeolites for Removal of MTBE from Water by Combination of Adsorption and Oxidation," vol. 47, no. 5, pp. 2353–2360, Feb. 2013, doi: https://doi.org/10.1021/es303885y.

[11] "Propane, 2-methoxy-2-methyl-," Nist.gov, 2023. https://webbook.nist.gov/cgi/cbook.cgi?ID=C1634044&Mask=4#Thermo-Phase [accessed Sep. 26, 2024].

[12] S. Viswanathan, M. Anand Rao, and L. Prasad, "Densities and Viscosities of Binary Liquid

Mixtures of Anisole or Methyl tert-Butyl Ether with Benzene, Chlorobenzene, Benzonitrile, and Nitrobenzene," Journal of Chemical & Engineering Data, vol. 45, no. 5, pp. 764–770, Jul. 2000, doi: https://doi.org/10.1021/je990288b.
[13] "GESTIS Substance Database MTBE," Dguv.de, 2024. https://gestis-database.dguv.de/data?name=040480 [accessed Sep. 26, 2024].
[14] KG Engineering Solutions, "Aspen Plus: Regression of experimental liquid liquid equilibrium data," YouTube, Mar. 26, 2023. https://www.youtube.com/watch?v=ZesSXCHbL28 [accessed Sep. 27, 2024].
[15] M. Rakhatkyzy, B. Suleimenova, M. Shaimardan, D. Shah, and Nurxat Nuraje, "Modeling Solubility of Acetylsalicylic Acid in Aspen Plus," Engineered Science, vol. Volume 26 December 2023, no. 0, pp. 987-, Oct. 2023, Accessed: Sep. 27, 2024. [Online]. Available: http://dx.doi.org/10.30919/es987
[16] J. Badra, F. Alowaid, A. Alhussaini, A. Alnakhli, and A. S. AlRamadan, "Understanding of the octane response of gasoline/MTBE blends," Fuel, vol. 318, p. 123647, Jun. 2022, doi: https://doi.org/10.1016/j.fuel.2022.123647.
[17] V. Matyash, G. Liebisch, T. V. Kurzchalia, A. Shevchenko, and D. Schwudke, "Lipid extraction by methyl-tert-butyl ether for high-throughput lipidomics," Journal of Lipid Research, vol. 49, no. 5, pp. 1137–1146, Feb. 2008, doi: https://doi.org/10.1194/jlr.d700041-jlr200.
[18] M. H. Eghbali, A. R. Soleimani Nazar, and T. Tavakoli, "An Experimental Study on the Operational Factors Affecting the Oil Content of Wax during Dewaxing Process: Adopting a DOE Method," Iranian Journal of Oil and Gas Science and Technology, vol. 2, no. 1, pp. 1–8, 2013, doi: https://doi.org/10.22050/ijogst.2013.3033.
[19] "Methyl Tert-Butyl Ether Market Size, Growth & Forecast 2032," Chemanalyst.com, 2022. https://www.chemanalyst.com/industry-report/methyl-tert-butyl-ether-market-2961#:~:text=The%20global%20Methyl%20Tert%2DButyl%20Ether%20(MTBE)%20market%20size
[20] "Methyl Tertiary Butyl Ether (MTBE) Market | 2021 - 26 | Industry Share, Size, Growth Mordor Intelligence," https://www.mordorintelligence.com/industry-reports/methyl-tertiary-butyl-ether-mtbe-market
[21] "Methyl Tertiary Butyl Ether Market by Manufacturing Process (Steam Cracker, Fluid Liquid Cracker, Dehydrogenation, Dehydration), Application (Gasoline Additive, Isobutene, Solvent), & Region for 2024-2031," Verified Market Research, Aug. 14, 2024. https://www.verifiedmarketresearch.com/product/methyl-tertiary-butyl-ether-market/
[22] "Oil production, gas supply, and investment attraction: Review of energy sector in Kazakhstan," PrimeMinister.kz. Accessed Nov. 15, 2024. [Online]. Available: https://primeminister.kz/en/news/reviews/oil-production-gas-supply-and-investment-attraction-review-of-energy-sector-in-kazakhstan
[23] "Kazakhstan to increase methanol imports," Globuc. Accessed Nov. 15, 2024. [Online]. Available: https://globuc.com/news/kazakhstan-to-increase-methanol-imports/
[24] "Development Bank of Kazakhstan: Press Release," KASE. Accessed Nov. 15, 2024. [Online]. Available: https://kase.kz/files/emitters/BRKZ/brkz_reliz_080921_1.pdf

[25] M. Ahmadi, “Production of Methyl Tertiary Butyl Ether (MTBE),” Department of Chemical and Biomedical Engineering, West Virginia University, 2010. [Online]. Available: https://cbe.statler.wvu.edu/files/d/075cb9f9-1ff4-4cc2-a663-1e302c44cbba/mtbe-b.pdf.
[26] E. C. Nelson, D. A. Storm, and M. S. Patel, “Preparation of MTBE from TBA and Methanol,” U.S. Patent 4,918,244, Apr. 17, 1990. [Online]. Available: https://patentimages.storage.googleapis.com/5c/dc/c3/869b9caa5628b4/US4918244.pdf
[27] Intratec Solutions, “MTBE Production from Butane (E41A),” Intratec Solutions, 2021. [Online]. Available: https://cdn.intratec.us/docs/reports/previews/mtbe-e41a-b.pdf.
[28] Chu, P. and Kühl, G. H. (1987). Preparation of Methyl-tert-Butyl Ether (MTBE) over Zeolite Catalysts. ACS, Ind. Eng. Chem. Res. 26, 365-369.
[29] Hatchings, G. J., Nicolaides, C. P., & Scurrell, M. S. (1992). Developments in the production of methyl tert-butyl ether. Catalysis Today, 15(1), 23–49. doi:10.1016/0920-5861(92)80121-3.
[30] Nicolaides, C. P., Stotijn, C. J., van der Veen, E. R. A., & Visser, M. S. (1993). Conversion of methanol and isobutanol to MTBE. Applied Catalysis A: General, 103(2), 223–232. doi:10.1016/0926-860x(93)85053-r.
[31] Zhang, T., & Datta, R. (1995). Integral analysis of methyl tert-butyl ether synthesis kinetics. Industrial & engineering chemistry research, 34(3), 730-740.
https://pubs.acs.org/doi/pdf/10.1021/ie00042a004
[32] - Technical Regulations of the Customs Union "On the requirements for motor and aviation gasoline, diesel and marine fuel, jet fuel and fuel oil" 013/2011.
[33] - National Standard of the Russian Federation "Methyl tert-butyl ether. Technical conditions" GOST R 58282-2018.
[34] Mohl, K. D., Kienle, A., Sundmacher, K., & Gilles, E. D. (2001). A theoretical study of kinetic instabilities in catalytic distillation processes: influence of transport limitations inside the catalyst. Chemical engineering science, 56(18), 5239-5254.
https://doi.org/10.1016/S0009-2509(01)00243-3
[35] PETRONAS Chemicals Group Berhad, "Methanol & Aromatics - MTBE," [Online]. Available: https://www.petronas.com/pcg/our-business/methanol-aromatics-mtbe
[36] Towler, G., & Sinnott, R. (2021). *Chemical engineering design: principles, practice and economics of plant and process design*. Butterworth-Heinemann.
[37]Q4A (n.d.) Stainless steel SCH 40S Pipe chart, dimensions, weight and pipe wall thickness. https://www.quest4alloys.com/images/documents/pdfs/pipe_charts_40S.pdf
[38] Kumaran, S. T., Baranidharan, K., Uthayakumar, M., & Parameswaran, P. (2021). Corrosion Studies on Stainless Steel 316 and their Prevention – A Review. *INCAS BULLETIN*, *13*(3), 245–251. https://doi.org/10.13111/2066-8201.2021.13.3.21
[39] F. S. Al-Harthi, I. S. Al-Mutaz, and A. E. Abasaeed, "Production of MTBE Using Reactive Distillation Technology," Proceedings of the Third International Conference on Modeling, Simulation and Applied Optimization (ICMSAO'09), Sharjah, U.A.E., 2009, pp. 1-4.

[40] "Alloy 316/316L Technical Information," Ulbrich Stainless Steels & Special Metals, Inc. [Online]. Available: https://www.upmet.com/sites/default/files/datasheets/316-316l.pdf
[41] J. Wang et al., "Corrosion Resistance and Mechanical Properties of Cr-Rich 316 Stainless Steel," Materials, vol. 16, no. 5, p. 11052491, 2024. [Online]. Available: https://www.ncbi.nlm.nih.gov/pmc/articles/PMC11052491/
[42] DuPont, "DuPont™ AmberLyst™ 15WET Polymeric Catalyst Product Data Sheet," Form No. 45-D00908-en, Rev. 2, Feb. 2023. [Online]. Available: https://www.vivaquainternational.com/_files/ugd/60aa39_1b37f404d860417d98aee59fb2b1fd3a.pdf
[43] Perry, R. H., Green, D. W., & Southard, M. Z. (2018). *Perry's chemical engineers' handbook* (9th ed.). McGraw-Hill Education.
[44] Seader, J. D., Henley, E. J., & Roper, D. K. (2016). *Separation process principles with applications using process simulators* (4th ed.) Ch.6 p.174. John Wiley & Sons, Inc.
[45] Branan, C. (2005). *Rules of thumb for chemical engineers: a manual of quick, accurate solutions to everyday process engineering problems*. Gulf Professional Pub.
[46] Sulzer Chemtech, "Regular packing for absorption and rectification processes" OOO "TI-SYSTEMS" ENGINEERING AND SUPPLY OF TECHNOLOGICAL EQUIPMENT
[47] American Society of Mechanical Engineers. (2020). *ASME B31.3: Process piping.* ASME.
[48] Towler, G., & Sinnott, R. (2012). *Chemical Engineering Design Principles, practice and economics of plant and Process Design*. Elsevier.
[49] Maxwell, C. (2020, May 28). *Cost indices*. Towering Skills. https://toweringskills.com/financial-analysis/cost-indices/
[50] Cheremisinoff, N. P. (2000). *Handbook of chemical processing equipment*. Elsevier.
[51] Wankat, P. C. (2006). *Separation process engineering*. Pearson Education.
[52] Sinnott, R. K., & Towler, G. (2020). Separation columns (distillation, absorption and extraction). *RK Sinnott, Coulson and Richardson's Chemical Engineering*, *6*
[53] Purosolv, "How to Properly Store Pharma-Grade Methanol for Long-Term Use," Purosolv, [Online]. Available: https://purosolv.com/how-to-properly-store-pharma-grade-methanol-for-long-term-use/.
[54] LyondellBasell Industries, "Global Product Strategy (GPS) Safety Summary: Isobutylene," Jun. 7, 2019. [Online]. Available: https://www.lyondellbasell.com/492c4f/globalassets/documents/safety-summaries/isobutylene.pdf
[55] Got Water, "How Long Can Water Be Safely Stored in a Tank?," Got Water, [Online]. Available: https://gotwater.co.za/how-long-can-water-be-safely-stored-in-a-tank/.
[56] Monument Chemical, "Methyl t-Butyl Ether (MTBE) - Technical Data Sheet," Monument Chemical, [Online]. Available: https://monumentchemical.com/uploads/files/TDS/MTBE_TDS.pdf?v=1635378633113.
[57] Shijiazhuang Zhengzhong Technology Co., Ltd., "Stainless Steel Industrial Wastewater Storage Tanks," CEC Tanks, [Online]. Available:

https://www.cectanks.com/sale-12643557-stainless-steel-industrial-wastewater-storage-tanks-durable-and-efficient-solutions-for-industrial-a.html.
[58] EuroTankWorks, "Vertical Steel Tank Vol.5000 cbm (AST-5000)," [Online]. Available: https://eurotankworks.com/storage-tanks/vertical-storage-tanks/vertical-tank-vol-5000/.
[59] EuroTankWorks, "Vertical Steel Tank Vol.50000 cbm (AST-50000)," [Online]. Available: https://eurotankworks.com/storage-tanks/vertical-storage-tanks/vertical-tank-vol-50000/.
[60] EuroTankWorks, "Vertical Steel Tank Vol.2000 cbm (AST-2000)," [Online]. Available: https://eurotankworks.com/storage-tanks/vertical-storage-tanks/vertical-tank-vol-2000/.
[61] EuroTankWorks, "Vertical Steel Tank Vol.30000 cbm (AST-30000)," [Online]. Available: https://eurotankworks.com/storage-tanks/vertical-storage-tanks/vertical-tank-vol-30000/.
[62] EuroTankWorks, "Vertical Steel Tank Vol.400 cbm (AST-400)," [Online]. Available: https://eurotankworks.com/storage-tanks/vertical-storage-tanks/vertical-tank-vol-400/.
[63] Methanol Institute, "Atmospheric Above Ground Tank Storage of Methanol," Methanol Institute, [Online]. Available: https://www.methanol.org/wp-content/uploads/2016/06/AtmosphericAboveGroundTankStorageMethanol-1.pdf.
[64] Balchem, "Safety Data Sheet: Isobutene, Liquefied, Under Pressure," Balchem, [Online]. Available: https://balchem.com/wp-content/uploads/2024/11/10340G_1.pdf.
[65] SEZ "Chemical Park Taraz.". Association of special economic zones participants in RK "SezUnion" (2019). http://sezunion.kz/en/component/k2/item/38-spetsialnaya-ekonomicheskaya-zona-khimicheskij-park-taraz.html
[66] About us. Special Economic Zone "Pavlodar." (2025). https://sezpv.com/en/About
[67] SEZ "National Industrial Petrochemical Technopark". Association of special economic zones participants in RK "SezUnion" (2019). http://sezunion.kz/ru/component/k2/item/33-spetsialnaya-ekonomicheskaya-zona-natsionalnyj-industrialnyj-neftekhimicheskij-tekhnopark.html
[68] SEZ «Aktau Seaport» (2025). General information. https://sez.kz/en/company/aboutsez
[69] Butadiene plant construction began in Kazakhstan. RUPEC. (2023). https://rupec.ru/news/52395/
[70] The plan of the territory SEZ "NIPT". SEZ "National Industrial Petrochemical Technopark" (2007). https://www.nipt.kz/investoram/57-interaktivnaja-karta-illjustrirujuschaja-obschuju-territoriju-sez.html
[71] Development Bank of Kazakhstan. (2021, September 8). Methyl-tret-butyl-ether plant has been successfully commissioned. WWW.KDB.KZ. https://www.kdb.kz/en/pc/news/press-releases/8943/
[72] Prospectus of "KazMunayGas" JSC. National Company "KazMunayGas" JSC. (2022). https://www.kmg.kz/upload/iblock/f04/8c8m61pg13pd9bq0be8hzqlo8ow71vql/Prospectus%20of%20JSC%20NC%20KazMunayGas%20(ENG).pdf

[73] Pulatov, A. B. (2024). The evolution of the automotive industry in Uzbekistan: Trends in manufacturing growth. European Journal of Applied Science, Engineering and Technology, 2(6), 178-184.
[74] Department of the Committee for Regulation of Natural Monopolies of the Ministry of National Economy of the Republic of Kazakhstan for Atyrau Region No. 23-03-03/861-I and No. 23-03-03/862-I. (2024). Tariffs on electric energy. Atyrau Energo. https://www.atyrauenergo.kz/page.php?page_id=289&lang=1
[75] Department of the Committee for Regulation of Natural Monopolies of the Ministry of National Economy of the Republic of Kazakhstan for Atyrau Region No. 93-OD. (2025). Water consuming and refining tariffs. SuArnasy. https://www.suarnasy.kz/ru/dlya-potrebitelej/tarify
[76] PJSC Sibur-Khimprom, (2025) "Isobutane-isobutylene fraction TU 2411-010-04605527-96".
https://shop.sibur.ru/catalog/toplivno_syrevye_produkty/szhizhennye_uglevodorodnye_gazy_sug/fraktsiya_izobutanovaya/fraktsiya_izobutan_izobutilenovaya_tu_2411_010_04605527_96_337647/
[77] PJSC Sibur-Khimprom, (2025) "Isobutylene, grade A, premium grade, TU 38.103504-81". https://shop.sibur.ru/catalog/organicheskiy_sintez/izobutilen_marka_a_sort_vysshiy_tu_38_103504_81_337694/
[78] Zhaik Petroleum. (2025). LTD "Zhaik Petroleum" Production. https://zhaikpetroleum.godaddysites.com/home
[79] KTZ Freight Transportation. (2025). Tariff guide (price list) part 1. https://ktzh-gp.kz/ru/activity/tariff-policy/cargo-transportation/tarifnoe-rukovodstvo-preyskurant-chast-1/
[80] KTZ Freight Transportation. (2025). Tariff guide (price list) part 3. https://www.ktzh-gp.kz/ru/activity/tariff-policy/cargo-transportation/tarifnoe-rukovodstvo-preyskurant-chast-3/
[81] Agency for Strategic Planning and Reforms of the Republic of Kazakhstan, Bureau of National Statistics. (2025). Population by gender and age groups at the beginning of 2025. https://stat.gov.kz/ru/industries/social-statistics/demography/publications/281562/
[82] Agency for Strategic Planning and Reforms of the Republic of Kazakhstan, Bureau of National Statistics. (2024). Current situation in the labor market, 2024. https://stat.gov.kz/ru/industries/labor-and-income/stat-empt-unempl/publications/341240/
[83] Agency for Strategic Planning and Reforms of the Republic of Kazakhstan, Bureau of National Statistics. (2024). Number and wages of employees in the Republic of Kazakhstan (IV quarter of 2024). https://stat.gov.kz/ru/industries/labor-and-income/stat-wags/publications/281058/
[84] Agency for Strategic Planning and Reforms of the Republic of Kazakhstan, Bureau of National Statistics. (2024). Structure and distribution of wages of employees in the Republic of Kazakhstan (Based on the results of 2024). https://stat.gov.kz/ru/industries/labor-and-income/stat-wags/publications/184053/

[85] “Liter” staff. (2021). Main ecological problems of Atyrau. What will happen to them, if ever. Liter.kz. https://liter.kz/top-5-ekologicheskih-problem-atyrau/
[86] IQAir. (2025). Air quality index in Atyrau region and air pollution in Kazakhstan. https://www.iqair.com/ru/kazakhstan/atyrau/atyrau
[87] Kazhydromet, Ministry of Ecology and Natural Resources of the Republic of Kazakhstan. (2024). Information bulletin on the state of the environment in Atyrau region. https://www.kazhydromet.kz/uploads/calendar/185/year_file/6798dbe5be26catyrau-russ-byulleten-za-2024.pdf
[88] Ryskalieva, D., Yessenamanova, M., Koroleva, E. G., Yessenamanova, Z., Tlepbergenova, A., Amanzholkyzy, S., & Turekeldiyeva, R. (2022). Monitoring study of the effect of Atyrau evaporation fields on the content of hydrogen sulfide in the air. International Journal of Sustainable Development and Planning, 17(6), 1789–1796. https://doi.org/10.18280/ijsdp.170613
[89] Ryskalieva, D., Yessenamanova, M., Syrlybekkyzy, S., Koroleva, E. G., Yessenamanova, Z., Tlepbergenova, A., Izbassarov, A., & Turekeldiyeva, R. (2023). Environmental assessment of the impact of atmospheric air pollution with hydrogen sulfide on the health of the population of Atyrau, republic of kazakhstan. International Journal of Sustainable Development and Planning, 18(7), 2199–2206. https://doi.org/10.18280/ijsdp.180724
[90] MeteoCast. (2025). Wind rose in Atyrau. https://ru.meteocast.in/windrose/kz/atyrau/
[91] Mackay, R. (2004). Practical pumping handbook. Elsevier. https://app.knovel.com/hotlink/toc/id:kpPPH00023/practical-pumping-handbook/practical-pumping-handbook
[92] Tidjma Engineers. (2024). Plant layout and spacing. https://www.tidjma.tn/en/art/plant-lay-out-and-spacing/
[93] Ministry of Emergency Situations of the Republic of Kazakhstan. (2021). On approval of the technical regulation "General requirements for fire safety" (Order No. 405). Registered with the Ministry of Justice on August 19, 2021 No. 24045. https://adilet.zan.kz/rus/docs/V2100024045
[94] Ministry of Emergency Situations of the Republic of Kazakhstan. (2021). On approval of the rules for ensuring industrial safety during the operation and repair of tanks for oil and oil products (Order No. 286). Registered with the Ministry of Justice on June 17, 2021 No. 23068. https://adilet.zan.kz/rus/docs/V2100023068
[95] Republic of Kazakhstan. (2011). Water disposal, external networks and structures: Building norms of the Republic of Kazakhstan 4.01-03-2011. https://online.zakon.kz/Document/?doc_id=31130718
[96] Tree Care Industry Association. (2012). ANSI A300 Part 5: Management of trees and shrubs during site planning, site development, and construction. West Chester Borough Document Center. https://west-chester.com/DocumentCenter/View/10142/A300-5
[97] Occupational Safety and Health Administration (n.d.). MTBE. https://www.osha.gov/chemicaldata/291?utm_source=chatgpt.com

[98] Airgas (n.d.) Isobutylene.
https://www.airgas.com/msds/010448.pdf?utm_source=chatgpt.com
[99] Airgas (n.d.) Methanol
https://www.airgas.com/msds/010448.pdf?utm_source=chatgpt.com
[100] LLP Crystal IG, “Methanol 99% — KZ #1779186,” Flagma-kg.com, 2024. [Online]. URL: https://flagma-kg.com/ru/metanol-bolee-99-methanol-99-o1779186.html [accessed Sep. 27, 2024].
[101] LLP KazNefteKhim Operating, “Technical methanol (grade A and B),” Flagma.kz, 2024. [Online]. URL: https://flagma.kz/metanol-tehnicheskiy-marka-a-i-b-methanol-o2425237.html [accessed Sep. 27, 2024].
[102] I. Group, “Methyl Tert-Butyl Ether (MTBE) Price Trend, News, Monitor, Forecast & Analysis,” Imarcgroup.com, 2023. https://www.imarcgroup.com/methyl-tert-butyl-ether-pricing-report (accessed Sep. 26, 2024)
[103]“Mtbe, China mtbe, mtbe Manufacturers, China mtbe catalog,” Made-in-china.com, 2024. [Online]. URL: https://www.made-in-china.com/productdirectory.do?subaction=hunt&style=b&mode=and&code=0&comProvince=nolimit&order=0&isOpenCorrection=1&org=top&keyword=&file=&searchType=0&word=mtbe [accessed Sep. 26, 2024].
[104] LLP KazNefteKhim Operating, “Methyl tert-butyl ether (MTBE),” Flagma.kz, 2024. [Online]. URL: https://flagma.kz/efir-metil-tret-butilovy-mtbe-o2603092.html [accessed Sep. 26, 2024].
[105]Стальные вертикальные резервуары в Астане [Steel Vertical Tanks in Astana]. (n.d.). Retrieved April 20, 2025, from https://kmicom.kz/catalog/rezervuary-vertikalnye-stalnye/
[106]World Salaries, "Average Chemical Engineer Salary in Kazakhstan," 2024. [Online]. Available: https://worldsalaries.com/average-chemical-engineer-salary-in-kazakhstan/
[107]Metcalf & Eddy, "Wastewater Engineering" (5th Ed.) https://www.abpsoil.com/images/Books/Wastewater_Engineering_Treatment_Resource_Recovery_Metcalf_Eddy_5th.pdf
[108]USEPA Design Manual (2010). Nutrient Control Design Manual. https://www.epa.gov/sites/default/files/2019-02/documents/nutrient-control-design-manual.pdf
[109] Indiamart (n.d.) Specialized Bacteria For Activated Sludge Process https://www.indiamart.com/proddetail/specialized-bacteria-for-activated-sludge-process-for-stp-etp-14090803391.html?srsltid=AfmBOorFNEK_smE9AWl5ppRI1DbpenHatpCCK1DFaOAid20cI4fO_3uF

Appendix A - Process Introduction

Table A.1. Chemical and physical properties of MTBE

Properties	**Aspen Plus**	**NIST Chemistry WebBook**	**Viswanathan et al. 2000 [8]**	**GESTIS Substance Database**
Molar mass, g/mol	88.1497	88.1482	-	88.15
Boiling point, °C	55.05	55.05	-	55
Melting point, °C	-108.6	-108.65	-	-109
Critical temperature, °C	223.95	223.25	-	-
Critical pressure, MPa	3.286	3.397	-	-
Density at 20 °C 1 atm, kg/m^3	741.269	-	742.5	740
Viscosity at 20 °C 1 atm, cP	0.35338	-	0.3861	-
Flash point (closed cup), °C	-	-	-	-28
Solubility in water at 20 °C 1 atm, g/l	16.56 (Table A2)	-	-	26

Table A.2. Data from Aspen for water solubility estimation of MTBE via experimental data regression

Model	NRTL	UNIFAC	UNIQUAC
Water density at 20 °C 1 atm in Aspen, g/L	996.473		
Water molecular weight in Aspen, g/mol	18.0153		
MTBE molar amount by Txx regression at 20 °C 1 atm, mol	0.010799	0.003384	0.013040
Water molar amount by Txx regression at 20 °C 1 atm, mol	0.989201	0.996616	0.986960
MTBE mass, g	0.951920	0.298316	1.149472
Water volume, L	0.017884	0.018018	0.017843
Solubility, g/L	53.227958	16.556675	64.420326
MTBE molar amount by Txx analysis at 20 °C 1 atm, mol	0.010882	0.003369	0.013009
Water molar amount by Txx analysis at 20 °C 1 atm, mol	0.989118	0.996631	0.986991
MTBE mass, g	0.959280	0.297013	1.146739
Water volume, L	0.017882	0.018018	0.017844
Solubility, g/L	53.644059	16.484122	64.265161

Table A.3. Studies on forecasts of the global demand for MTBE

Forecast Period	CAGR (%)	Production Rate or USD Value initial (Year)	Production Rate or USD Value final (Year)	Source
2024-2032	4.89	17.6 mln ton (2022)	28.5 mln ton (2032)	ChemAnalyst, 2024

2024-2034	4.6	USD 15.98 bn (2024)	USD 25.06 bn (2034)	Fact.Mr, 2024
2024-2031	4.3	USD 17.29 bn (2024)	USD 23.48 bn (2031)	Verified Market Research, 2024

Table A.4. Comparison of different pathways of MTBE production

Aspect	**Direct Etherification**	**TBA Route**	**Butane Route**
Feedstock	C4 streams (raffinate-1, FCC-C4)	TBA	n-Butane
Process Steps	Etherification	Dehydration → Etherification	Isomerization → Dehydrogenation → Etherification
Catalyst	Acidic ion-exchange resins	Acidic ion-exchange resins	Platinum (isomerization), Chromium (dehydrogenation), Acidic resins (etherification)
Energy Requirements	Moderate	Moderate	High (due to isomerization and dehydrogenation)
Byproducts	Minimal	Water	Hydrogen
Commercial Use	Widely adopted	Moderate	Less common

Table A.5. Comparison of different catalysts in liquid phase MTBE production

Zeolite	**ZSM-5**			**ZSM-11**		**Amberlyst 15**		
Molar ratio of methanol/isobutene	1.00	1.05	1.10	1.05	1.10	1.00	1.05	1.10
Weight hourly space velocity, h^{-1}	1.75	1.71	1.68	1.49	1.41	1.03	1.01	1.01
Peak temperature, °C	108			86	90	77	70	62
Isobutene conversion, %	89.6	89.8	90.1	88.7	90.2	93.1	93.4	94.5
MTBE yield, %	89.6	89.8	90.1	88.7	90.2	86.0	89.4	92.7
MTBE selectivity, %	100					92.4	95.7	98.1

Production Rate Calculation

Initial demand (2022): 17.6 million tonnes

CAGR (average): 4.6%

Projected demand (2029):

$$MTBE\ global\ demand\ in\ 2029\ =\ 17.6\ mln\ ton\times(1\ +\ 0.046)^{7}\ =\ 23.112\ mln\ ton \quad \text{(A.1)}$$

Global GDP (2029): USD 139,048.77 billion

CIS GDP excluding Russia (2029): USD 926.5 billion

$$GDP\ ratio\ =\frac{CIS\ GDP}{Global\ GDP}=\frac{USD\ 926.5\ bn}{USD\ 139{,}048.77\ bn}\ =\ 0.00666 \quad \text{(A.2)}$$

$$MTBE\ \ demand\ in\ 2029\ =\ 23.112\ mln\ ton\times 0.00666\ =\ 153,998\ tonnes/year \quad \text{(A.3)}$$

Target plant share (25%):

$$153,998\ ton\times 0.25\ =\ 38,500\ tonnes/year \quad \text{(A.4)}$$

Kinetic Rate Expression (Zhang & Datta)

$$-r_{IB}=k_1\left(\frac{\alpha_{IB}}{\alpha_{MeOH}}-\frac{1}{K}\cdot\frac{\alpha_{MTBE}}{\alpha_{MeOH}^2}\right) \quad \text{(A.5)}$$

, where k_1 is the rate constant, defined by (A.6), and K is equilibrium constant, expressed through the (A.7). $\alpha_{IB}, \alpha_{MeOH}, \alpha_{MTBE}$ are activities of isobutylene, methanol, and MTBE, respectively. The rate constant, k_1, is defined by the Arrhenius equation as expressed below:

$$k_1=A_0\cdot\exp\left(\frac{-E_a}{RT}\right) \quad \text{(A.6)}$$

, where A_0 is the pre-exponential constant, E_a is the activation energy, R is the universal constant, and T is the reaction temperature.

$$\ln K=-13.482+\frac{4388.7}{T}+1.2353\ln T-0.013849T+2.5923\times10^{-5}T^2-3.1881\times10^{-8}T^3 \quad \text{(A.7)}$$

, where T is the temperature (K). Activity of species j is defined by the following equation:

$$\alpha_j=x_j\gamma_j \quad \text{(A.8)}$$

, where j is MeOH, IB, MTBE, x_j is the mole fraction of species j and γ_j is the activity coefficient of species j. The activity coefficients, γ_j, were determined using the UNIFAC method.

The mole fractions of isobutylene, x_{IB}, methanol, x_{MeOH}, and MTBE, x_{MTBE} are defined through the methanol to isobutylene ratio, θ_{MeOH}, and fractional isobutylene conversion, X, as indicated in (A.9-11).

$$x_{IB} = \frac{1 - X}{1 + \theta_{MeOH} - X} \tag{A.9}$$

$$x_{MeOH} = \frac{\theta_{MeOH} - X}{1 + \theta_{MeOH} - X} \tag{A.10}$$

$$x_{MTBE} = \frac{X}{1 + \theta_{MeOH} - X} \tag{A.11}$$

, where $X = i\Delta X$ and $\Delta X = \frac{X_{IB}}{N}$ $(i = 0, 1, \ldots N)$. X_{IB} is the isobutylene conversion coming out of the reactor and N is the intervals for the integration of (A.14).

To account for the intraparticle diffusion in determining the appropriate kinetic model of MTBE, the catalyst effectiveness factor needs to be considered which is defined by (A.12).

$$\eta = \frac{\sqrt{2\int_{C^*_{MeOH}}^{1} R^* \, dC^*_{MeOH}}}{\varphi_s} \tag{A.12}$$

The intraparticle diffusion influence on the reaction rate was investigated with the help of Thiele modulus, which is defined as

$$\varphi_g = \frac{\varphi_s}{\sqrt{2\int_{C^*_{MeOH,c}}^{1} R^* \, dC^*_{MeOH,e}}} \tag{A.13}$$

, where $\varphi_g, \varphi_s, C^*_{MeOH,c}, C^*_{MeOH,e}, R^*$ is the generalized Thiele modulus, Thiele modulus, dimensionless methanol concentrations, and dimensionless reaction rate. Therefore, it was proposed to include intraparticle diffusion impact in determining the rate expression of MTBE production by involving the effectiveness factor, which can be described by the (A.14).

$$\frac{W_{cat}}{F_{IB,i}} = \int_0^{X_{IB}} \frac{1}{\eta(-r_{IB})_s} \, dX \tag{A.14}$$

, where $W_{cat}(g)$ is the weight of the catalyst, $F_{IB,i}$ is the inlet molar flow rate of isobutylene (mol/h).

Table A.6. MTBE grading and purity specifications

Grading	Grade A (Top grade)	Grade B (First grade)	Grade C (Second grade)
Purity, %	98.0	96.0	94.0

Appendix B - H-101 heat exchanger design

Table B.1. Square pitch arrangement constants

Triangular Pitch, p_t=1.25d_o		
No. Passes	**K_1**	**n_1**
1	0.319	2.142
2	0.249	2.207
4	0.175	2.285
6	0.0743	2.499
8	0.0365	2.675
Square Pitch, p_t=1.25d_o		
No. Passes	**K_1**	**n_1**
1	0.215	2.207
2	0.156	2.291
4	0.158	2.263
6	0.0402	2.617
8	0.0331	2.643

Table B.2. Fouling coefficients

Fluid	**Coefficient (W/m^{2}C)**	**Factor (m^{2}C/W)**
River water	3000–12000	0.0003–0.0001
Sea water	1000–3000	0.001–0.0003
Cooling water (towers)	3000–6000	0.0003–0.00017

Town water (soft)	3000–5000	0.003–0.0002
Town water (hard)	1000–2000	0.001–0.0005
Steam condensate	1500–5000	0.00067–0.0002
Steam (oil free)	4000–10000	0.0002–0.0001
Steam (oil traces)	2000–5000	0.0005–0.0002
Refrigerated brine	3000–5000	0.003–0.0002
Air and industrial gases	5000	0.0004
Flue gases	2000–5000	0.0005–0.0002
Organic vapors	5000	0.0002
Organic liquids	5000	0.0002
Light hydrocarbons	5000	0.0002
Heavy hydrocarbons	2000	0.0005
Boiling organics	2500	0.0004
Condensing organics	5000	0.0002
Heat transfer fluids	5000	0.0002
Aqueous salt solutions	3000–5000	0.0003–0.0002

Table B.3. Standard Dimensions for Steel Tubes

Outside Diameter (mm)	**Wall Thickness (mm)**				
16	1.2	1.7	2.1	—	—
19	—	1.7	2.1	2.8	—
25	—	1.7	2.1	2.8	3.4
32	—	1.7	2.1	2.8	3.4
38	—	—	2.1	2.8	3.4
50	—	—	2.1	2.8	3.4

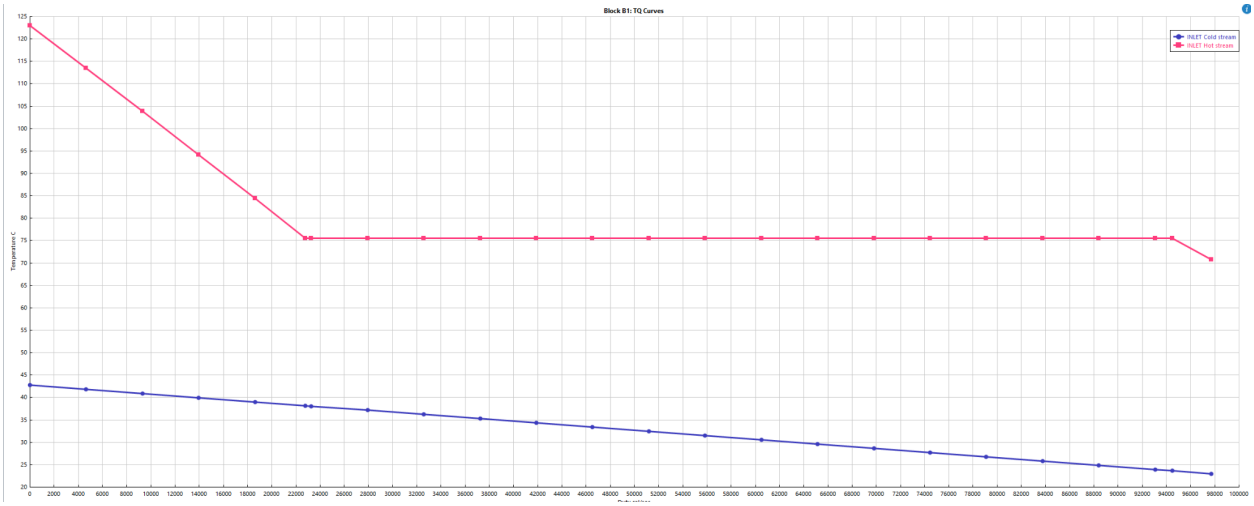

Figure B.1. Temperature curve

Appendix C - H-102 heat exchanger design

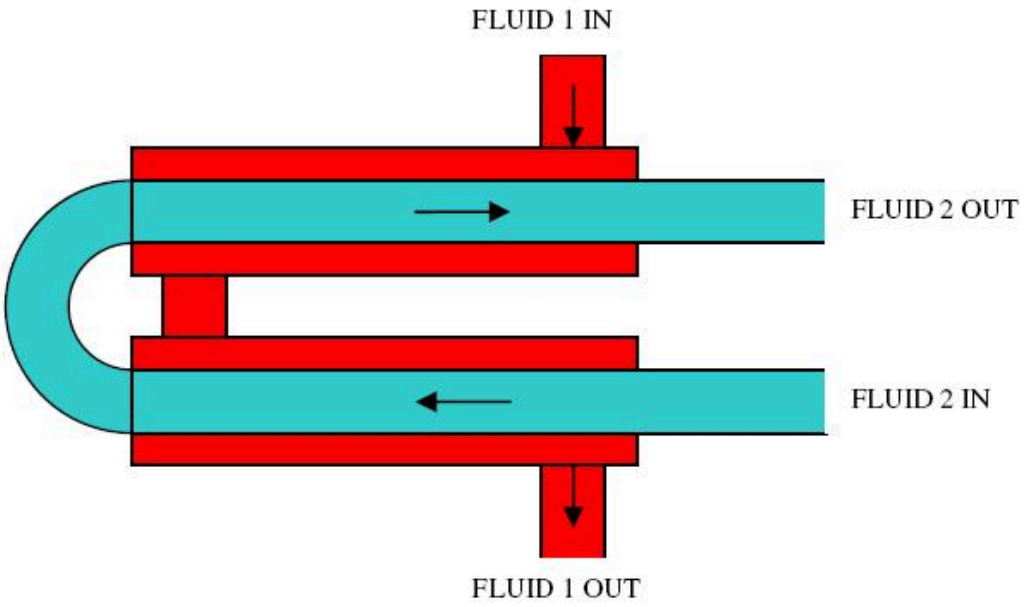

Figure C.1. Double pipe heat exchanger

Appendix D - T-101 distillation column design

Table D.1. Antoine coefficients employed in design of T-101 and T-103

Component	A	B	C
MTBE	5.896	708.69	179.9
Water	8.07131	1730.63	233.426
MEOH	8.0724	1574.99	238.87
IB	6.84134	923.2	240

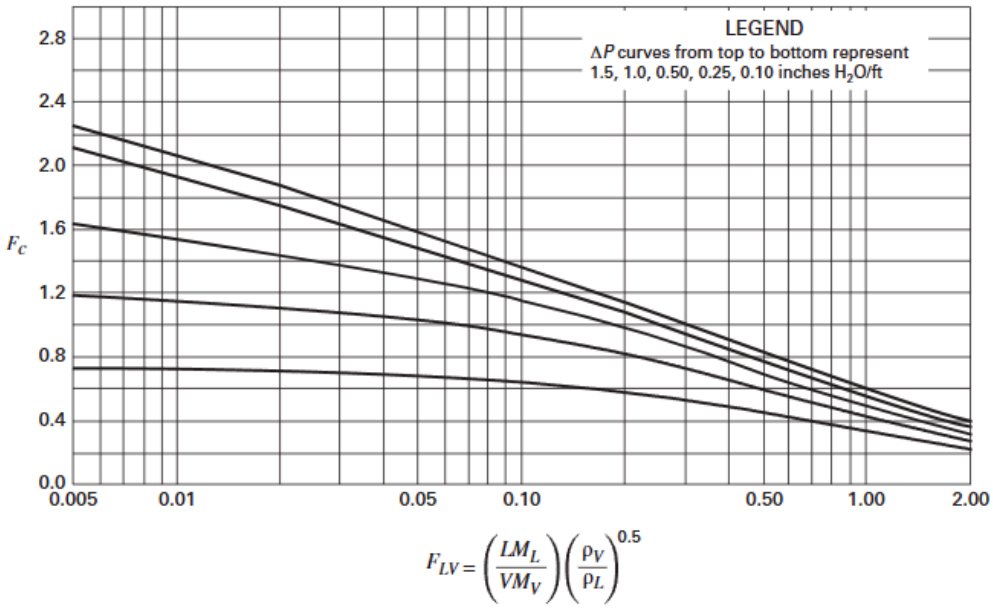

Figure D.1. Sherwood-Eckert generalized pressure-drop correlation for structured packing

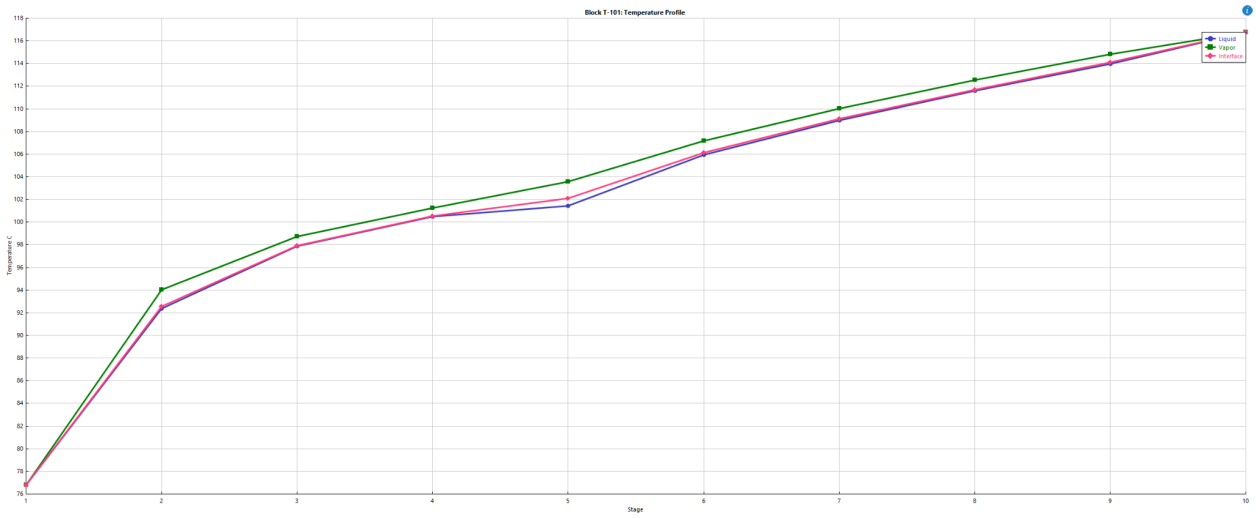

Figure D.2. T-101: Temperature Profile

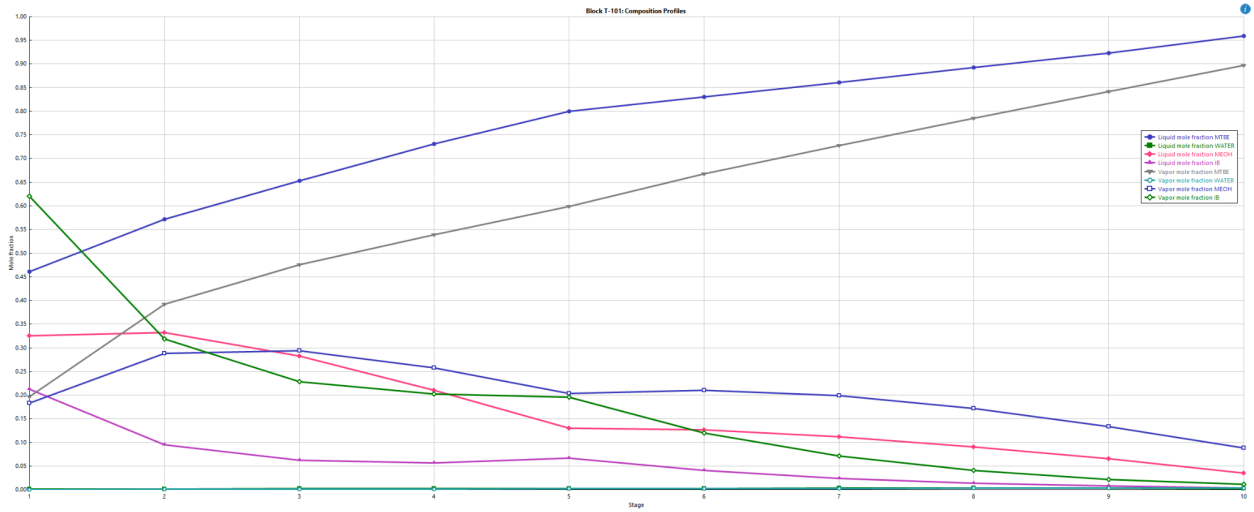

Figure D.3. T-101: Composition Profiles

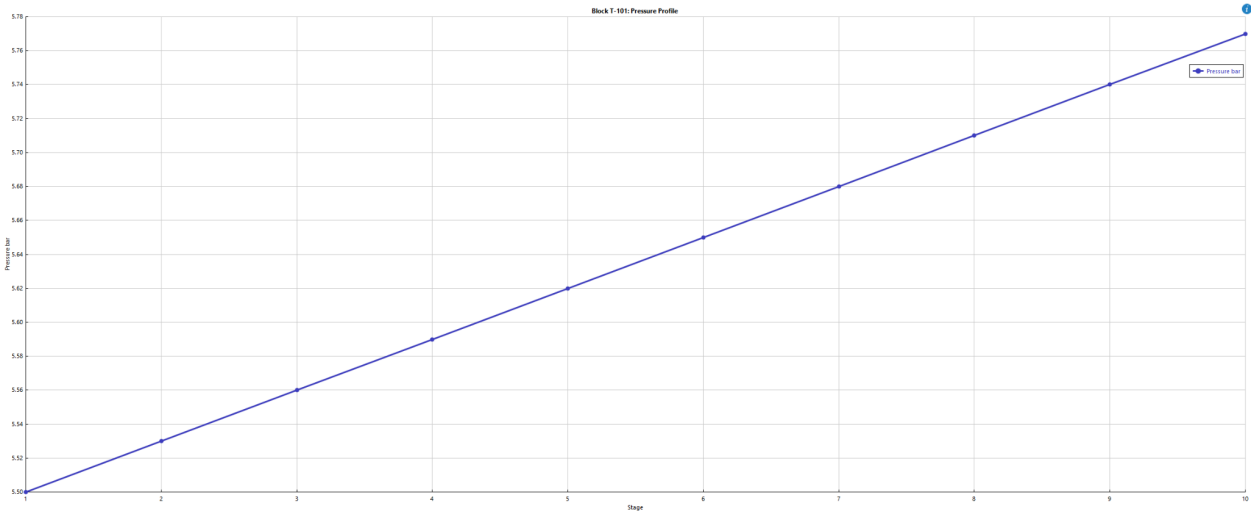

Figure D.4. T-101: Pressure Profile

Appendix E - T-102 absorption column design

Table E.1. Characteristics of Random Packings

Name	Material	Nominal size (mm)	Surface area (m^2/m^3)	% Voids	Packing factor (m^{-1})	Vendor
Intalox saddles "IMTP"	Metal	(No. 25)	97	97	135	NorPro-Ste. Gobain Akron, Ohio USA
		(No. 40)	98	94	97	
		(No. 50)	97	96	125	
Pall rings*	Metal	16	205	94	184	(Generic)
		25	130	95	181	
		38	370	94	88	
		50	115	92	88	
		90	92	97	59	
Pall rings*	Plastic	16	340	87	310	(Generic)
		25	205	90	180	
		50	100	92	110	
Intalox saddles	Ceramic	13	100	92	660	NorPro-Ste. Gobain Akron, Ohio USA
		25	625	78	197	
		50	255	77	197	
		75	118	79	98	
Intalox saddles	Plastic	20	131	92	410	NorPro-Ste. Gobain Akron, Ohio USA
		25	108	94	59	
Raschig rings	Ceramic	13	370	64	1900	(Generic)
		25	190	74	587	
		38	74	74	213	
		50	72	74	213	
		75	62	75	121	
Raschig rings	Metal	19	245	73	750	(Generic)
		25	185	86	470	
		38	130	92	270	
		50	115	96	180	
		75	95	105	105	

*Through-flow packing.

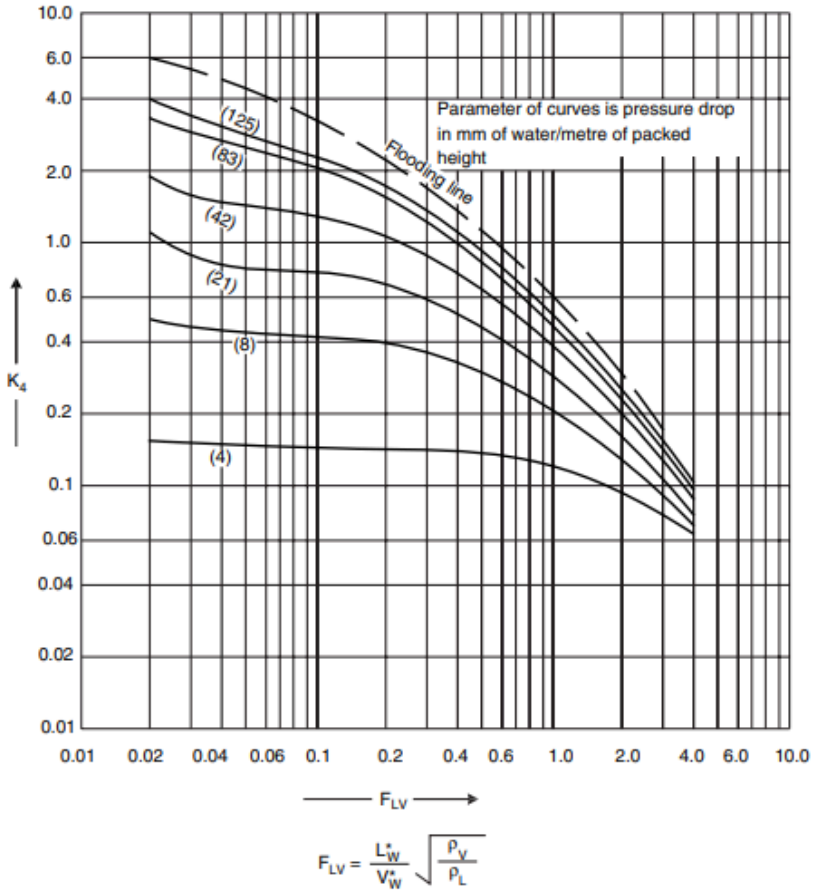

Figure E.1. Relation between K4 and Flow Parameter

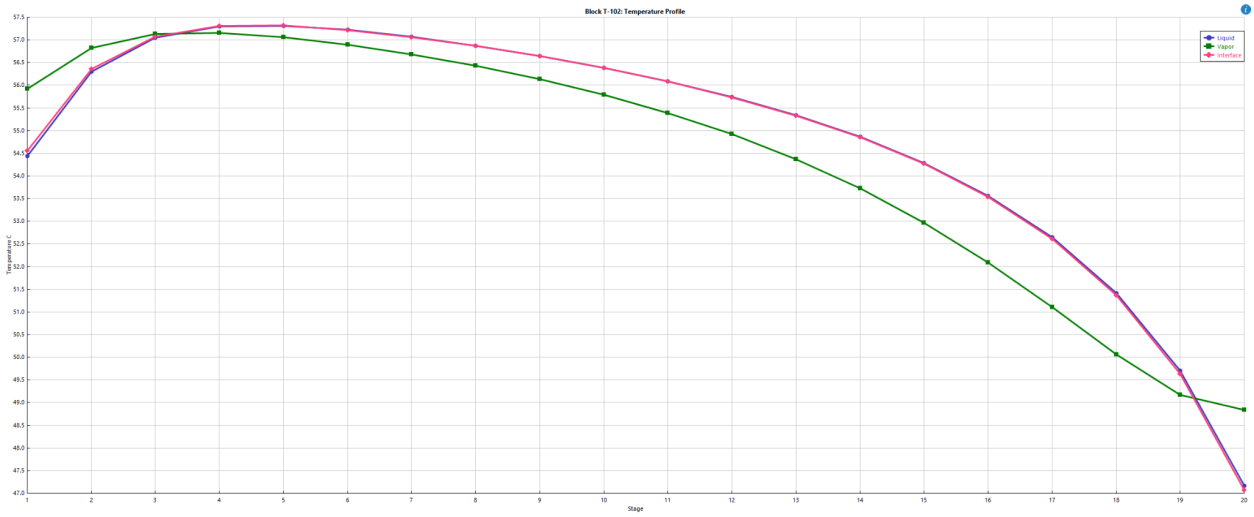

Figure E.2. T-102: Temperature Profile

Appendix F - T-103 distillation column design

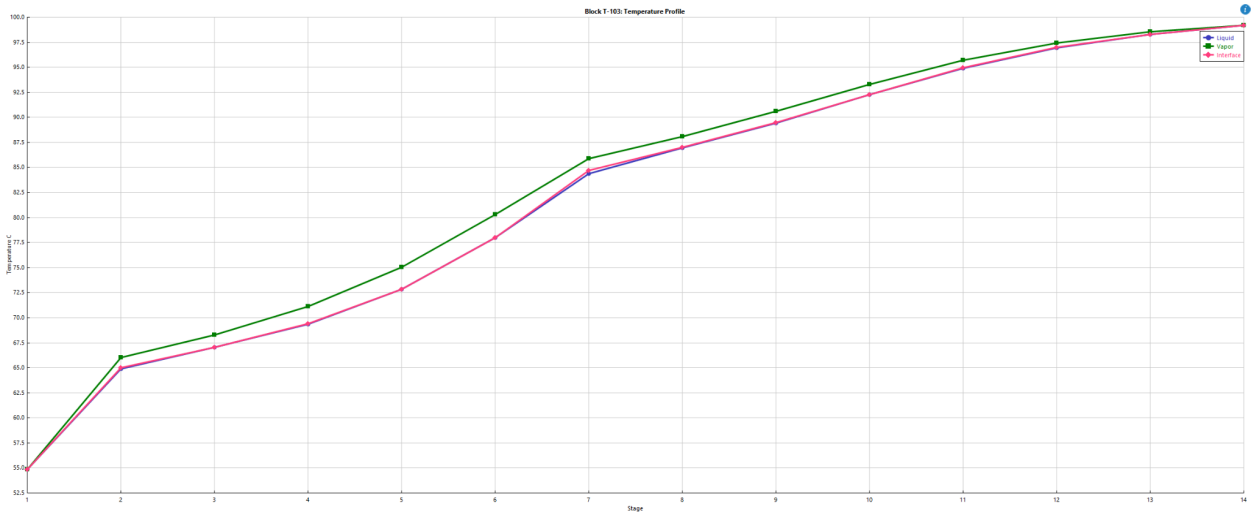

Figure F.1. T-103: Temperature Profile

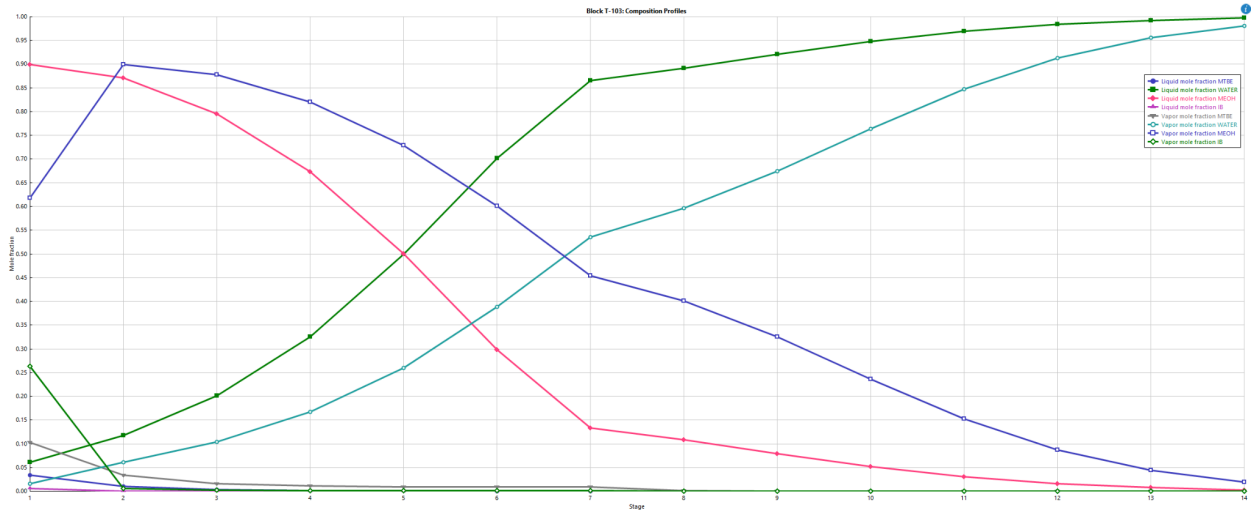

Figure F.2. T-103: Composition Profiles